

Part I

Moving towards the sustainable fisheries framework for
Pacific herring: data, models, and alternative assumptions.

Part II

Stock Assessment and Management Advice for the British
Columbia Pacific Herring Stocks:
2011 Assessment and 2012 Forecasts

Steven Martell, Jake Schweigert, Jaclyn Cleary, Vivian Haist

August 9, 2011

Abstract

Executive summary

DRAFT August 9, 2011 DRAFT

Contents

Abstract

Contents	i
List of Figures	iii
List of Table	viii
	x

I Moving towards a sustainable fisheries framework for Pacific herring: data, models and alternative assumptions

1.1 Introduction	1
1.2 Methods	2
1.2.1 Analytical methods	2
1.2.2 Sustainable Fisheries Framework reference points	4
1.2.3 Simulation testing	4
1.2.4 Comparison of HCAM with <i>iSCAM</i>	5
1.3 Results	7
1.3.1 Simulation testing	7
1.3.2 Comparison of HCAM with <i>iSCAM</i>	7
1.3.3 Alternative assumptions about catchability, mortality & selectivity	13
1.3.4 Preliminary assessments for all other areas	16

II Stock Assessment and Management Advice for the British Columbia Pacific Herring Stocks: 2011 Assessment and 2012 Forecasts

2.4 Introduction	18
2.5 BC Herring Stocks	19
2.6 Methods	19
2.6.1 Input data & assumptions	19
2.6.2 Analytical methods	32
2.6.3 Retrospective analysis	32
2.6.4 Abundance and recruitment forecasts	32
2.6.5 Catch advice	32
2.7 Results	32
2.7.1 Maximum likelihood fits to the data	33
2.7.2 Biomass estimates & reference points	36
2.7.3 Estimates of mortality	42
2.7.4 Selectivity	46
2.7.5 Recruitment and stock-recruitment relationships	48
2.7.6 Retrospective analysis	49
2.7.7 Marginal posterior distributions	49
2.7.8 Parameter confounding	54
2.7.9 Marginal posterior distributions	54
2.7.10 Forecast and catch advice based on the joint posterior distribution	54
2.8 Stock assessments for minor stock areas	54

2.8.1	Maximum likelihood estimates of biomass	66
2.8.2	Estimates of recruitment and reference points	66
2.8.3	Retrospective analysis	69
2.8.4	Marginal posterior distributions and trace plots	69
2.8.5	Catch advice	69
2.9	Acknowledgements	74
	References	75

III Appendixes

A.1	Technical description of <i>iSCAM</i>	77
A.1.1	Analytic methods	78
A.1.2	Equilibrium considerations	78
A.1.3	MSY based reference points	78
A.1.4	Dynamic age-structured model	81
A.1.5	Options for selectivity	84
A.1.6	Options for natural mortality	86
A.1.7	Residuals, likelihoods & objective function value components	86
A.1.8	Catch data	87
A.1.9	Relative abundance data	87
A.1.10	Age composition data	88
A.1.11	Stock-recruitment	89
A.1.12	Parameter Estimation and Uncertainty	89
A.1.13	Negative loglikelihoods	90
A.1.14	Constraints	90
A.1.15	Priors for parameters	90
A.1.16	Survey priors	91
A.1.17	Convergence penalties	91
B.2	Data and Control files	93
B.2.1	Haida Gwaii	93
B.2.2	Prince Rupert District	94
B.2.3	Central Coast	97
B.2.4	Strait of Georgia	99
B.2.5	West Coast of Vancouver Island	101
B.2.6	Area 2W	103
B.2.7	Area 27	104
B.2.8	Control file for the simulation studies	106
C.3	Bayesian prior for the dive survey spawn index proportionality constant q	107
C.3.1	The process	107
C.3.2	Factors affecting q and their distributions	107
C.3.3	Simulating the dive survey spawn index q	108
D.4	Landings and Survey data	113

List of Figures

1.1	B.C. herring major stock areas: Haida Gwaii (HG or QCI 2E), Prince Rupert District (PRD), Central Coast (CC), Strait of Georgia (SOG), West Coast Vancouver Island (WCVI), and minor stock areas: Area 2W and Area 27.	3
1.2	True (thin line) and estimated (thick shaded line) spawning biomass (a), fishing mortality rates by gear (b), observed and predicted relative abundance (c), and residuals between observed and predicted relative abundance (d) for the SOG herring simulation with perfect information and a deterministic stock-recruitment relationship.	8
1.3	Estimates of precision and bias in key model parameters and MSY based reference points for 50 simulated data sets conditioned on the Strait of Georgia herring catch. The log2 ratio of estimated versus true value is plotted; values of 1 and -1 correspond to a twice or half the true value, respectively.	9
1.4	Maximum likelihood estimates of pre-fishery biomass (defined as the numbers-at-age times the mean weight-at-age at the start of the year) and post fishery spawning biomass in the Strait of Georgia (a), spawning biomass depletion (b), age-2 recruits (c), stock-recruitment relationship and unfished reference points (d), components of total mortality (log-scale, e), and observed (points) and predicted (lines) spawn survey data (f). These results are based on trying to configure the $iSCAM$ model as similar as possible to the previous HCAM assessment; the red line in panel (a) is the MLE estimate of spawning biomass from HCAM.	11
1.5	From top to bottom in the left column: the log residuals between observed and predicted catch for each gear, the residuals between the observed and predicted spawn survey index, and the annual deviations between age-2 recruitment and that predicted by the Beverton-Holt model and the estimated spawning stock biomass. Right column: residual patterns in the age-composition data (observed - predicted, where black is a positive residual) for each of the three commercial gears in the Strait of Georgia.	12
1.6	A comparison of the estimated biomass and spawning biomass and fits to the survey data when q is either fixed at 1 for Survey 2, or estimated using an informative prior with an expected mean of 0 and a log standard deviation of 0.274.	14
1.7	A comparison of fits to the survey data and estimated components of average mortality by year when M is allowed to vary via a random walk process or is estimated and assumed time invariant.	15
1.8	Residuals in the age-composition data when gill net selectivity is a function of mean weight-at-age (left column with q Fixed in each caption) and or is a logistic function of age and time invariant (right column with Fixed Gillnet in each caption).	16
1.9	A comparison of estimated spawning stock biomass between HCAM and $iSCAM$ for the five major stock assessment regions using data from 1951 to 2010 and setting up $iSCAM$ similar to HCAM.	17
2.1	Historical catch of herring in the five major stock areas between 1951 and 2011 for the winter purse seine fishery (dark bars), seine-roe fishery (grey bars), and gill net fishery (light grey bars). Units of catch are in thousands of metric tons.	20
2.2	Preliminary Spawning activity for Haida Gwaii (top panel) and Prince Rupert District (bottom) in 2011.	22
2.2	Preliminary Spawning activity for Central Coast (top panel) and Strait of Georgia (bottom) in 2011.	23

2.2	Preliminary Spawning activity in 2011 for the West Coast of Vancouver Island (includes minor stock area 27)	24
2.3	Spawn survey index for Strait of Georgia between 1951 and 2011. The units are actual estimates of spawning biomass (1000s tons), but only the trend information is used in the model fitting.	25
2.4	Bubble plots showing the proportions-at-age versus time for the winter purse seine fishery (top), seine roe fishery (middle) and the gill net fishery (bottom) in Haida Gwaii. The area of the circle is proportional to cohort abundance, each column sums to 1, zeros are not shown, and age 10 is a plus group. Also shown is the mean age of the catch (line) and the approximate 95% distribution of ages (shaded polygon) for each year.	26
2.5	Bubble plots showing the proportions-at-age versus time for the winter purse seine fishery (top), seine roe fishery (middle) and the gill net fishery (bottom) in Prince Rupert District. The area of the circle is proportional to cohort abundance, each column sums to 1, zeros are not shown, and age 10 is a plus group. Also shown is the mean age of the catch (line) and the approximate 95% distribution of ages (shaded polygon) for each year.	27
2.6	Bubble plots showing the proportions-at-age versus time for the winter purse seine fishery (top), seine roe fishery (middle) and the gill net fishery (bottom) in the Central Coast region. The area of the circle is proportional to cohort abundance, each column sums to 1, zeros are not shown, and age 10 is a plus group. Also shown is the mean age of the catch (line) and the approximate 95% distribution of ages (shaded polygon) for each year.	28
2.7	Bubble plots showing the proportions-at-age versus time for the winter purse seine fishery (top), seine roe fishery (middle) and the gill net fishery (bottom) in the Strait of Georgia. The area of the circle is proportional to cohort abundance, each column sums to 1, zeros are not shown, and age 10 is a plus group. Also shown is the mean age of the catch (line) and the approximate 95% distribution of ages (shaded polygon) for each year.	29
2.8	Bubble plots showing the proportions-at-age versus time for the winter purse seine fishery (top), seine roe fishery (middle) and the gill net fishery (bottom) in the West Coast Vancouver Island region. The area of the circle is proportional to cohort abundance, each column sums to 1, zeros are not shown, and age 10 is a plus group. Also shown is the mean age of the catch (line) and the approximate 95% distribution of ages (shaded polygon) for each year.	30
2.9	Empirical mean weight-at-age data by cohort from 1951 to 2011 for ages 2 to 10 in the five major Stock Assessment Regions.	31
2.10	Residual for the log difference between observed and predicted catch for the five major SARs for each gear type (Gear 1 = winter seine fishery, Gear 2 = seine-roe fishery, Gear 3 = gillnet fishery).	33
2.11	Residual patterns for the log difference between observed and predicted spawn survey abundance for the five major SARs. Spawn survey data based on surface estimates are show as solid lines and data based on diver surveys is shown as dashed lines.	34
2.12	Observed (points) and predicted (lines) relative abundance data (spawn survey data) for each of the five major SARs. In each panel, the corresponding scalar (q) is presented for each of the surveys.	35
2.13	Residual difference between the observed and predicted proportions-at-age for HG for each of the three gear types (Gear 1 = winter seine, Gear 2 = seine-roe, Gear 3 = gillnet). The area of each circle is proportional to the residua, black is positive, and red is negative. The corresponding MLE estimates of the residual variance is displayed in each panel.	37
2.14	Residual difference between the observed and predicted proportions-at-age for PRD for each of the three gear types (Gear 1 = winter seine, Gear 2 = seine-roe, Gear 3 = gillnet). The area of each circle is proportional to the residua, black is positive, and red is negative. The corresponding MLE estimates of the residual variance is displayed in each panel.	38
2.15	Residual difference between the observed and predicted proportions-at-age for CC for each of the three gear types (Gear 1 = winter seine, Gear 2 = seine-roe, Gear 3 = gillnet). The area of each circle is proportional to the residua, black is positive, and red is negative. The corresponding MLE estimates of the residual variance is displayed in each panel.	39

2.16	Residual difference between the observed and predicted proportions-at-age for SOG for each of the three gear types (Gear 1 = winter seine, Gear 2 = seine-roe, Gear 3 = gillnet). The area of each circle is proportional to the residua, black is positive, and red is negative. The corresponding MLE estimates of the residual variance is displayed in each panel.	40
2.17	Residual difference between the observed and predicted proportions-at-age for WCVI for each of the three gear types (Gear 1 = winter seine, Gear 2 = seine-roe, Gear 3 = gillnet). The area of each circle is proportional to the residua, black is positive, and red is negative. The corresponding MLE estimates of the residual variance is displayed in each panel.	41
2.18	Estimates of total biomass at the start of the year (numbers times empirical weight-at-age) and spawning stock biomass (post fishery) for the five major SARs.	43
2.19	Estimates of spawning biomass depletion (B_t/B_0) for each of the five major stock areas. Horizontal dotted lines represent 25% and 40% depletion levels, and the shaded regions demarcate reference points based on <40% B_{MSY}/B_0 (critical zone) and 40–80% B_{MSY}/B_0 (cautious zone) and >80% B_{MSY}/B_0 (healthy zone).	44
2.20	Maximum likelihood estimates of the components of average total mortality for each of the five major stock assessment regions. Note that the y-axis is plotted on a log scale, natural mortality (grey) is age-independent, fishing mortality is age-specific and the average fishing mortality rate over all age-classes is plotted here.	45
2.21	Maximum likelihood estimates of age-specific selectivity coefficients for the winter seine fishery for each of the major stock areas.	46
2.22	Maximum likelihood estimates of age-specific selectivity coefficients for the seine-roe fishery for each of the major stock areas.	47
2.23	Estimates of selectivity for the gillnet fleet for each of the five major stock assessment regions. In this case selectivity is a logistic function of the empirical weight-at-age data; due to declining growth there is a tendency for selectivity to shift to older ages.	48
2.24	Maximum likelihood estimates of age-2 recruits for each of the five major stock areas. The horizontal divisions demarcate the 0.33 and 0.66 quantiles that define poor, average, and good recruitment.	50
2.25	Maximum likelihood estimates of age-2 recruits versus estimated spawning stock biomass in each of the five major assessment regions. The green and red circles indicate the start (recruits in 1952) and end (recruits in 2011) of the series, the circle plus (red) corresponds to the maximum likelihood estimate of unfished spawning biomass (B_0) and unfished age-2 recruitment R_0 , the line is the Beverton-Holt stock recruitment model fitted to these data.	51
2.26	Log residual differences between estimated age-2 recruits and the recruitment predicted by the Beverton-Holt model and estimated spawning stock biomass. The standard deviations of the residuals along with the MLE estimate of the process error standard deviations are displayed at the top of each panel.	52
2.27	Retrospective estimates of spawning stock biomass for each of the five major stock assessment areas. The model was sequentially fitted to the full data set, then from 1951:2010, 1951:2009, ... 1951:2001.	53
2.28	A systematic sample of 2,000 from an MCMC chain of length 1,000,000 of leading parameters and derived variables used in reference point calculations for HG. Green circle corresponds to the MLE estimates and the solid line is a lowess smooth fit to the data ($f=1/4$), and the dashed line is the mean of the distribution.	55
2.29	A systematic sample of 2,000 from an MCMC chain of length 1,000,000 of leading parameters and derived variables used in reference point calculations for PRD. Green circle corresponds to the MLE estimates and the solid line is a lowess smooth fit to the data ($f=1/4$), and the dashed line is the mean of the distribution.	56
2.30	A systematic sample of 2,000 from an MCMC chain of length 1,000,000 of leading parameters and derived variables used in reference point calculations for CC. Green circle corresponds to the MLE estimates and the solid line is a lowess smooth fit to the data ($f=1/4$), and the dashed line is the mean of the distribution.	57

2.31 A systematic sample of 2,000 from an MCMC chain of length 1,000,000 of leading parameters and derived variables used in reference point calculations for SOG. Green circle corresponds to the MLE estimates and the solid line is a lowess smooth fit to the data ($f=1/4$), and the dashed line is the mean of the distribution.	58
2.32 A systematic sample of 2,000 from an MCMC chain of length 1,000,000 of leading parameters and derived variables used in reference point calculations for WCVI. Green circle corresponds to the MLE estimates and the solid line is a lowess smooth fit to the data ($f=1/4$), and the dashed line is the mean of the distribution.	59
2.33 Pairs plot and marginal distributions for leading parameters in HG region (200 random samples). The dotted lines correspond to the means of the distributions, circle is the mean, and the red square is the mode of the distribution.	60
2.34 Pairs plot and marginal distributions for leading parameters in PRD region (200 random samples). The dotted lines correspond to the means of the distributions, circle is the mean, and the red square is the mode of the distribution.	61
2.35 Pairs plot and marginal distributions for leading parameters in CC region (200 random samples). The dotted lines correspond to the means of the distributions, circle is the mean, and the red square is the mode of the distribution.	62
2.36 Pairs plot and marginal distributions for leading parameters in SOG region (200 random samples). The dotted lines correspond to the means of the distributions, circle is the mean, and the red square is the mode of the distribution.	63
2.37 Pairs plot and marginal distributions for leading parameters in WCVI region (200 random samples). The dotted lines correspond to the means of the distributions, circle is the mean, and the red square is the mode of the distribution.	64
2.38 Marginal posterior densities (histograms) and prior densities (lines) for the seven leading parameters for each of the five major assessment regions.	65
2.39 Catch and survey data for minor stock Areas 2W and Area 27.	66
2.40 Age composition data for Area 2W and Area 27 for the seine-roe fishery (Gear 2) and the gillnet fishery (Gear 3).	67
2.41 Maximum likelihood estimates of total biomass, spawning biomass, spawning depletion and fits to the spawn survey data for the two minor stock areas.	68
2.42 Maximum likelihood estimates of age-2 recruits, spawner-recruit relationships with the fitted Beverton Holt model and unfished reference points (B_o, R_o), and the residuals between the estimated age-2 recruits and that predicted by the Beverton-Holt model.	70
2.43 Retrospective estimates of spawning stock biomass for each of the minor stock assessment areas. The model was sequentially fitted to the full data set, then from 1951:2010, 1951:2009, ... 1951:2001.	71
2.44 A systematic sample of 2000 points from a chain of length 1,000,000 from the joint posterior distribution for areas 2W and area 27.	72
2.45 Marginal distributions for the leading parameters based on a systematic sample of 2000 points from a chain of length 1,000,000 from the joint posterior distribution for areas 2W and area 27.	73
A.46 Equilibrium yield (a), recruits (b), biomass (c) and spawner per recruit (ϕ_e/ϕ_E) (d) versus instantaneous fishing mortality F_e for two different values of the recruitment compensation ratio ($\kappa = 12$ solid lines, $\kappa = 4$ dashed lines). Vertical lines in each panel correspond to F _{MSY} and horizontal lines correspond to various reference points that would achieve MSY.	80
A.47 Example of a natural cubic spline interpolation for estimating selectivity coefficients. In <i>iSCAM</i> the user specifies the number of nodes (circles) to estimate; then age-specific selectivity coefficients are interpolated using a natural cubic spline.	85
A.48 Example of a time-varying cubic spline (left) and bicubic spline (right) interpolation for selectivity. The panel on the left contains 165 estimated selectivity parameters and the bicubic interpolation estimates 85 selectivity parameters, or 5 age nodes and 17 year nodes. There are 495 actual nodes (selectivity parameters) being interpolated.	86
A.49 An example of the prior distributions used for $\ln(R_o)$, h , $\ln(M)$, $\ln(\bar{R})$, ρ , ϑ . The actual values used for the SOG herring assessment can be found in the control file in the appendix.	91

C.1 Distribution of the log of the simulated spawn index q estimates, overlaid with a normal distribution based on the mean and standard deviation of the simulated values.	109
---	-----

List of Tables

1.1	A comparison of key parameters from $i\text{SCA}_M$ and the HCAM model	10
1.2	Summary statistics for alternative structural assumptions about the Strait of Georgia herring assessment from 1951 to 2010. Definitions are No. is the number of estimated parameters, f the objective function value, B_0 unfished spawning biomass, h steepness, \bar{M} is the average natural mortality rate, B_{MSY} the biomass at maximum sustainable yield, q survey scalers for pre and post 1988.	13
2.1	Summary of maximum likelihood estimates for each of the five major stock areas. No. is the total number of estimated parameters, F_{MSY} the average instantaneous fishing rate to achieve the maximum sustainable yield (MSY), B_0 is the unfished spawning biomass, B_{MSY} is the spawning biomass that achieves maximum sustainable yield, B_t is the spawning biomass at the end of the 2011 fishing season, and B_t/B_0 is the spawning depletion level at the end of the 2011 fishing season.	42
2.2	Maximum likelihood estimates of gillnet selectivity parameters, where μ_a is the age-at-50% vulnerability, σ_a is the standard deviation in selectivity, and $\lambda^{(a)}$ is the coefficient that describes the influence of growth on selectivity ($\lambda^{(a)}=0$ implies no effect, $\lambda^{(a)} > 0$ implies a positive effect).	49
2.3	Estimated spawning stock biomass, age-4+ biomass and pre-fishery biomass for poor average and good recruitment, old cutoffs, and available harvest based on median values from the joint posterior distribution.	60
2.4	Estimated spawning stock biomass, age-4+ biomass and pre-fishery biomass for poor average and good recruitment, new cutoffs (based on median value of $0.25B_0$ estimated within the $i\text{SCA}_M$ model), and available harvest based on the median values from the joint posterior distribution.	61
2.5	Summary of maximum likelihood estimates for the two minor stock areas. No. is the total number of estimated parameters, F_{MSY} the average instantaneous fishing rate to achieve the maximum sustainable yield (MSY), B_0 is the unfished spawning biomass, B_{MSY} is the spawning biomass that achieves maximum sustainable yield, B_t is the spawning biomass at the end of the 2011 fishing season, and B_t/B_0 is the spawning depletion level at the end of the 2011 fishing season.	69
2.6	Estimated spawning stock biomass, age-4+ biomass and pre-fishery biomass for poor average and good recruitment, cutoffs, and available harvest based on median values of the joint posterior distribution for the two minor areas. All units are in tonnes.	70
A-1	Steady-state age-structured model assuming unequal vulnerability-at-age, age-specific natural mortality, age-specific fecundity and Beverton-Holt type recruitment.	79
A-2	Partial derivatives, based on components in Table A-1, required for the numerical calculation of F_{MSY} using (A.1).	81
A-3	Statistical catch-age model using the Baranov catch equation and C^* and F^* as leading parameters.	82
A-4	An incomplete list of symbols, constants and description for variables used in $i\text{SCA}_M$	83
C-1	Factors affecting the q prior and their assumed distributions.	108
C-2	Estimated means and standard deviations for the simulated q prior and natural log of the q prior.	109
C-3	Summary of west coast North America herring egg loss literature.	110

C-4	Estimates of the instantaneous daily egg loss rate (Z) from herring egg loss studies conducted in the Pacific Northwest. The Z estimates for the Haegele and Schweigert (1989, 1991) studies were calculated from their reported egg loss rates over the study period.	111
C-5	Criteria for selecting herring spawn survey data records for estimating days between spawning and surveys. The "number of records" is the records retained after each successive selection criterion.	111
C-6	Average number of days between spawn deposition and spawn survey by stock assessment region and year.	112
D-1	Observed catch by gear type and year for each stock.	114
D-2	Abundance for each survey by year for each stock.	116

Part I

Moving towards a sustainable fisheries framework for Pacific herring: data, models and alternative assumptions

1.1 Introduction

There are four major objectives of this paper: (1) to describe in detail an alternative integrated statistical catch-age model (iSCAM), (2) examine parameter estimation performance using iSCAM, (3) perform a side-by-side comparison of the previous HCAM and iSCAM on the five major herring stocks, and (4) explore alternative assumptions about selectivity, catchability, and natural mortality using iSCAM. The most recent assessment of BC herring stocks was conducted in 2010 using the Herring Catch Age Model (HCAMv2) which is documented in [Cleary and Schweigert \(2010\)](#). Furthermore, a review sponsored by the Herring Research and Conservation Society (HRCS) was conducted June 17-18, 2010 in Nanaimo, BC where an expert panel addressed specific questions about the current implementation of the HCAMv2 model and suggested recommendations for each of the questions. This paper also attempts to address some of the points brought up in the review.

BC herring are currently managed as five major stocks and 2 minor stocks (Figure 1.1). Annual catch advice for each of these areas is based on current estimates of stock status, and a 20% exploitation rate if the stock is above the cutoff level for the five major stocks and a 10% exploitation rate for the two minor stocks. Cutoff levels for the five major stocks are based on $0.25B_o$, and estimates of unfished biomass were established first in 1985 ([Haist et al., 1986](#)). Estimates of B_o were updated most recently in 1996, and in last years HCAM assessment marginal posterior distributions for B_o were also presented but were not used to update cutoffs. These cutoffs are currently thought to be more conservative than the current default Limit Reference Point of $0.4B_{MSY}$ ([Fisheries and Oceans Canada, 2006](#)). However, estimates of B_o and MSY based reference points have not been examined for Pacific herring for some time. In this paper we also describe the methods for updating estimates of B_o and MSY based reference points using the iSCAM model framework. We also compare estimates of MSY based reference points for the Strait of Georgia herring under the previously mentioned alternative assumptions (see point (4) in the previous paragraph).

We do not provide a detailed description of HCAMv2 in this paper and we refer the reader to [Schweigert et al. \(2009\)](#) and [Cleary and Schweigert \(2010\)](#). We first begin with a description of the input data required and assumptions about the data, followed by a detailed description of the analytical methods and assumptions in iSCAM. We then present the analytical methods and assumptions for exploring alternative hypotheses about selectivity, catchability and natural mortality, followed by a description of the elements that make up the joint posterior distribution (i.e., likelihoods, priors, and penalties). Parameter estimating and quantifying uncertainty is carried out using AD Model Builder ([ADMB Project, 2009](#)). We then explore estimation performance in iSCAM using simulation experiments where the model is used to generate simulated observations with known parameter values, then estimate parameter, and repeat this exercise a number of times to evaluate bias and precision in parameter estimates. Finally, we present forecast of pre-fishery biomass and available harvest options using the cutoffs (e.g., reproduce Table 5 in [Cleary and Schweigert, 2010](#)) as well as available harvest options based on the Sustainable Fisheries Framework (i.e., [Fisheries and Oceans Canada, 2006](#)) for comparison.

1.2 Methods

1.2.1 Analytical methods

We present a new stock assessment platform for the assessment of BC Pacific herring. This platform is based on the general statistical catch age model first described by [Fournier and Archibald \(1982\)](#). The software platform used is called $iSCAM$, which stands for integrated Statistical Catch Age Model. The source code and documentation for $iSCAM$ is freely available from <https://sites.google.com/site/iscamproject/>, or from a subversion repository at <http://code.google.com/p/iscam-project/>. The subversion repository is more likely to be up to date; whereas, the project website has periodic updates with corresponding version numbers. Ideally, the results of this report could easily be repeated just by downloading the necessary software and using the data and control files presented in the appendix of this paper. A complete technical description of $iSCAM$ is provided in Appendix A.1 of this report.

In short, for each stock two input files are required for $iSCAM$: (1) a data file that contains the historical catch, survey, life-history and age-composition information, and (2) a control file that specifies initial pa-

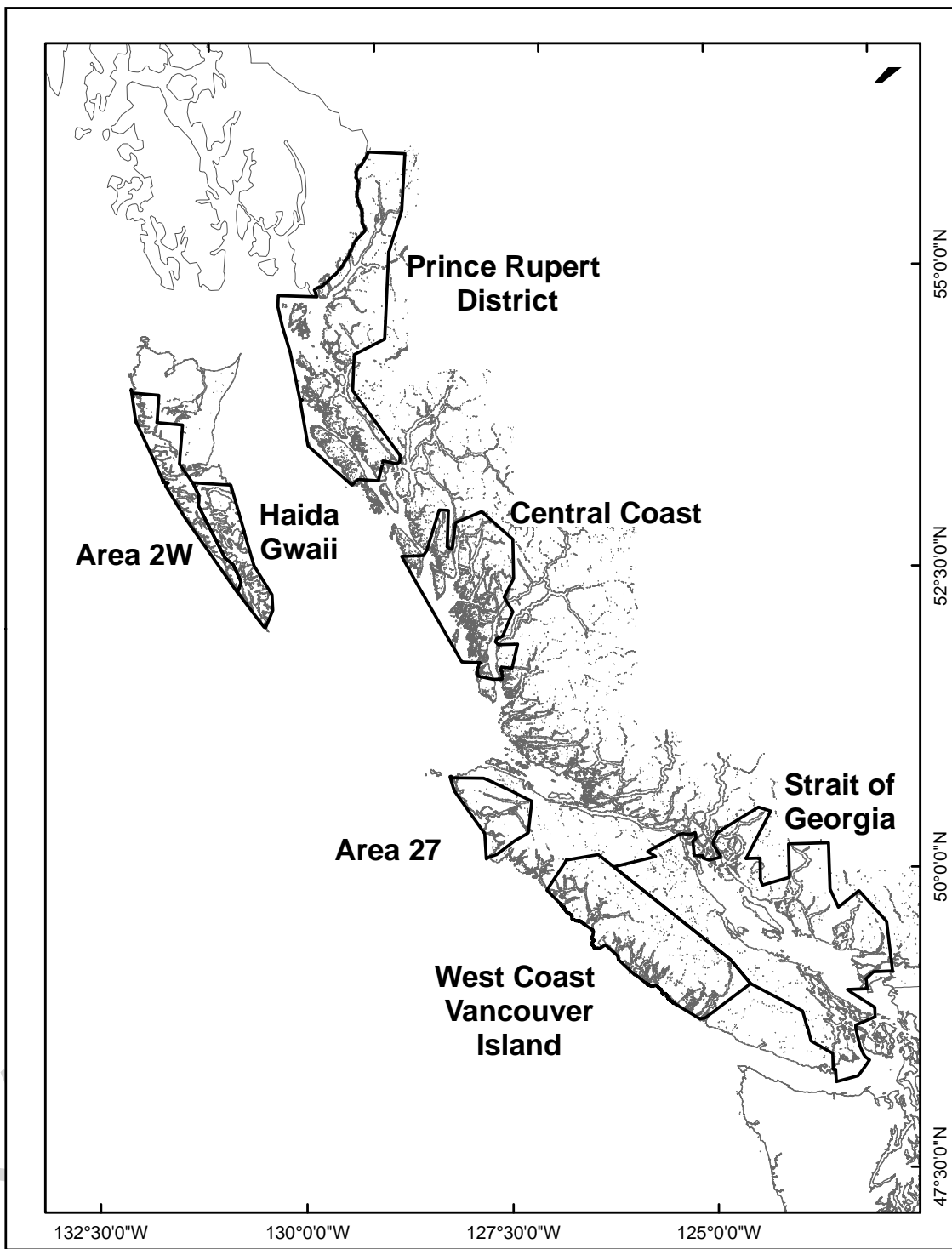


Figure 1.1: B.C. herring major stock areas: Haida Gwaii (HG or QCI 2E), Prince Rupert District (PRD), Central Coast (CC), Strait of Georgia (SOG), West Coast Vancouver Island (WCVI), and minor stock areas: Area 2W and Area 27.

rameter values, priors, selectivity options, and various other controls that specify options for time-varying natural mortality, type of recruitment model, etc. Each major and minor stock has its own data and control file and these are provided in Appendix B.2 such that these results can be verified by an independent reviewer using the *ⁱSCA_M* software.

Estimated model parameters includes the initial numbers-at-age, annual age-2 recruits, annual fishing mortality rates for each gear, selectivity parameters, natural mortality rates, parameters that describe the observation error and process error variance, and the unfished age-2 recruits and the steepness of the stock recruitment relationship. The total number of estimated parameters differs for each stock assessment region depending on the number of years of active fishing, assumptions about selectivity, and the number of assumed nodes in natural mortality rates.

1.2.2 Sustainable Fisheries Framework reference points

The general framework for developing a harvest strategy that is compliant with the precautionary approach is to divide the stock into three stock status zones; healthy, cautious, and critical zones (*Fisheries and Oceans Canada, 2006*). In this work we define these stock status thresholds as $0.4B_{MSY}$ and $0.8B_{MSY}$ when crossing from the critical-cautious zone and cautious-healthy zone, respectively. A critical component to this interpretation is the definition of B_{MSY} . In the case of a single fishing fleet using a fixed gear type, B_{MSY} is normally defined as the spawning stock biomass that would, on average, support the largest surplus yield. In the case of multiple fishing fleets, each using a different gear with different selectivities, the definition of B_{MSY} is more complex and is a function of allocation of mortality to each gear type. For example, if one gear harvest fish at a much younger age than the other gear, an increase in allocation to the gear that catches younger sexually immature fish will shift B_{MSY} upwards. Also, changes in selectivity over time (perhaps due to changes in growth) will also result in changing B_{MSY} . This precise definition for B_{MSY} increases the difficulty in estimating reference points when there are non-stationary parameters in the model (i.e., time-varying natural mortality rates, selectivity, growth in the case of Pacific herring).

Estimates of reference points are based on equilibrium calculations (see Appendix A.1), where the average natural mortality rate over the time period in question is used along with the most recent empirical estimates of weight-at-age and fecundity. The ratios of average catch over the past 20 years for each gear type, in each SAR, are used for allocation purposes.

1.2.3 Simulation testing

The purpose of conducting simulation testing is two fold: (1) to demonstrate that the model is capable of estimating model parameters given perfect information, and (2) to examine precision and bias in parameter estimates (and corresponding management quantities) in the presence of observation and process errors. To conduct simulation testing using *ⁱSCA_M*, the following command line option `-sim 1234` is used, where 1234 is a unique random number seed. There is also a special seed number `-sim 000` that generates data with no error. That is the simulation model is deterministic, the relative abundance data are directly proportional with 0 observation error, and the age-composition data replicates precisely the true vulnerable proportions-at-age. The simulation model is conditioned on the historical catch data specified in the data file, and the true parameter values used to simulate the data are those that are specified in the control file.

Estimation performance with perfect information

When simulating data with perfect information, there are a couple of things that need to be highlighted here when trying to estimate parameters from data that contain no error. First, the phases for the precision and variance partitioning parameters (ϑ and ρ) should be set to a negative number. There are no error in the data, therefore, there is no need to estimate the variance terms for the error distributions. Second, in the control file, the initial value for the precision (ϑ) should be set to an extremely large number (e.g., 4999.999, assuming the upper bound is 5000). The reason to set this number large is to minimize the slight bias due to the lognormal bias correction in the stock recruitment relationship (i.e., the $-0.5\tau^2$ term in T3.13, or T3.14). The control file used to simulate the fake data is provided in Appendix B.2.8.

Bias & precision with observation & process errors

To determine bias and precision of parameter estimates when the model is confronted with both observation error and process error, a series of Monte Carlo trials are performed and \log_2 ratios are used to measure the distribution of estimated parameters ($\hat{\theta}$) from the true value(θ). The log2 ratio

$$\log_2 \left(\frac{\hat{\theta}}{\theta} \right)$$

is zero when $\hat{\theta} = \theta$, is 1 when $2\hat{\theta} = \theta$, and is -1 when $0.5\hat{\theta} = \theta$. Box plots are used to examine the distribution of 50 trials where a unique random number seed is used for each trial. For the purposes of the simulation experiments only, we assume that the proportion of the total variance associated with observation error is known ($\rho = 0.25$) and estimate the total variance. The total precision is set to 2.50 which is equivalent to a total standard deviation of 0.4 (i.e., $1/2.50=0.4$). The control file used for the Monte Carlo procedures is provided in Appendix B.2.8, on page 106.

1.2.4 Comparison of HCAM with $i\text{SCAM}$

There are a number of different statistical assumptions and structural differences between the previous assessments using HCAM (Herring Catch Age Model) and $i\text{SCAM}$. Here we briefly summarize the differences and similarities between the two approaches, and we first attempt to formulate the $i\text{SCAM}$ model to be as similar as possible to the last implementation of HCAM used in Cleary and Schweigert (2010).

The objective function in the HCAM model has four major components to it: 1) the likelihood of the age composition data, 2) the likelihood of the commercial catch data, 3) the likelihood of the spawn data, and 4) the prior densities for estimated model parameters. In the following subsections are more detailed descriptions of how the $i\text{SCAM}$ model was set up to best approximate the HCAM implementation.

For the gill net fishery, HCAM implements a time varying selectivity scheme as a function of the average weight-at-age. A similar implementation was also developed in $i\text{SCAM}$. Alternative options for changes in selectivity will be investigated further later in this paper. For the remainder of this paper and especially in the Figures, the definitions for Gear is as follows: Gear 1 = winter purse seine fishery, Gear 2 = seine-roe fishery, Gear 3 = gill net fishery.

Age-composition data

There are two alternative likelihoods specified for the age-composition data in the HCAM model (see Table 8 in Appendix B in Cleary and Schweigert, 2010); a multinomial likelihood (T8.1), and a robust normal approximation to the multinomial(T8.2). In the $i\text{SCAM}$ model, a multivariate logistic negative log-likelihood for age-composition data is used (see equation A.10 above), with the intention of weighting these data based on the conditional maximum likelihood estimate of the variance. In addition, we require a minimum observed proportion of at least 2% in each age class. In years and ages where the observed proportion is less than 2% the consecutive ages are grouped into a single age-class which reduces the effective number of age-classes (this is some what analogous to a plus group).

Commercial catch data

In the HCAM assessment, commercial catch was assumed to be know with a high degree of certainty; observation errors were assumed lognormal, and the standard deviation specified in the code is fixed at 0.0707 (variance of 0.005) for all three periods. To implement these assumptions in $i\text{SCAM}$ we fix the assumed standard deviation for the catches in the last phase to 0.0707.

Spawn survey data

For the Strait of Georgia spawn survey, the assumed standard deviations in HCAM were specified at 0.35 and 0.3 for the pre and post 1988 periods. To carry out the same assumptions in $i\text{SCAM}$ the relative weights

for the pre and post 1988 survey data were fixed at 1.0 and 1.1666, respectively. In $i\text{SCA}_M$ the total error (or precision=1/variance) is estimated and partitioned into components of observation error (spawn survey residuals) and process error (recruitment deviations). To implement the same observation error and process errors in the $i\text{SCA}_M$ model (standard deviations of 0.35 and 0.8, respectively for observation errors and process errors in HCAM) the total precision was fixed at $\vartheta = 1/1.15$, and the proportion assigned to observation error was fixed at $\rho = 0.35/1.15$.

Specification of prior distributions

Starting with the prior density for natural mortality in HCAM, the average natural mortality rate is assumed to be normal with a mean of 0.45, and a standard deviation of 0.2 (see Table 3 in Cleary and Schweigert, 2010). The average natural mortality rate in $i\text{SCA}_M$ is estimated in the log scale; using a normal prior for the $\ln(M)$ is equivalent to a lognormal prior for M . A lognormal prior is appropriate for this parameter as natural mortality rates must be positive; however, there is no equivalent analytical transformation to the normal distribution that was used in the HCAM assessment. Here we have specified a normal prior for $\ln(M)$ with a log mean of $\ln(0.45) = -0.7985$ and a log standard deviation of 0.4 to approximate the variance specified in the normal distribution used in the previous HCAM assessment.

The base HCAM model also allows for a random walk in natural mortality rate implemented as:

$$M_t = \begin{cases} \psi, & t = t' \\ M_{t-1} \exp(d_t^M), & t > t' \end{cases}$$

where d_t^M are annual natural mortality deviations that are assumed to be normally distributed with a mean 0 and a standard deviation of 0.10, and ψ is an estimated initial value for natural mortality. The implementation of time varying natural mortality is similar in $i\text{SCA}_M$ in that it is a random walk process, but the components of the objective function include a prior for the initial value of M (as specified in the previous paragraph) and that the first differences between natural mortality deviations are normally distributed. Again, this structure allows natural mortality rates to drift away from central tendency and long-term changes in M could have profound effects on reference point calculations. For the comparison with the HCAM model, the first differences in annual natural mortality deviations were assumed to have a mean 0 and a standard deviation of 0.10.

Annual recruitment deviations in the HCAM implementation were assumed to be normally distributed on a log scale with a mean of zero and a standard deviation of 0.8. To set up an equivalent assumption in $i\text{SCA}_M$, the total variance (ϑ) and ratio of the total variance (ρ) that explains observation error in the spawn survey must be specified *a priori*. In the HCAM model the variance terms for the observation errors and process errors are not estimated and assumed to be known; the standard deviation for recruitment variation was set at 0.8 and the standard deviation for observation errors in the spawn survey was fixed at 0.35 and 0.3 for the pre and post 1988 data, respectively. These variance terms can be estimated within the $i\text{SCA}_M$ model, or treated as fixed constants; however, $i\text{SCA}_M$ estimates the total error and partitions the variance into observation (σ^2) and process error (τ^2) components. To make the same assumptions about the variance terms in $i\text{SCA}_M$ as those that were used in HCAM the following values were used $\vartheta = 1/1.15 = 0.8695652$, and $\rho = 0.3043478$, and the weights assigned to the post 1988 spawn data were set at 1.1666 and 1.0 for the pre 1988 spawn data.

The prior for steepness in the HCAM model was based on a lognormal distribution with a logmean of 0.67 and a standard deviation of 0.17. For the Beverton-Holt stock recruitment model, steepness must lie in the interval of $0.2 < h \leq 1.0$; a Beta distribution is an appropriate density function for this parameter. In the $i\text{SCA}_M$ implementation, a Beta distribution is used and to approximate the distribution used in the HCAM model, the shape and rate parameters specified are 10.0 and 4.925373, respectively. These values corresponds to a mean of 0.67 and a standard deviation of 0.1178 for the Beta prior.

The last informative prior that is not explicit in the table of priors in the HCAM model is the scaling parameter (q) for the spawn survey. The spawn survey data are broken into two separate time series, pre and post 1988 when the survey switch from a surface estimate to dive surveys for estimating total egg deposition. In the HCAM implementation, a very informative prior for q in the post 1988 period was used where the mean was fixed at $q = 1.0$ and not permitted to vary (i.e., $\sigma_q = 0$). The scaling parameter in the

first period was then freely estimated. Again, to emulate these assumptions in the $i\text{SCAM}$ implementation a normal prior for $\ln(q)$ with a mean =0 and a standard deviation of 0.001 was used for the post 1988 data and a uniform prior for the pre 1988 data.

1.3 Results

1.3.1 Simulation testing

Estimation performance with perfect information

Given perfect information about trends in relative abundance and age composition information, and a deterministic stock-recruitment relationship, $i\text{SCAM}$ was able to estimate 216 parameters without any substantial errors. Estimation performance is easily demonstrated by comparing estimates of spawning biomass and fishing mortality rates to the true values that were used to simulate the data. As shown in Figure 1.2 estimates of spawning biomass and fishing mortality rates were exactly the same as the true values. There is no measurable difference between the observed and predicted trends in the relative abundance information (Figs. 1.2cd).

Residuals between the observed and predicted age-composition data (not shown) were also extremely small and are easily summarized by the conditional maximum likelihood estimates of the residual variance $\hat{\tau}^2$ for the winter seine fishery $\hat{\tau}^2 = 2.49e - 03$, the seine roe fishery $\hat{\tau}^2 = 1.25e - 27$, and the gill net fishery $\hat{\tau}^2 = 1.24e - 27$.

This perfect fit to the data is used only to judge if the code is syntactically correct and to determine if it is capable of estimating model parameters exactly given perfect information. In the following section, observation errors and process errors are introduced to determine bias and precision in parameter estimates.

Bias & precision with observation & process errors

In the simulation experiments conducted with both observation error and process error included in the simulated data, there was no appreciable bias in the estimates of unfished biomass ($\ln(R_o)$) and the natural mortality rate ($\ln(M)$), the average recruitment ($\ln(\bar{R})$) and the initial recruitment ($\ln(\dot{R})$, Figure 1.3). There was, however, a very slight upward bias in the estimate of the steepness parameter for the Beverton-Holt stock recruitment relationship. Also, steepness was estimated with the least amount of precision. The estimability of steepness depends on many factors including the precision of the observations, but also the history of exploitation, the true value of steepness and the natural mortality rate (Conn et al., 2010).

Its not surprising to see a slight upward bias in h for these simulations because the true value of natural mortality was set quite high ($M = 0.45$) along with steepness ($h = 0.8$). These high values of M and h imply a very productive stock, and the spawning biomass would have to be driven to very low levels in order to generate data that would be informative about the underlying production function. Note that M and h are confounded because M is required to calculate the spawning stock biomass per recruit in unfished conditions. Furthermore, the simulated exploitation history involved a strong depletion signal between the 1950s and 1960's followed by very light exploitation from 1970 onward. On average the assumed parameter values for the simulation and the catch time series generated sufficient contrast to reliably estimate key model parameters without the use of informative priors.

The lower panel of Figure 1.3 shows the apparent precision and bias in the estimates of MSY based reference points. There is a very slight upward bias in the estimate of F_{MSY} associated with the slight upward bias in steepness. Estimates of B_{MSY} are also slightly biased in a downward direction, and MSY in a slight upward direction. Overall, MSY is the most precisely estimated and F_{MSY} is the least precisely estimated management variable.

1.3.2 Comparison of HCAM with $i\text{SCAM}$

Based on the description of the priors and model setup in Section 1.2.4 on page 5, a comparison of the spawning stock biomass between $i\text{SCAM}$ and HCAM were very similar (Figure 1.4a) for the Strait of Georgia stock. Between 1951 and 1969 the absolute difference in spawning biomass is minimal and post 1970

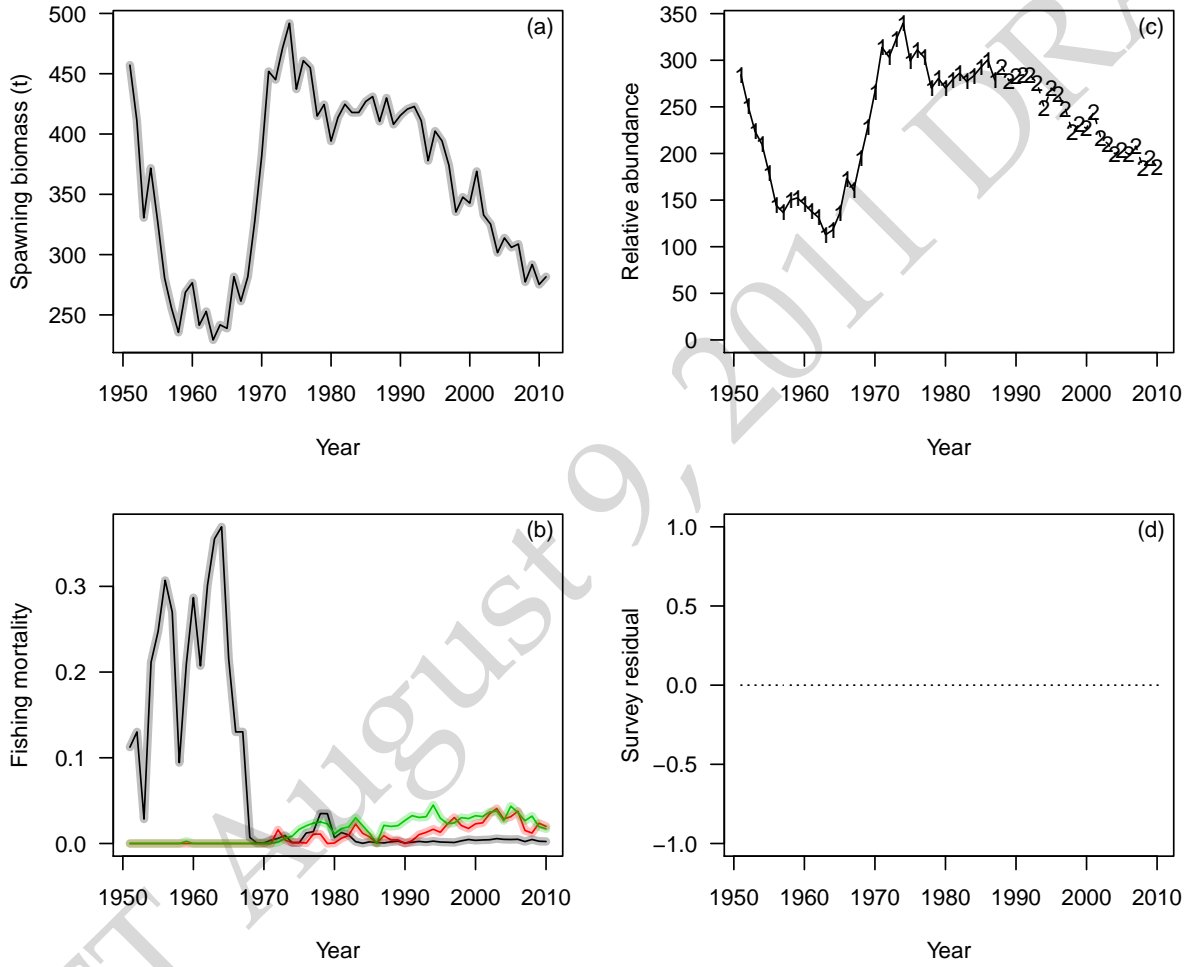


Figure 1.2: True (thin line) and estimated (thick shaded line) spawning biomass (a), fishing mortality rates by gear (b), observed and predicted relative abundance (c), and residuals between observed and predicted relative abundance (d) for the SOG herring simulation with perfect information and a deterministic stock-recruitment relationship.

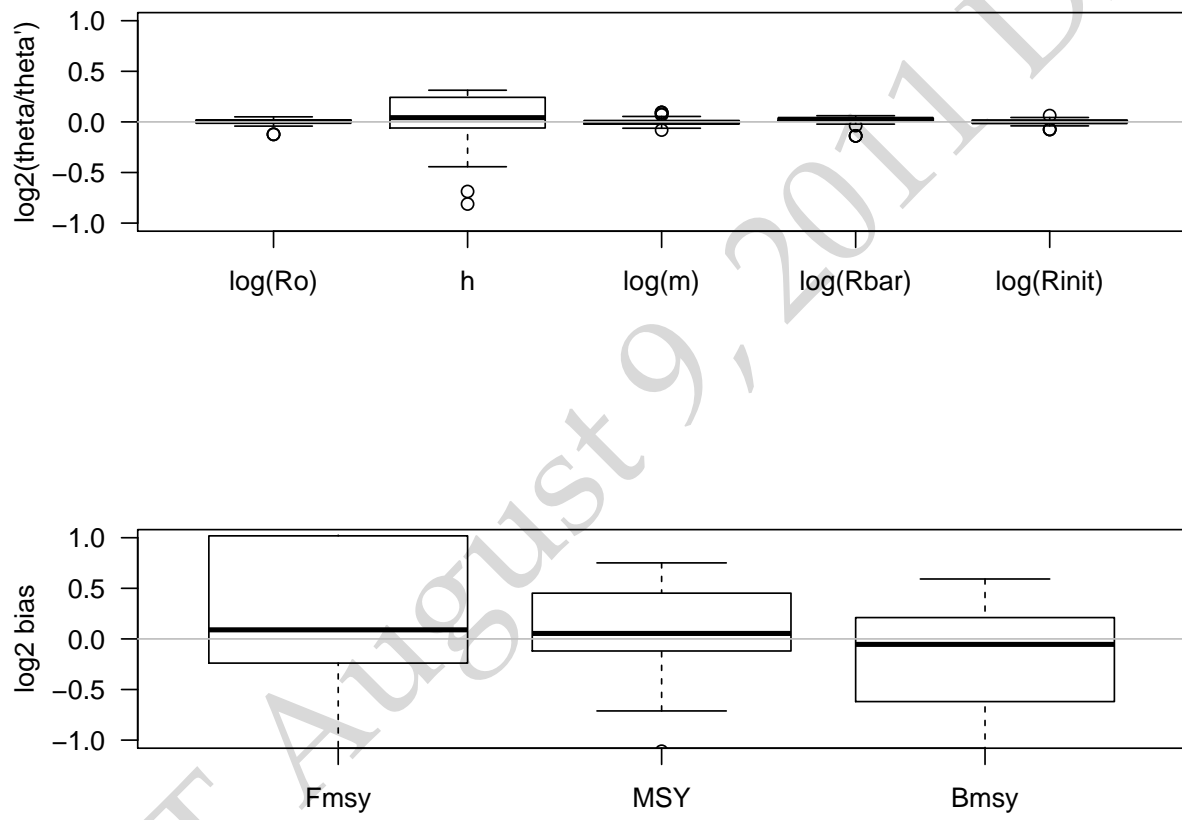


Figure 1.3: Estimates of precision and bias in key model parameters and MSY based reference points for 50 simulated data sets conditioned on the Strait of Georgia herring catch. The \log_2 ratio of estimated versus true value is plotted; values of 1 and -1 correspond to a twice or half the true value, respectively.

estimates of spawning biomass are slightly higher for the HCAM model. The only real difference between the two models during this period is a differences in the assumptions about the error structure for the age-composition data.

Estimates of spawning depletion are based on the post fishery spawning biomass relative to the estimated unfished spawning biomass (Figure 1.4b). The three coloured zones demarcate the critical zone, cautious zone, and healthy zones with transitions defined by $0.4B_{MSY}$ and $0.8B_{MSY}$, respectively.

Maximum likelihood estimates of key model parameters for both $iSCA_M$ and HCAM are summarized in Table 1.1. The $iSCA_M$ model tends to have a lower estimate of B_o in comparison to the HCAM model and a higher value of steepness (h). These two parameters are usually negatively correlated and it is expected that if B_o was higher in one model in comparison to the other, then h would normally be lower to compensate. Information to estimate B_o and h come from the apparent stock-recruitment data and the structural form of the stock recruitment relationship. In $iSCA_M$ annual recruitment is freely estimated and the residuals are based on the Beverton-Holt stock recruitment model and the estimates of spawning stock biomass. Similarly, in HCAM recruitment is a function of the spawning stock biomass and the Beverton-Holt model and the annual deviations are estimated and assumed to be normally distributed random variables.

Table 1.1: A comparison of key parameters from $iSCA_M$ and the HCAM model

Parameter	$iSCA_M$	HCAM
Unfished spawning biomass (B_o 1000 t)	114.492	190.817
Steepness (h)	0.786	0.683
Average natural mortality rate	0.535	0.334
Survey q for period 1	1.101	1.1105

Average natural mortality rate is higher in the $iSCA_M$ model (Table 1.1), and the survey q for the pre-1988 spawn survey data is nearly identical in the two models (Figure 1.4f). The more contemporary survey data were both forced to scale with $q = 1.0$. There is some pattern in the residuals for the overall fits to the survey data (Figure 1.4f), the model fails to predict the large increases in abundance in the late 1970s and early 2000s and the recent sharp decline in the mid 2000s. The assumed standard deviation for the survey errors was 0.35 and 0.3 for the pre and post 1988 survey data, the standard deviation of the residual errors in Figure 1.4d is 0.335 and 0.334, respectively.

Estimates of the components of total mortality for the comparison with the HCAM model are shown in Figure 1.4e. The fishing mortality rates for each gear represent the average fishing mortality rate over all age-classes, and the natural mortality rate is assumed to be age-independent. During the 1950s through to 1968, fishing mortality rates for Pacific herring in the Strait of Georgia were extremely high; this period was almost exclusively a winter purse-seine fishery where fish were taken for fishmeal (the reduction fishery). After the fishery reopened in the early 1970s fishing mortality rates were greatly reduced and targeted the spring spawning aggregations as the market was for herring roe.

Estimates of natural mortality are based on a random walk process, initially starting at a value of 0.401 in 1951 and declining to a very low value of 0.217 in 1959, then increasing to a maximum of 0.915 in 1969 (Figure 1.4e). Information to estimate natural mortality rates comes from the age-composition data, and assumptions about selectivity in the fishery. In this comparison, the $iSCA_M$ model assumes selectivity is invariant for the purse seine gears and is a function of weight-at-age for the gill net gear. Much of the residual variation in the age-composition is explained by variation in M and variation in age-2 recruits (see Figures 1.4c & d for age-2 recruitment and stock recruitment relationship). The HCAM model has a very similar trend in the estimates of natural mortality but the variability is much less than that of the $iSCA_M$ assessment. This is almost certainly due to the differences in the assumptions about the error structure in the age-composition data (or relative weights associated with the age-composition).

There is good correspondence between the observed and predicted catch, however, the residual patterns do not appear to be iid for each of the fleets (Fig. 1.5). Recall that the fit to the catch data is largely determined by an assumed variance for the observation errors in the reported catch ($\sigma_C^2 = 0.005$).

The fit to the spawn survey data in Strait of Georgia is nearly iid for the 1951:1987 time period. There is some pattern in the residuals post 1988 that appears to be in contradiction with other information (i.e., age-

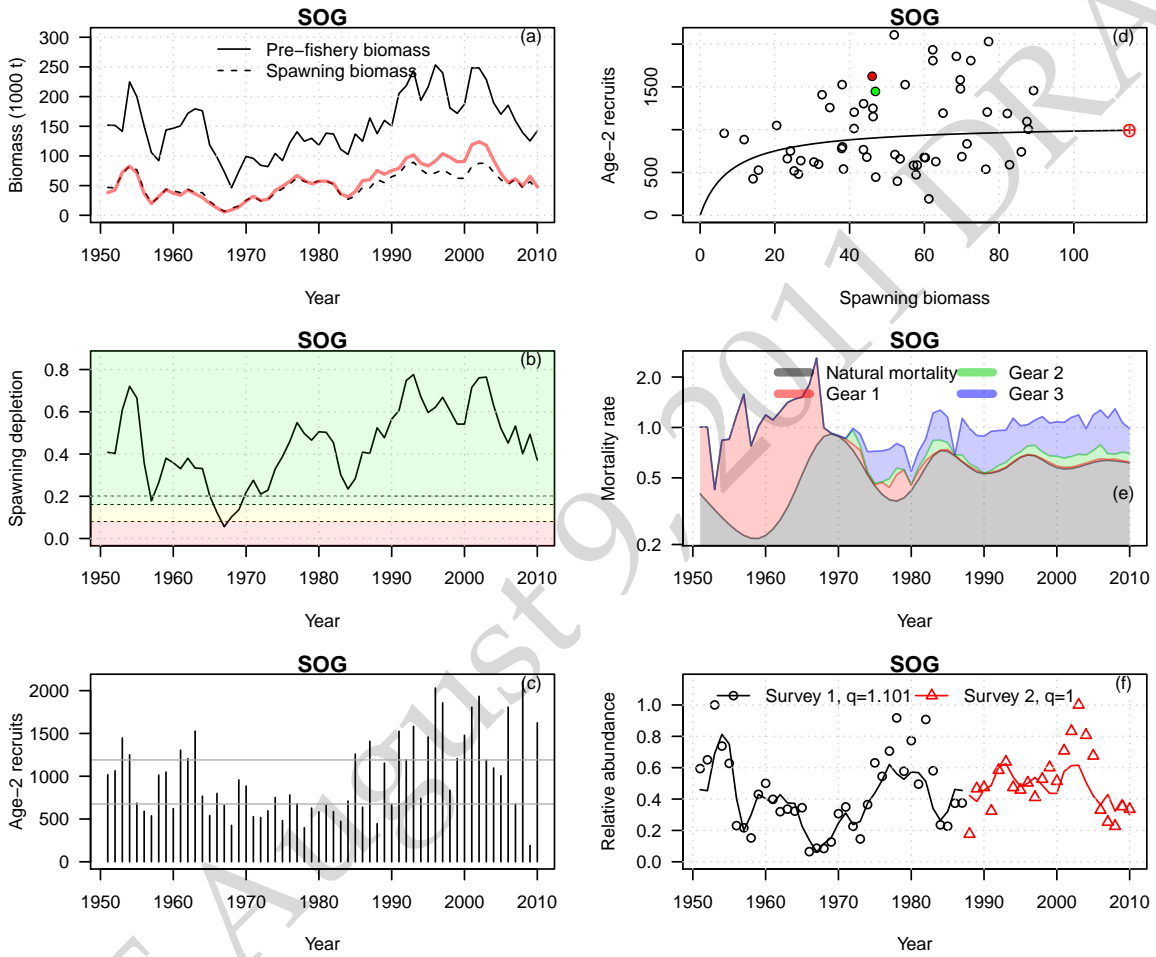


Figure 1.4: Maximum likelihood estimates of pre-fishery biomass (defined as the numbers-at-age times the mean weight-at-age at the start of the year) and post fishery spawning biomass in the Strait of Georgia (a), spawning biomass depletion (b), age-2 recruits (c), stock-recruitment relationship and unfished reference points (d), components of total mortality (log-scale, e), and observed (points) and predicted (lines) spawn survey data (f). These results are based on trying to configure the *iSCAM* model as similar as possible to the previous HCAM assessment; the red line in panel (a) is the MLE estimate of spawning biomass from HCAM.

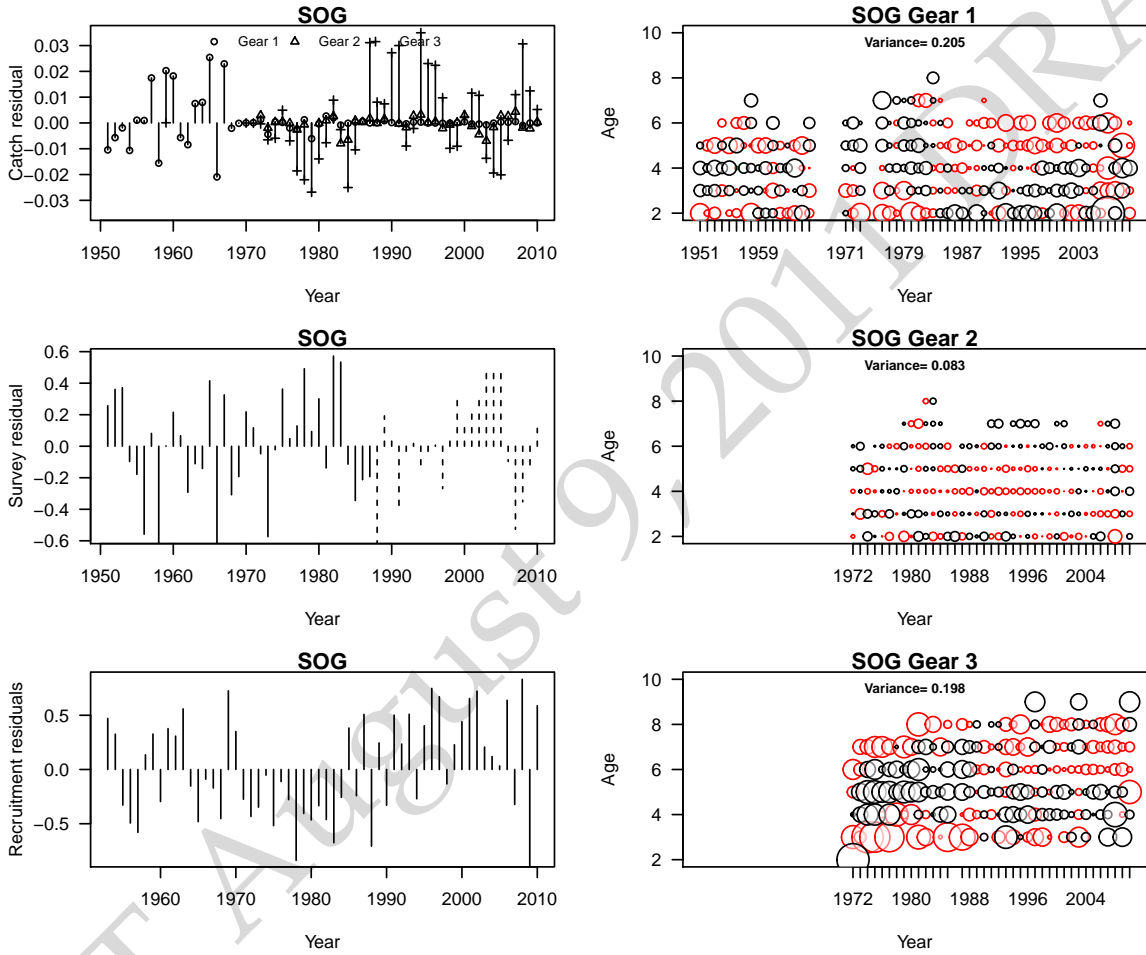


Figure 1.5: From top to bottom in the left column: the log residuals between observed and predicted catch for each gear, the residuals between the observed and predicted spawn survey index, and the annual deviations between age-2 recruitment and that predicted by the Beverton-Holt model and the estimated spawning stock biomass. Right column: residual patterns in the age-composition data (observed - predicted, where black is a positive residual) for each of the three commercial gears in the Strait of Georgia.

composition data and structural assumptions about selectivity) (Fig. 1.5). The pattern in the recruitment residuals for the Strait of Georgia suggest periods of below average-recruitment in the 1970s and early 1980s and above average recruitment starting in the early 1990s.

Fits to the age-composition data for the purse seine-roe fishery were best in comparison to the winter seine and gillnet fisheries. The conditional maximum likelihood estimates of the variance of the age-composition data are 0.205, 0.083, and 0.198 for the winter purse seine, seine-roe, and gill net fisheries, respectively. The smaller the standard deviation, the better correspondence between the observed and predicted age-composition data. Also the pattern of residuals does indicate some model mis-specification (e.g., the gillnet fishery in the Strait of Georgia).

1.3.3 Alternative assumptions about catchability, mortality & selectivity

Here we briefly explore the differences between relaxing the informative prior on catchability for the survey, reducing the number of natural mortality parameters being estimated and exploring alternative selectivity options to try and reduce the residual pattern in the gillnet fishery age-composition data. For the comparisons, we only examine the maximum likelihood fits to the data and the overall objective function value.

The following table presents a few summary statistics in the following section for easier comparison.

Table 1.2: Summary statistics for alternative structural assumptions about the Strait of Georgia herring assessment from 1951 to 2010. Definitions are No. is the number of estimated parameters, f the objective function value, B_o unfished spawning biomass, h steepness, M is the average natural mortality rate, B_{MSY} the biomass at maximum sustainable yield, q survey scalers for pre and post 1988.

Model	No.	f	B_o	h	M	B_{MSY}	q_1	q_2
Fixed q	279	-1165.77	114.93	0.786	0.53	23.114	1.01	1.0
Prior q	279	-1161.49	116.98	0.766	0.58	24.370	0.988	0.878
Fixed M	219	-1051.92	126.59	0.706	0.68	28.510	0.681	0.795
Gill net Selectivity	279	-1196.06	121.65	0.76	0.655	25.27	0.817	0.795

Impacts of informative priors on q 's

The implication of relaxing the informative prior on q for the contemporary spawn survey data was examined by using a less informative prior for the spawn survey q . The results shown in Fig. 1.6 is a comparison of the HCAM parameterized version of the model as shown in previous sections with a version where the prior on $\ln(q)$ was assumed normal ($\mu = 0, \sigma = 0.274$) for both the contemporary and surface survey data.

The net result of relaxing this prior on q is a slight increase in the global scaling (the spawn biomass increases by roughly 12%) in comparison to the fixed $q = 1$ scenario. There is no appreciable difference in the overall fits to the data (see objective function value in Table 1.2).

Implications of variable natural mortality rate M_t

In this next scenario we use the same prior for $\ln(q)$ but do not allow natural mortality rates to vary over time (i.e., fixed M). The natural mortality rate and q are confounded so it does not make sense to fix q and estimate M because the corresponding estimate of M would simply be conditional on the assumed value of q .

In the case where M is assumed to be time invariant, estimates of average M over the entire time series does increase slightly as well as the overall scaling of population size (Table 1.2). There are 60 fewer estimated parameters in this case but the overall fit to the data is slightly degraded (Fig 1.7, and see objective function values in Table 1.2).

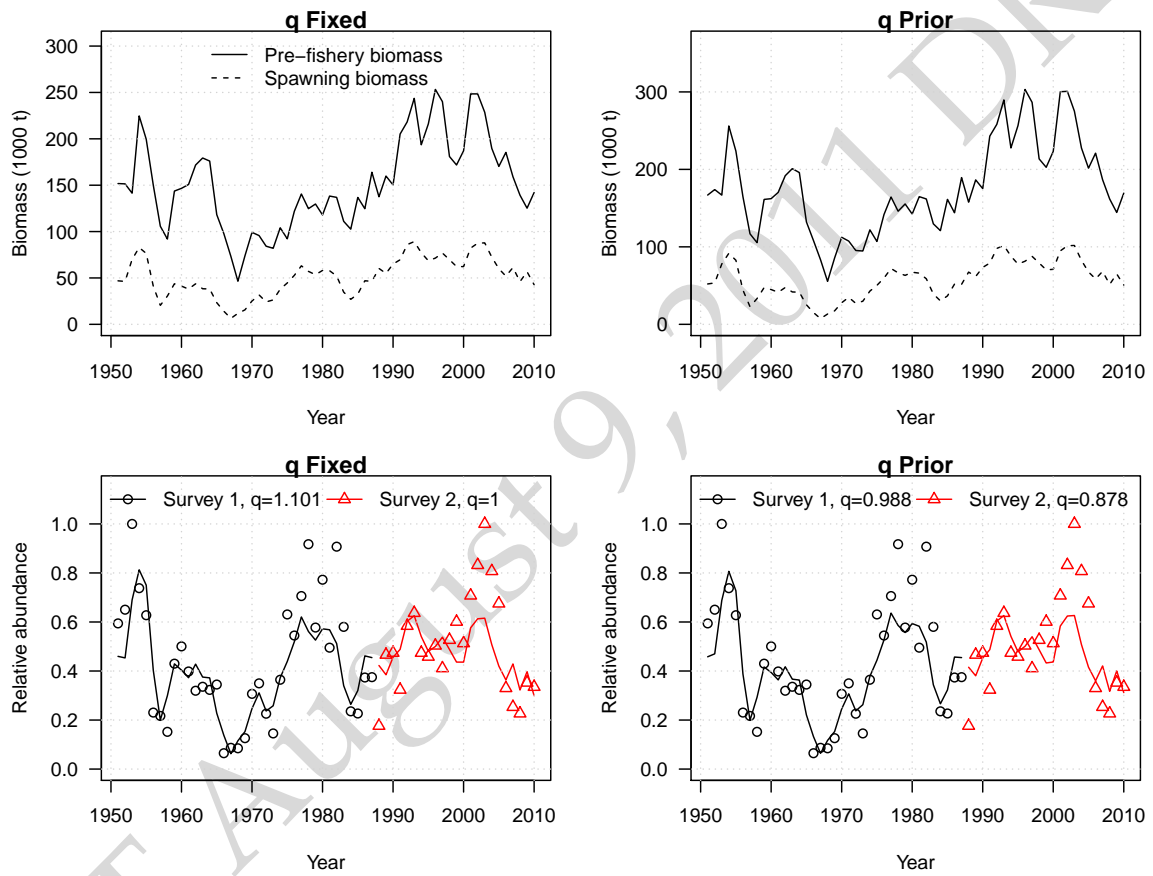


Figure 1.6: A comparison of the estimated biomass and spawning biomass and fits to the survey data when q is either fixed at 1 for Survey 2, or estimated using an informative prior with an expected mean of 0 and a log standard deviation of 0.274.

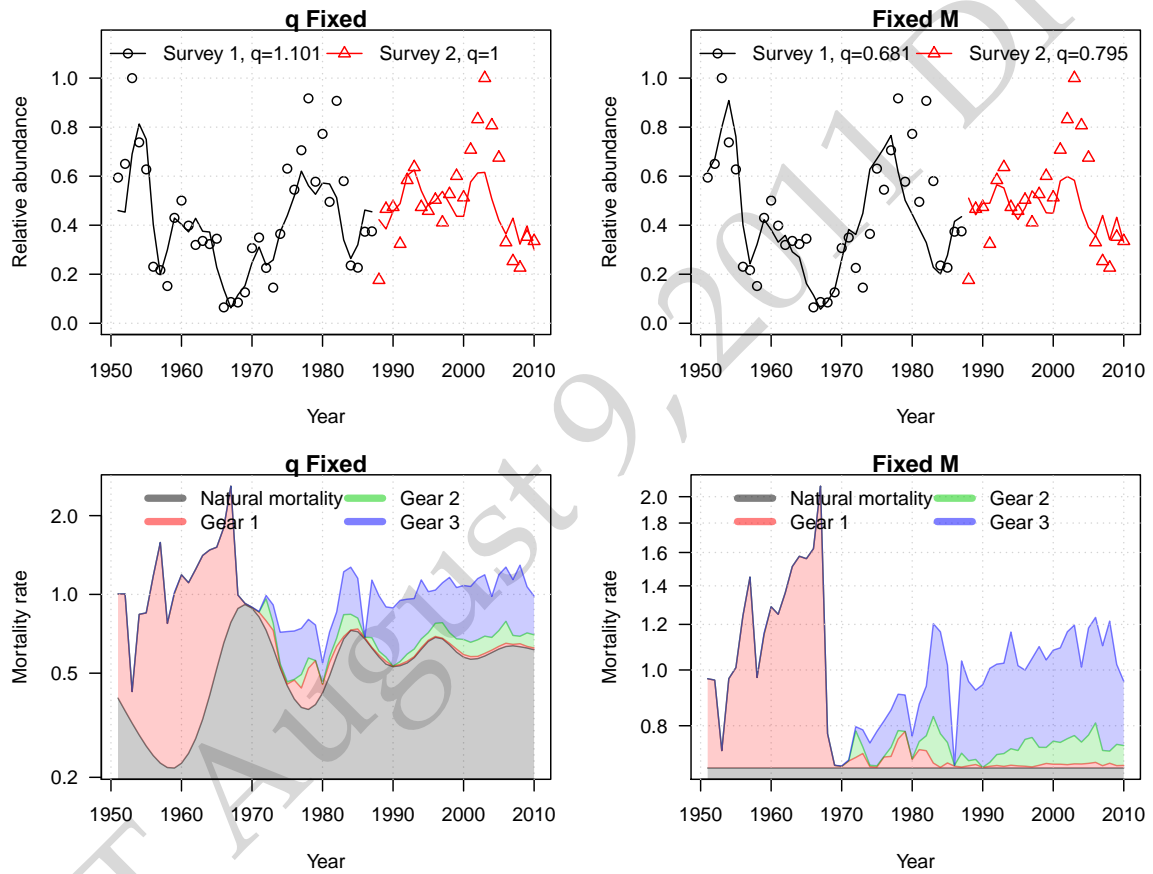


Figure 1.7: A comparison of fits to the survey data and estimated components of average mortality by year when M is allowed to vary via a random walk process or is estimated and assumed time invariant.

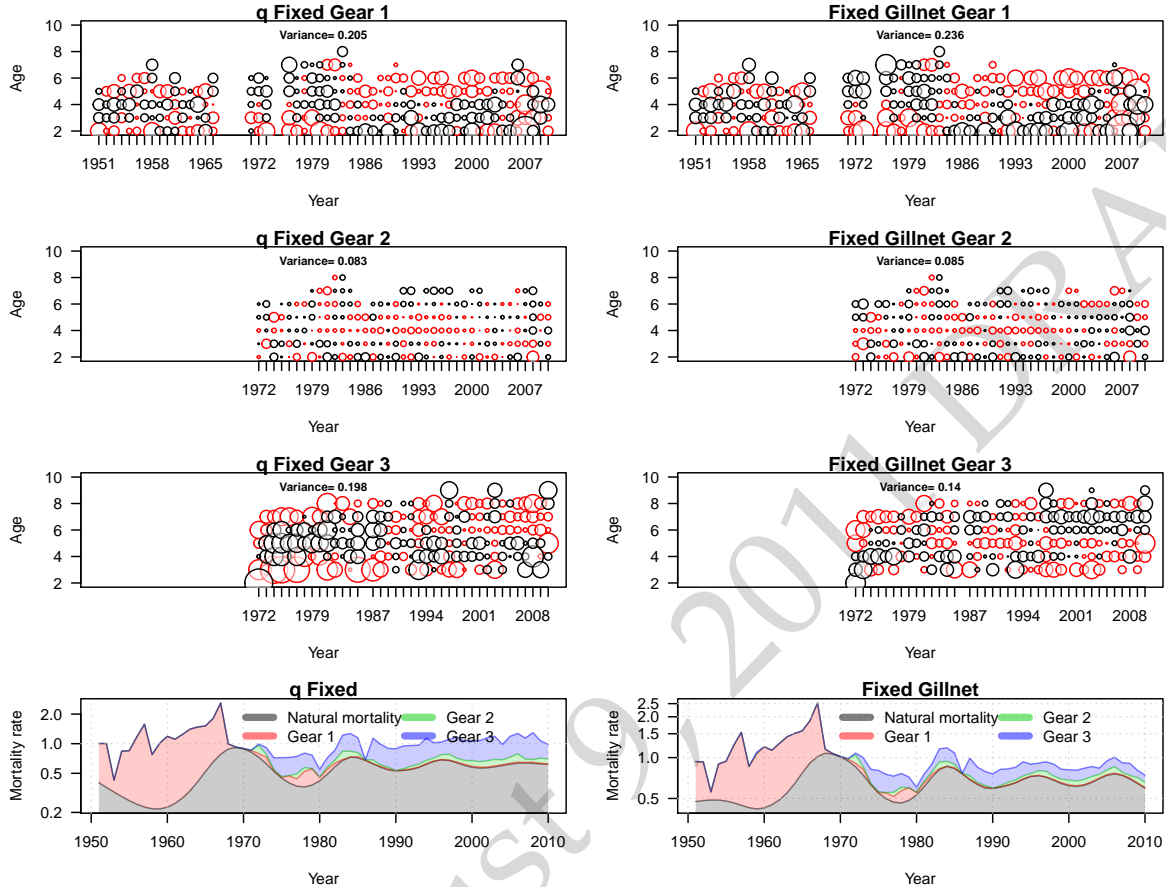


Figure 1.8: Residuals in the age-composition data when gill net selectivity is a function of mean weight-at-age (left column with q Fixed in each caption) and or is a logistic function of age and time invariant (right column with Fixed Gillnet in each caption).

Implications of variable selectivity in directed fisheries

Finally, we also explored the option of treating the gill net selectivity as time invariant and estimated two parameters that describe age-specific selectivity using a logistic curve. In this case we also allowed for a random walk process in natural mortality rates so the total number of estimated parameters remains the same.

Slightly better fits were obtained to the gill net fishery age-composition data with a constant selectivity, and the residual pattern also appears to improve under the assumption of constant selectivity (Fig. 1.8). There was also a slight degradation to the age composition data in the winter purse seine fishery (Gear 1), but residual patterns were nearly identical in both the seine fisheries (Fig. 1.8). The same number of model parameters were estimated and there was a slight improvement in the overall objective function with constant selectivity (Table 1.2). However, there is much more variability in the estimates of natural mortality rates when the gill net selectivity is assumed constant.

1.3.4 Preliminary assessments for all other areas

For the five major stock assessment regions there was very good correspondence between the estimated spawning stock biomass between the HCAM and new $i\text{SCA}_M$ models (Fig. 1.9). The control file used for

each of the assessment regions was the same as that used for the Strait of Georgia. No additional changes were required (i.e., each SAR had the same initial starting parameter values etc.).

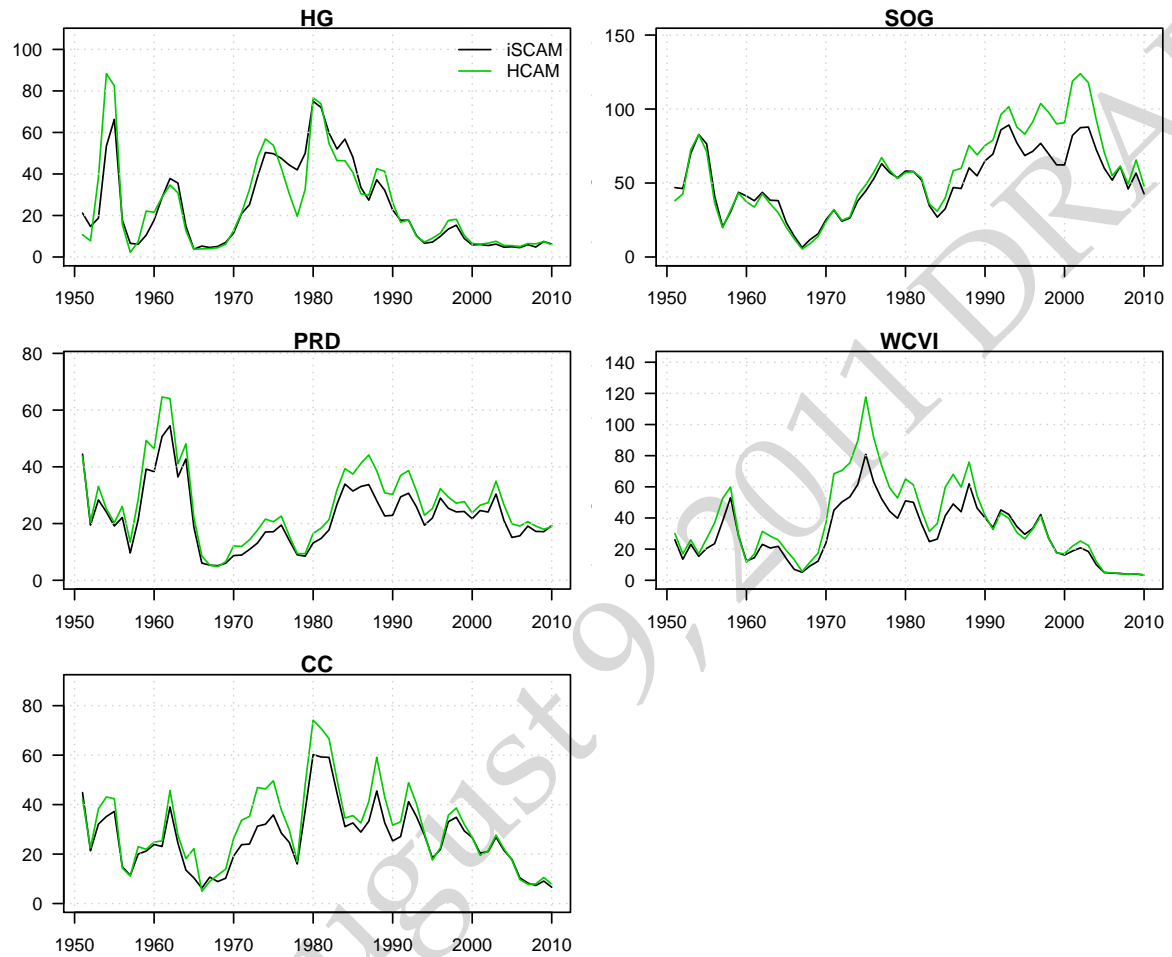


Figure 1.9: A comparison of estimated spawning stock biomass between HCAM and $iSCAM$ for the five major stock assessment regions using data from 1951 to 2010 and setting up $iSCAM$ similar to HCAM.

Part II

Stock Assessment and Management Advice for the British Columbia Pacific Herring Stocks: 2011 Assessment and 2012 Forecasts

2.4 Introduction

The objectives of this section of the report are: (1) present the data used in the 2011 assessment, (2) provide a summary overview of the integrated statistical catch-age model (hereafter, $iSCA_M$), (3) present the 2011 stock assessment and forecast for 2012, and (4) describe in detail the decision table used to provide advice to fisheries management.

BC herring are currently managed as five major stocks and 2 minor stocks (Figure 1.1). Annual catch advice for each of these areas is based on current estimates of stock status, and a 20% exploitation rate if the stock is above the cutoff level for the five major stocks and a 10% exploitation rate for the two minor stocks. Cutoff levels for the five major stocks historically were based on the 1996 estimate of $0.25B_o$. These cutoffs are currently thought to be more conservative than the suggested default Limit Reference Point of $0.4B_{MSY}$ (*Fisheries and Oceans Canada, 2006*). Alternative cutoffs based on updated estimates of B_o are also provided in this document.

This years assessment is based on a new model, $iSCA_M$, where alternative assumptions about survey q , and the form of the error distribution for the age-composition data are the major differences in comparison to the 2010 assessment using HCAM.

2.5 BC Herring Stocks

The geographic boundaries used to delineate the B.C. herring stock assessment regions have remained consistent since 1993. Boundaries and locations of the major stock and minor stock areas are identified in Figure 1.1. The Haida Gwaii (HG) or Queen Charlotte Islands (QCI2E) stock assessment region includes most of Statistical Area 2E, spanning from Cumshewa Inlet in the north to Louscoone Inlet in the south. The Prince Rupert District (PRD) stock assessment region encompasses Statistical Areas 03 to 05. The Central Coast (CC) assessment region separates the major migratory stocks from the minor spawning populations in the mainland inlets. The Central Coast assessment region includes Statistical Area 07 plus Kitas Bay in Area 06, Kwakshua Channel in Section 085 and Fitz Hugh Sound in Section 086. The Strait of Georgia (SOG) stock assessment region includes all of Statistical Areas 14 to 19, 28, and 29 (excluding Section 293), Deepwater Bay and Okisollo Channel, both in Section 132, and Section 135. The west coast of Vancouver Island (WCVI) assessment region encompasses Statistical Areas 23 to 25. The minor stocks include all of Area 27 and Area 2W (excluding Louscoone Inlet in Section 006). Current geographic stock boundaries are outlined in *Midgley (2003)*, although note that SOG sections 280 and 291 do not appear as they were added in 2006.

2.6 Methods

2.6.1 Input data & assumptions

Catch data

For each of the statistical areas, the required input data for $iSCA_M$ consists of a catch time series for each of the fishing fleets. For the BC herring fishery, the annual total removals has been partitioned into three distinct fishing fleets (or fishing periods, see Figure 2.1). The first fleet is a winter seine fishery that has been in operation since the start of the assessment in 1951, the second is a seine-roe fishery that commenced in 1972 in the Strait of Georgia, and the third fleet is a gillnet fishery that targets females on the spawning grounds. The model is fit to the catch time series information and assumes measurement errors are lognormal, independent and identically distributed. The assumed standard deviation in the catch observations must be specified in the control file and it is assumed that measurement errors in the catch is the same for all fishing periods. The units of the catch are given in 1000s of metric tons.

In addition to the commercial catch, removals from fisheries independent surveys must also be specified in $iSCA_M$. Two additional fleets are specified to represent the spawn survey, where the spawn survey is broken into two distinct time periods pre-1988 and post-1988, the year when the survey switched from surface surveys to dive surveys. This partitioning of the data is done for two reasons: (1) to allow for

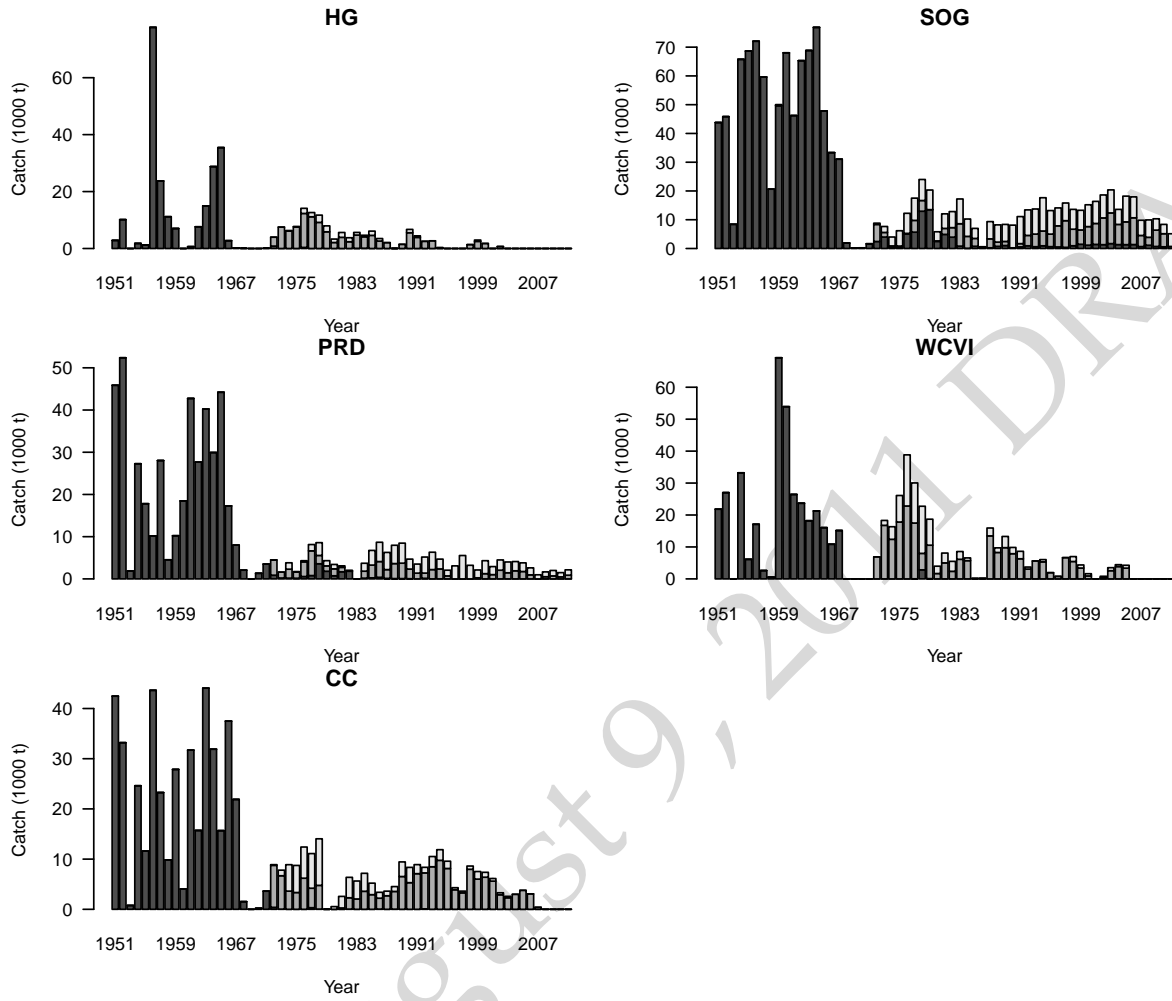


Figure 2.1: Historical catch of herring in the five major stock areas between 1951 and 2011 for the winter purse seine fishery (dark bars), seine-roe fishery (grey bars), and gill net fishery (light grey bars). Units of catch are in thousands of metric tons.

different catchability coefficients to be specified for the early and late periods, and to allow for more weight to be placed on the contemporary data due to improved precision in the estimates of egg layers.

In the case where the test fishery data has been separated from the seine roe fishery, an additional fleet is specified in the data file and fishing mortality rates for the test fishery are also estimated in years when the catch is greater than 0.

Relative abundance data

Herring spawn surveys have been conducted throughout the B.C. coast beginning in the 1930s. Prior to 1988, spawn surveys were conducted from the surface either by walking the beach at low tide or using a drag from a skiff to estimate the shoreline length and width of spawn. Egg layers were sampled visually and are used to calculate egg densities following the methods of Schweigert (2001). Beginning in 1988, herring spawn surveys using SCUBA methods were introduced and were implemented coastwide within a couple of years initially being conducted by DFO staff and eventually through contract divers hired through the test fishing program. Prior to the 2006 Larocque ruling, the test fishing program was funded through

an allocation of fish by industry. In years since the 2006 Larocque ruling, the availability of resources to conduct dive surveys in all areas has been reduced. For the 2010 survey, dive surveys were conducted in all major and minor assessment regions, with the exception of Area 2W where snorkelling and surface survey methods were also used. As in earlier years, a few minor spawning beds outside the main assessment areas were surveyed by SCUBA or surface methods where resources permitted.

The locations of the spawning beds for the five major and two minor stock areas are shown in Figure 2.2. Egg density estimates are used to calculate a fishery-independent index of herring spawning biomass, referred to as the spawn survey index hereafter (Schweigert et al., 2001).

The spawn survey is conducted after the fisheries in the area have been completed; therefore, it is assumed that all the mortality for the year has occurred just prior to commencing the spawning survey. The fisheries independent survey estimates egg density and total spawn area, and from this information the total female spawning biomass can be estimated assuming the 200 eggs per gram of female or 100 eggs per gram of mature individuals (Hay, 1985; Hardwick, 1973). The assumed selectivity for the spawn survey is fixed to the maturity schedule for herring.

Biological samples

Biological samples are collected from both commercial catch and from the test fishery program. Commencing in 1975, test fishery charters supplemented biological samples in areas with poor sampling that was not representative of the stock in that area (i.e., fishing solely on spawning aggregations), or in closed areas. Prior to 2006, test fishing charters were funded through an allocation of fish to the test program; the program is now fully funded by DFO. Through a contract with DFO, the Herring Conservation and Research Society (HCRS) sub-contracts a number of vessels to collect biological samples. Industry also conducts pre-season test sets for roe-quality testing in open areas and supplementary biological samples are provided as part of this program. The following data are collected for all biological samples: fish length, weight, sex, and maturity. Subsequently these sources of data are combined and information on weight-at-age and proportion-at-age become input data for the stock assessment model.

During the 2010/2011 season a total of XXX biological samples were collected, of which XXX were collected from the test fishery, XXX were collected from the roe fishery, XXX from the food & bait fishery, XXX from Spawn on Kelp (SOK) operations, and XXX from the summer trawl research survey (Table ??). Note that the definition of a sample is roughly 100 individual fish. A summary of biological samples collected from commercial and pre-fishery charters from 2002/03–2010/11 is presented in Table ??).

Age composition data

Ageing data, through the reading of fish scales, are collected from the biological samples taken from the commercial fisheries and test fishery charters. Age composition data is used to determine proportions-at-age and is an essential source of input data to the herring stock assessment model.

Catch-at-age data from the winter seine fishery (top panels of Figures 2.4-2.8) tend to consist of younger fish in comparison to the age composition data from the seine-roe and gillnet fleets post 1970. The shaded polygons in Figures 2.4-2.8 approximates the 95% distribution of ages in the catch. Roughly 90% of the fish landed in the winter seine fishery were younger than age-7, and younger than age-6 in recent years. In both the winter seine and seine-roe fishery age-2 fish are frequently landed; whereas, age-2 fish are rarely landed in the gill net fishery, and fish do not appear to fully recruit to the gear until at least 4-5 years of age. The mean age of the catch appears to be increasing between 2008 and 2010 in both the gill net and winter seine fishery, and there is no obvious trend in the seine roe fishery. There is however a declining trend in the older ages caught in the seine-roe fishery since 2006 (erosion of age-structure).

Mean weight-at-age data

From the mid-1970s until the present, there has been a measurable decline in weight-at-age for all ages in all major stock areas (Figure 2.9). Samples collected during the 2009/10 fishing year indicate weights-at-age that are among the lowest on record. This declining weight-at-age may be attributed to any number of

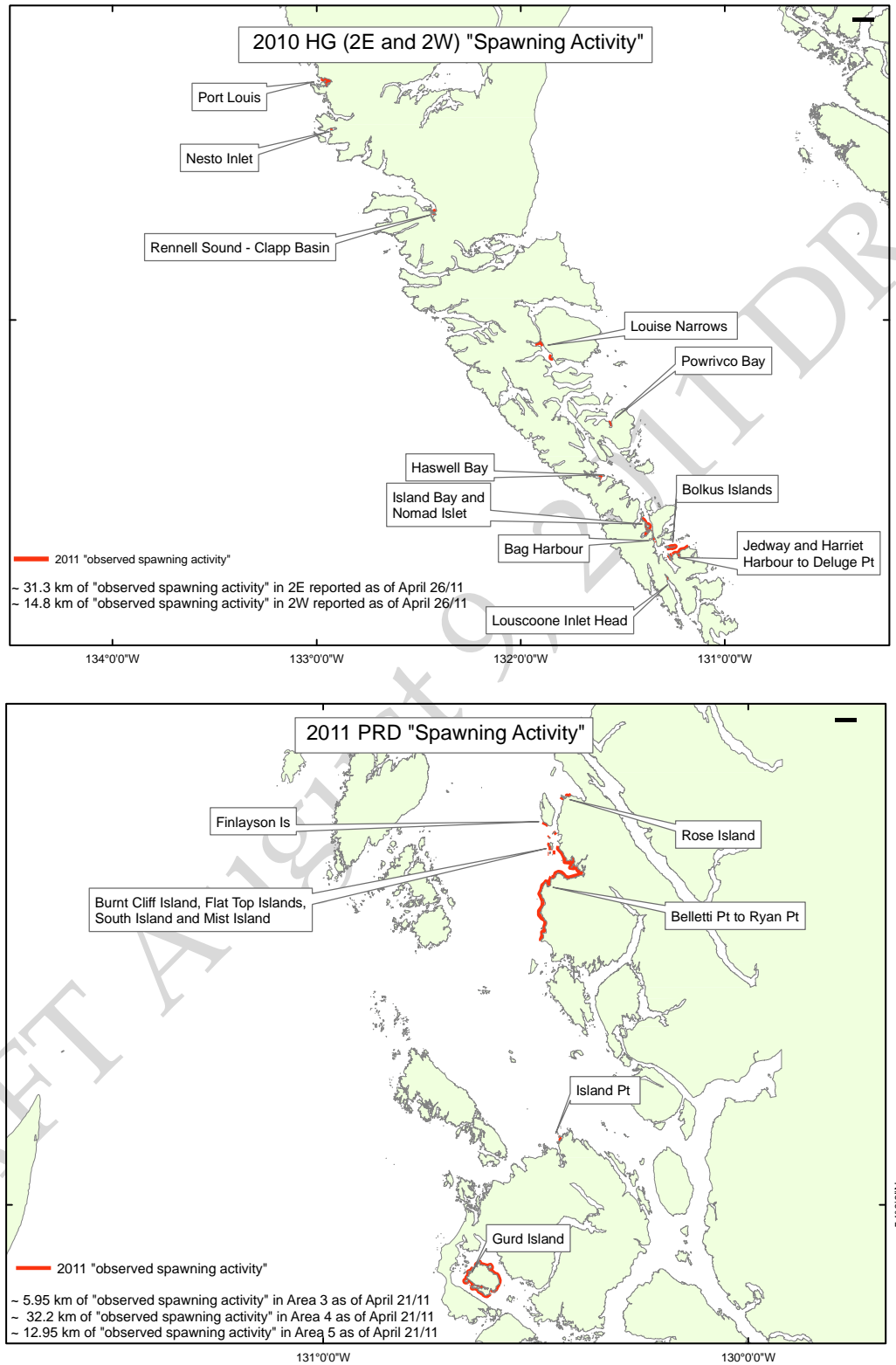


Figure 2.2: Preliminary Spawning activity for Haida Gwaii (top panel) and Prince Rupert District (bottom) in 2011.

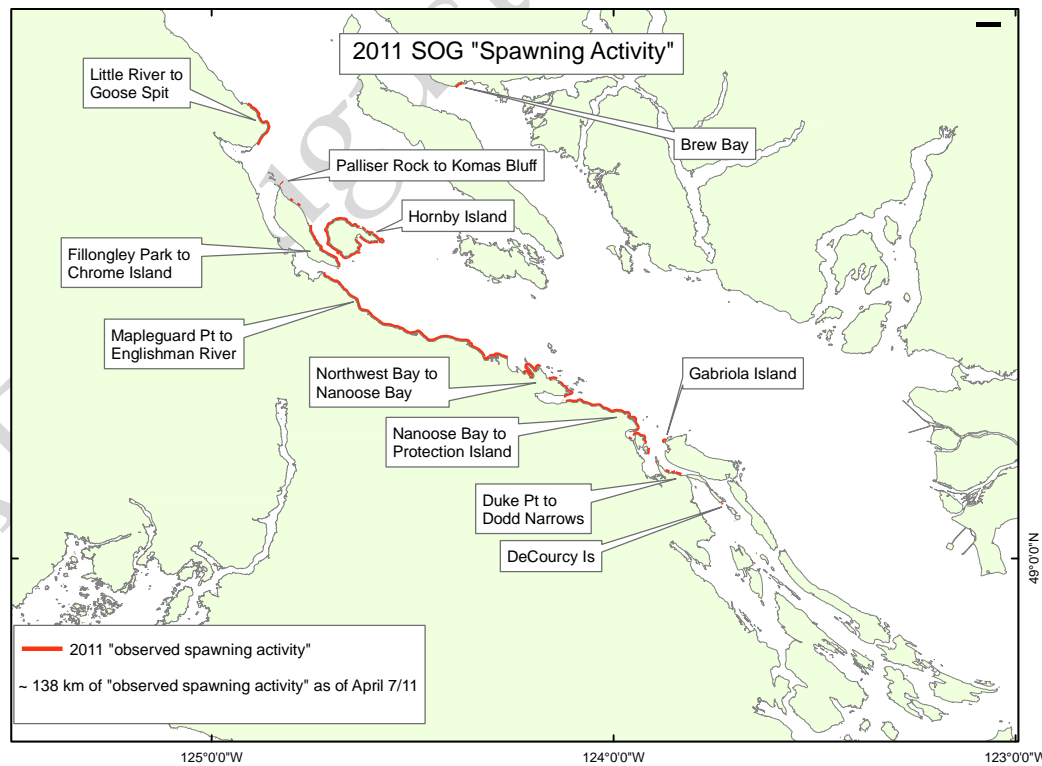
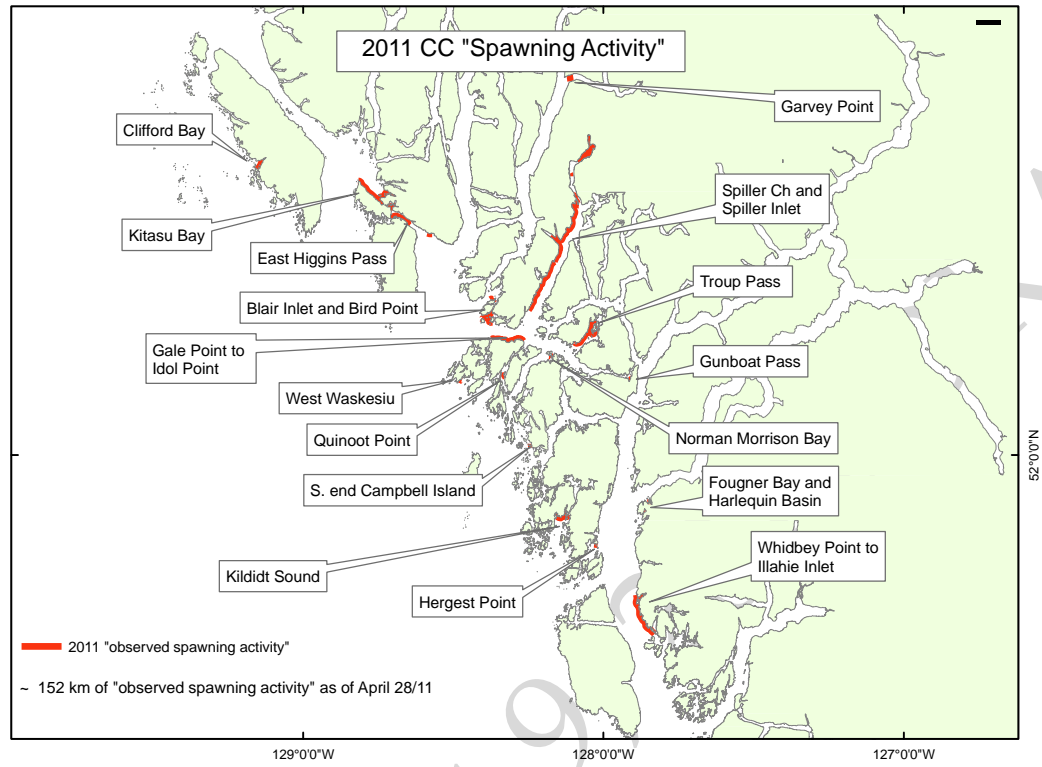


Figure 2.2: Preliminary Spawning activity for Central Coast (top panel) and Strait of Georgia (bottom) in 2011.

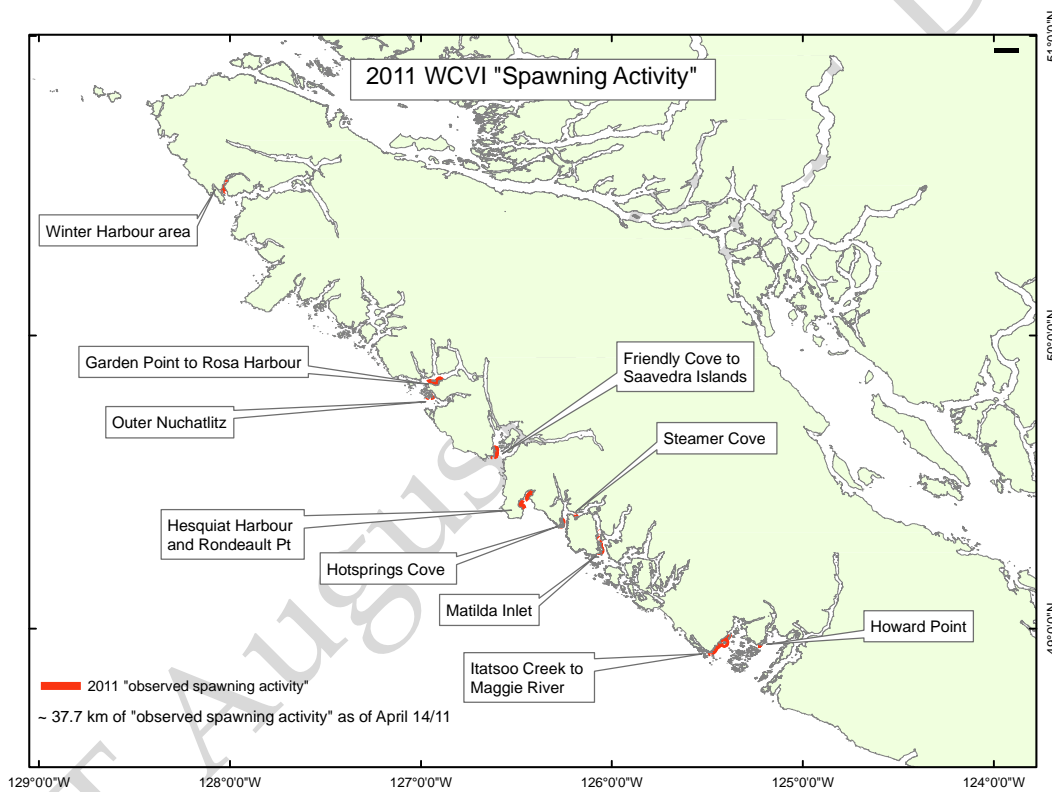


Figure 2.2: Preliminary Spawning activity in 2011 for the West Coast of Vancouver Island (includes minor stock area 27).

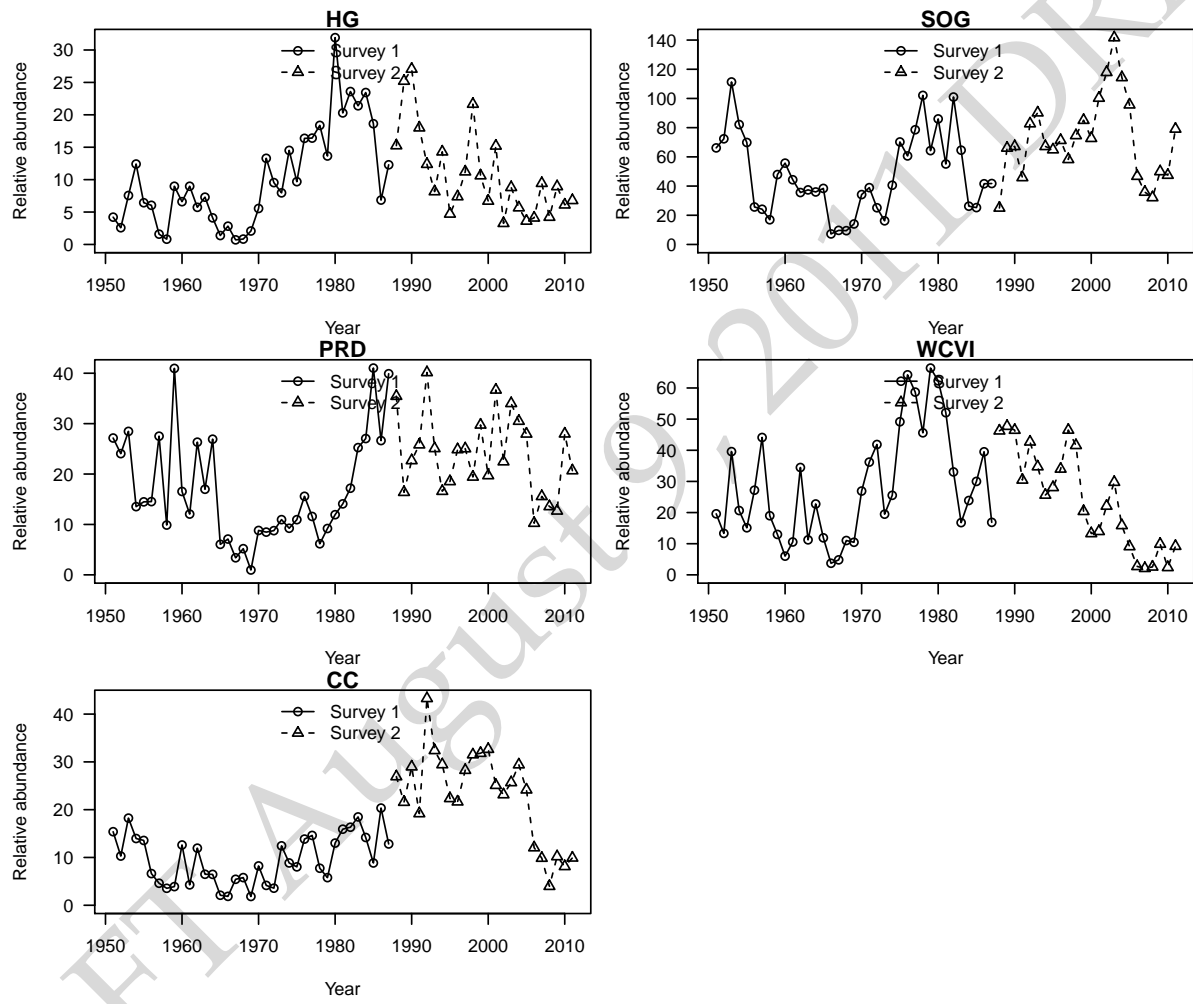


Figure 2.3: Spawn survey index for Strait of Georgia between 1951 and 2011. The units are actual estimates of spawning biomass (1000s tons), but only the trend information is used in the model fitting.

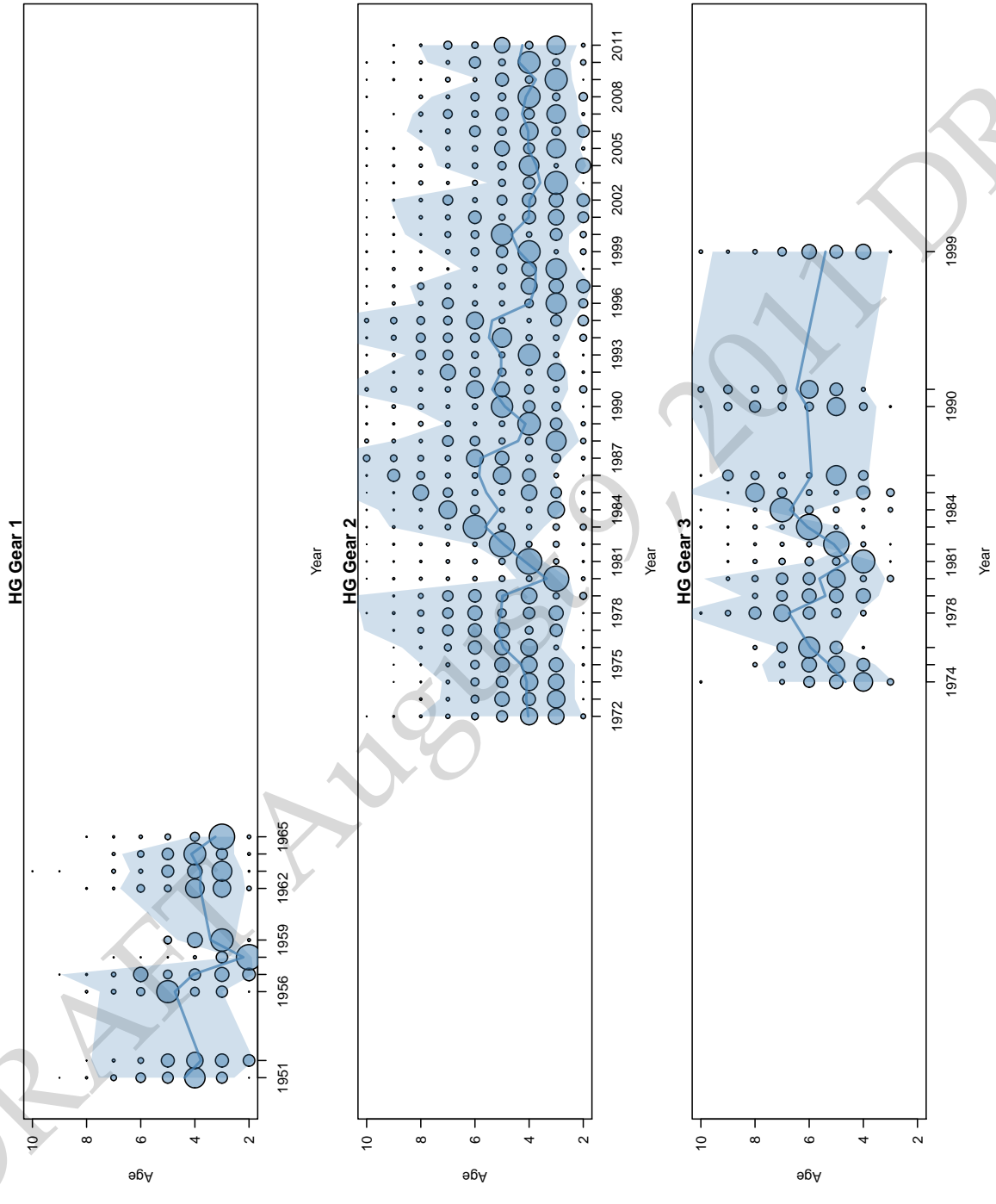


Figure 2.4: Bubble plots showing the proportions-at-age versus time for the winter purse seine fishery (top), seine roe fishery (middle) and the gill net fishery (bottom) in Haida Gwaii. The area of the circle is proportional to cohort abundance, each column sums to 1, zeros are not shown, and age 10 is a plus group. Also shown is the mean age of the catch (line) and the approximate 95% distribution of ages (shaded polygon) for each year.

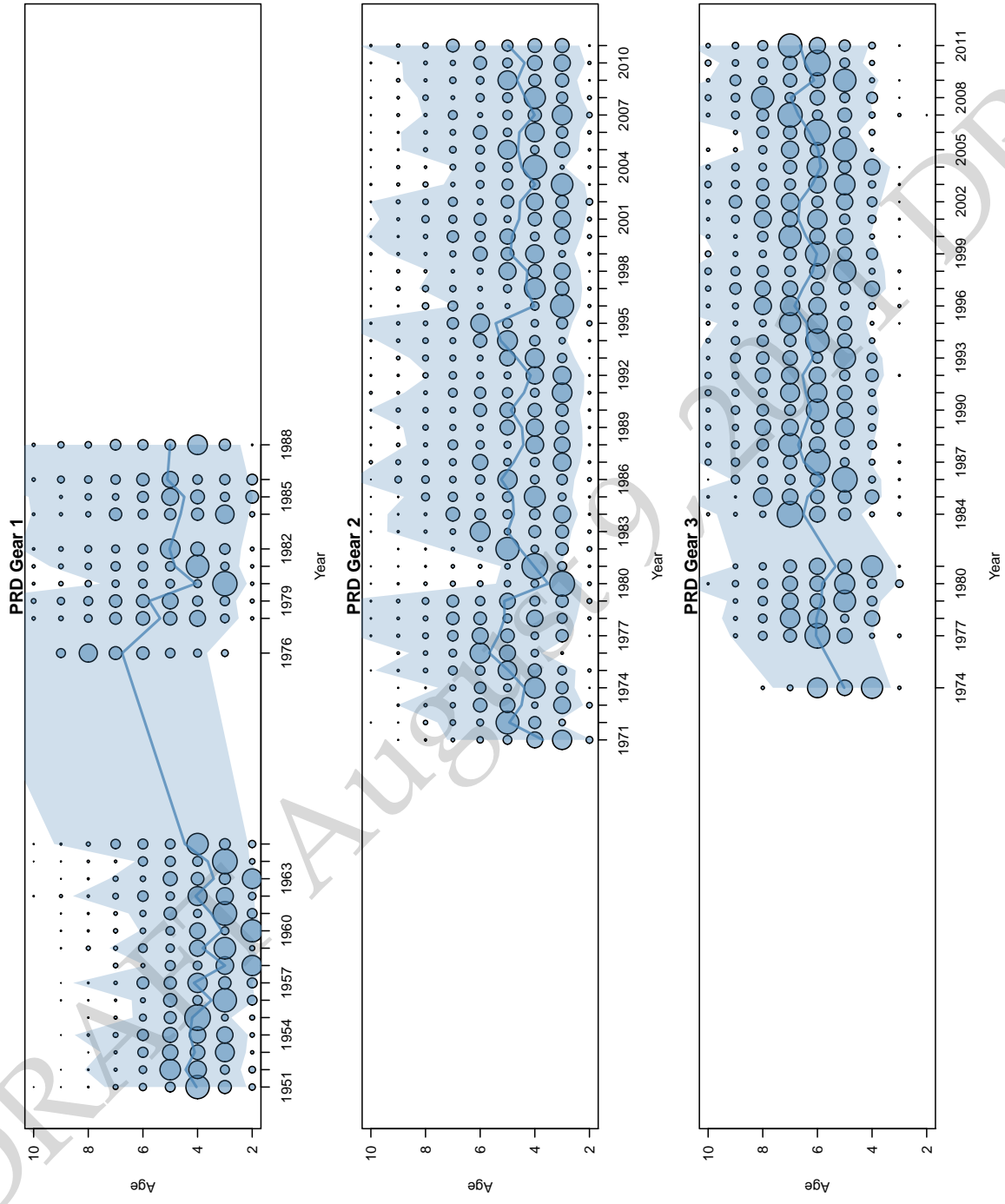


Figure 2.5: Bubble plots showing the proportions-at-age versus time for the winter purse seine fishery (top), seine roe fishery (middle) and the gill net fishery (bottom) in Prince Rupert District. The area of the circle is proportional to cohort abundance, each column sums to 1, zeros are not shown, and age 10 is a plus group. Also shown is the mean age of the catch (line) and the approximate 95% distribution of ages (shaded polygon) for each year.

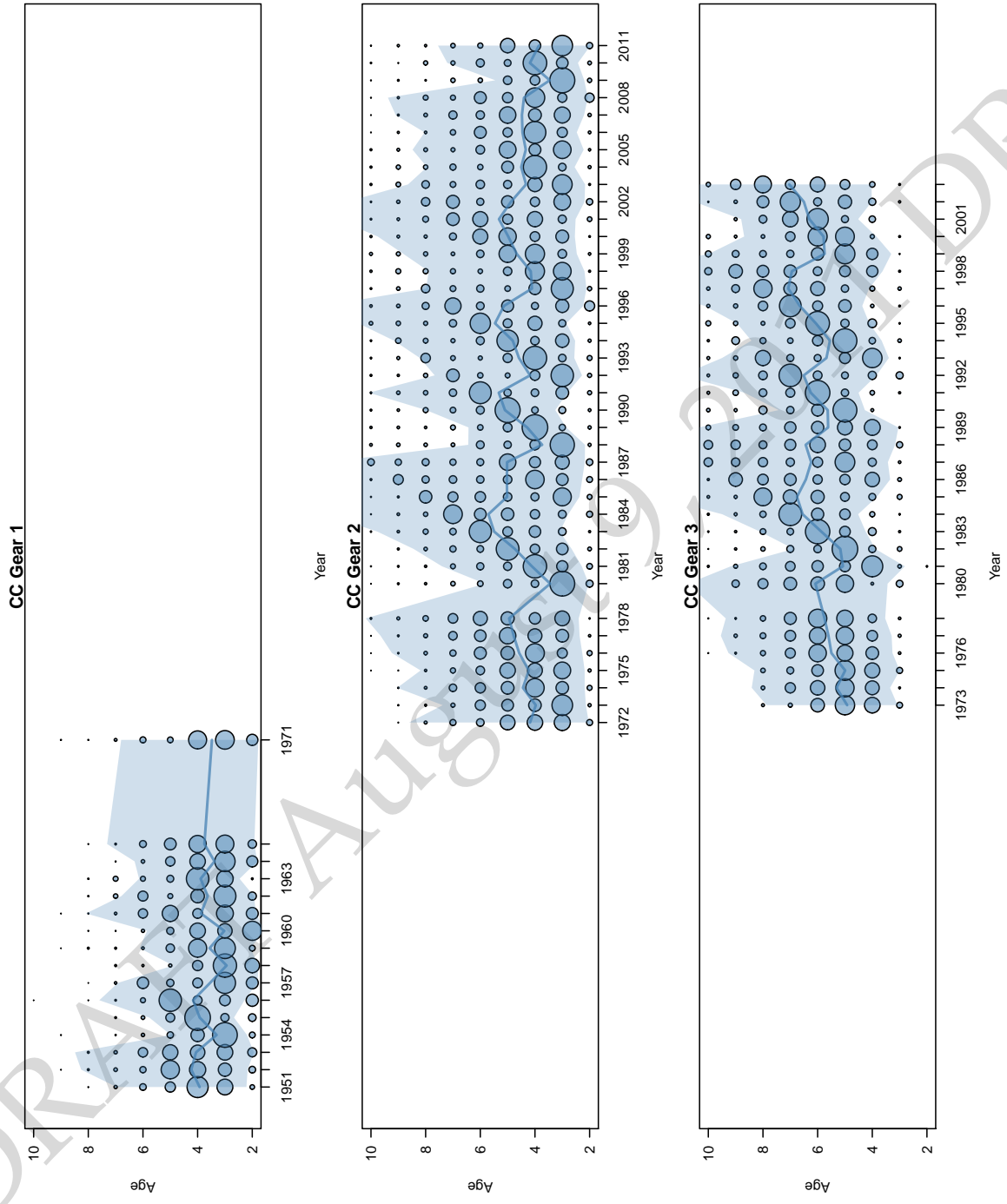


Figure 2.6: Bubble plots showing the proportions-at-age versus time for the winter purse seine fishery (top), seine roe fishery (middle) and the gill net fishery (bottom) in the Central Coast region. The area of the circle is proportional to cohort abundance, each column sums to 1, zeros are not shown, and age 10 is a plus group. Also shown is the mean age of the catch (line) and the approximate 95% distribution of ages (shaded polygon) for each year.

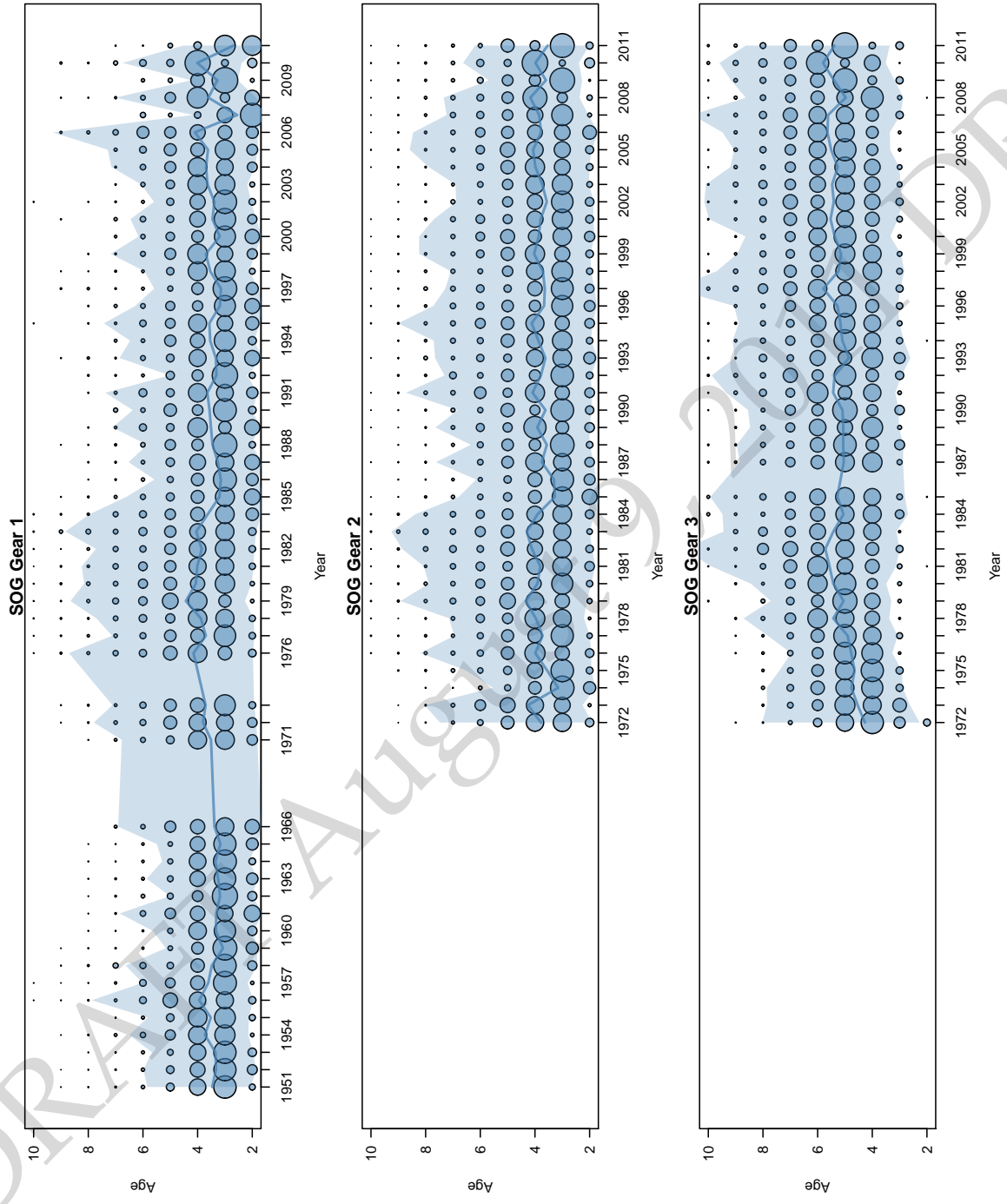


Figure 2.7: Bubble plots showing the proportions-at-age versus time for the winter purse seine fishery (top), seine roe fishery (middle) and the gill net fishery (bottom) in the Strait of Georgia. The area of the circle is proportional to cohort abundance, each column sums to 1, zeros are not shown, and age 10 is a plus group. Also shown is the mean age of the catch (line) and the approximate 95% distribution of ages (shaded polygon) for each year.

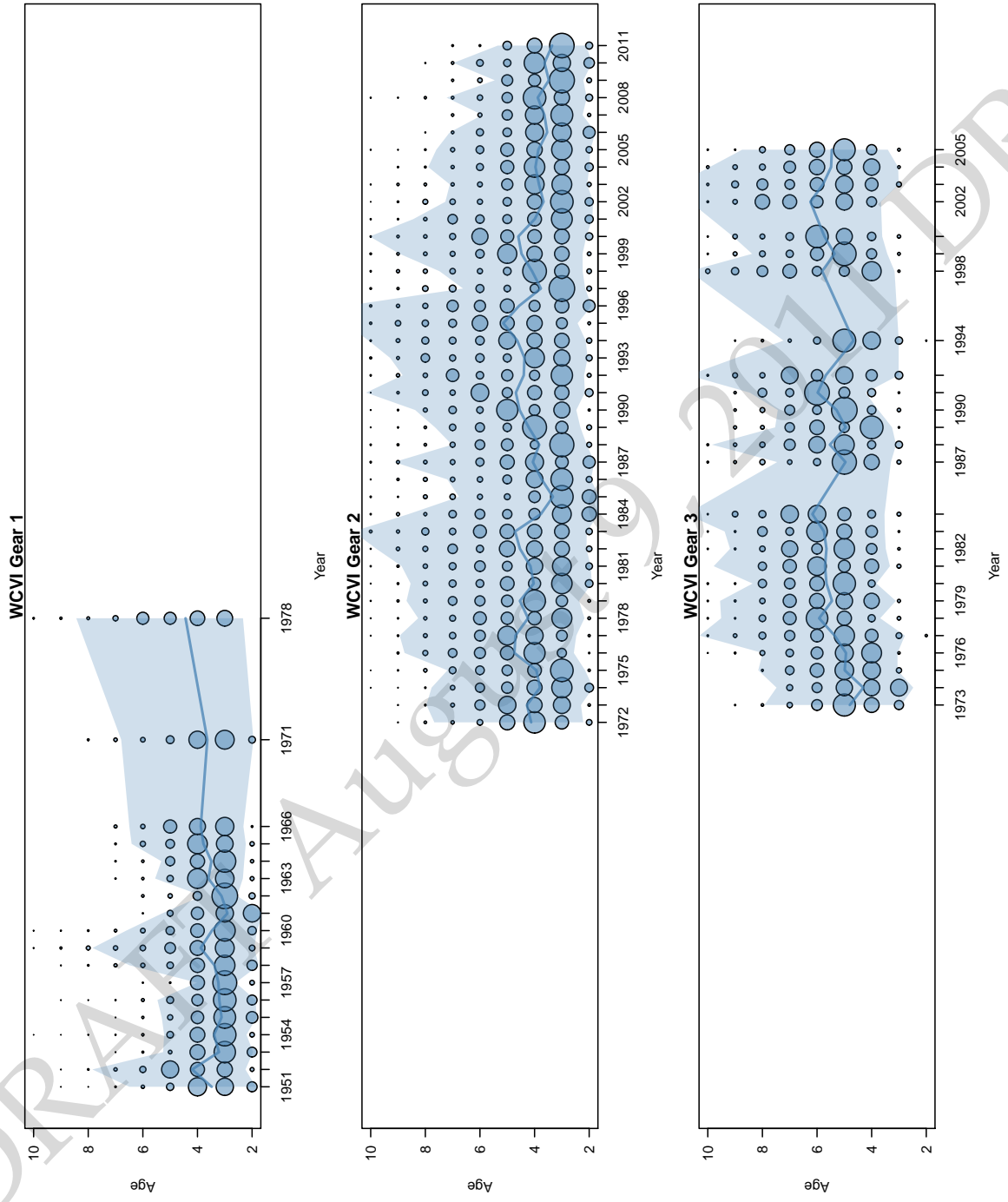


Figure 2.8: Bubble plots showing the proportions-at-age versus time for the winter purse seine fishery (top), seine roe fishery (middle) and the gill net fishery (bottom) in the West Coast Vancouver Island region. The area of the circle is proportional to cohort abundance, each column sums to 1, zeros are not shown, and age 10 is a plus group. Also shown is the mean age of the catch (line) and the approximate 95% distribution of ages (shaded polygon) for each year.

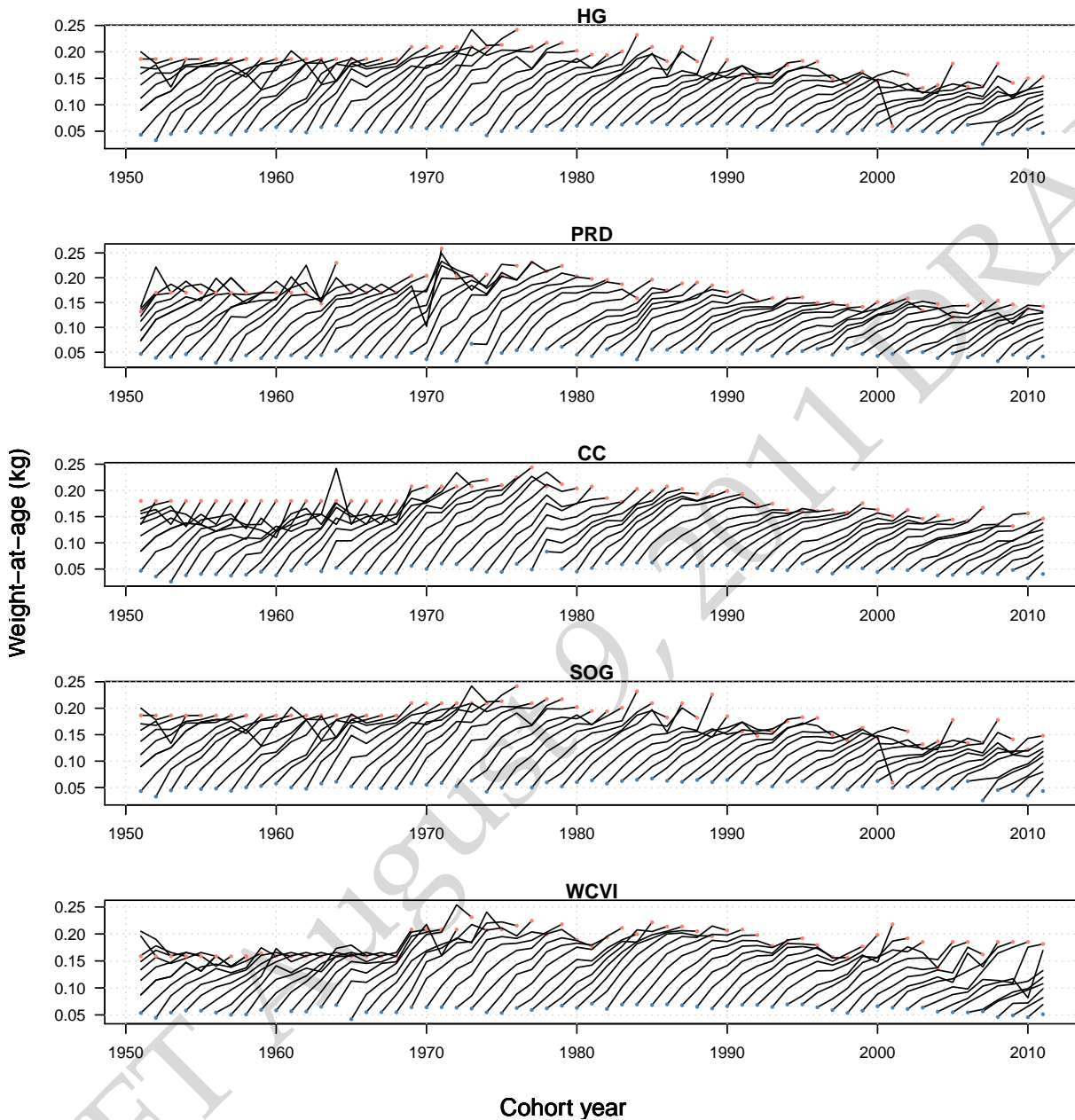


Figure 2.9: Empirical mean weight-at-age data by cohort from 1951 to 2011 for ages 2 to 10 in the five major Stock Assessment Regions.

factors, including: fishing effects (i.e., gear selectivity), environmental effects (changes in ocean productivity), or it may even be attributed to changes in sampling protocols (shorter time frame over which samples are collected). Declining weight-at-age has been observed in all five of the major stocks, and despite area closures over the last 10-years, has continued to occur in the QCI and WCVI stocks. Although the direct cause of this decline is still to be investigated, this trend has been observed in B.C. and U.S. waters, from California to Alaska (Schweigert, 2002), and merits further research. The observed mean weight-at-age data appear to have a few errors that need to be investigated as well; for example, see the apparently small age-10 fish in 2001 in Figure 2.9.

2.6.2 Analytical methods

For the 2011 BC herring assessment, $iSCA_M$ was used to conduct the stock assessment for each of the five major Stock Assessment Regions (SAR) and two minor assessment areas (Area 2W and Area 27). The technical details of this model can be found in Appendix A.1.

2.6.3 Retrospective analysis

A retrospective analysis was conducted for each of the major and minor SARs. The retrospective analysis successively removes the last 10-years of data and examines changes in estimates of terminal spawning biomass. The results are then plotted on a single panel to compare how estimates of spawning biomass change as successive years of data are omitted from the analysis.

2.6.4 Abundance and recruitment forecasts

The abundance forecast for the upcoming fishing season, also referred to as pre-fishery biomass, is defined as the predicted biomass of age-4 fish and older plus the number of age-3 fish recruiting in year $T + 1$. The abundance estimates are based on the median values from the sampled posterior distribution. Age-3 recruits are based on poor, average, and good recruitment scenarios; see next paragraph for definitions of poor, average and good.

The recruitment forecasts are based on the surviving number of age-3 fish at the start of the fishing season times the average weight-at-age 3 in the last 5 years. The definitions of poor, average, and good recruitment are as follows: **Poor** is the average recruitment from the 0-33 percentile, **Average** is the average recruitment from the 33-66 percentile, and **Good** is the average recruitment from the 66-100 percentile. Note that all cohorts from 1951 to 2010 were included in the calculation of recruitment quantiles.

2.6.5 Catch advice

Catch advice is based on the application of the harvest control rule (HCR). The herring HCR has three components:

1. Reference points (LRP, USR, and cutoffs)
2. Harvest rate
3. Decision rules

For each of the five major stocks, the limit reference point (LRP) is the cutoff value, which is defined here as $0.25B_0$ and the Upper Stock Reference (USR) is defined as the 1.05^*LRP ($0.25B_0 + 0.2*0.25B_0 = LRP + 0.05LRP$). **For clarification, references to B_0 throughout this document refer to the mature spawning stock biomass.** The default harvest rate if the stock is at or above USR is 0.2, and declines linearly to 0 when the stock is at or below the LRP (a default harvest rate of 0.1 is used for the minor stock areas). The decision rule for the major stock areas operates as follows:

- If the forecast run is less than the LRP (cutoff) then the area is closed to all commercial harvest (i.e., stock is deemed to be in the critical zone).
- If the forecast run is greater than the LRP and less than the USR (i.e., cautious zone), then total allowable catch is based on a reduced harvest rate that would deplete the stock to the LRP level.
- If the forecast run is greater than USR, then the total allowable catch is set at 20% of the forecast run.

2.7 Results

The results section is broken down into three major subsections, Maximum likelihood fits to the data, marginal posterior distributions, and stock forecasts and catch advice based on samples from the joint posterior distribution.

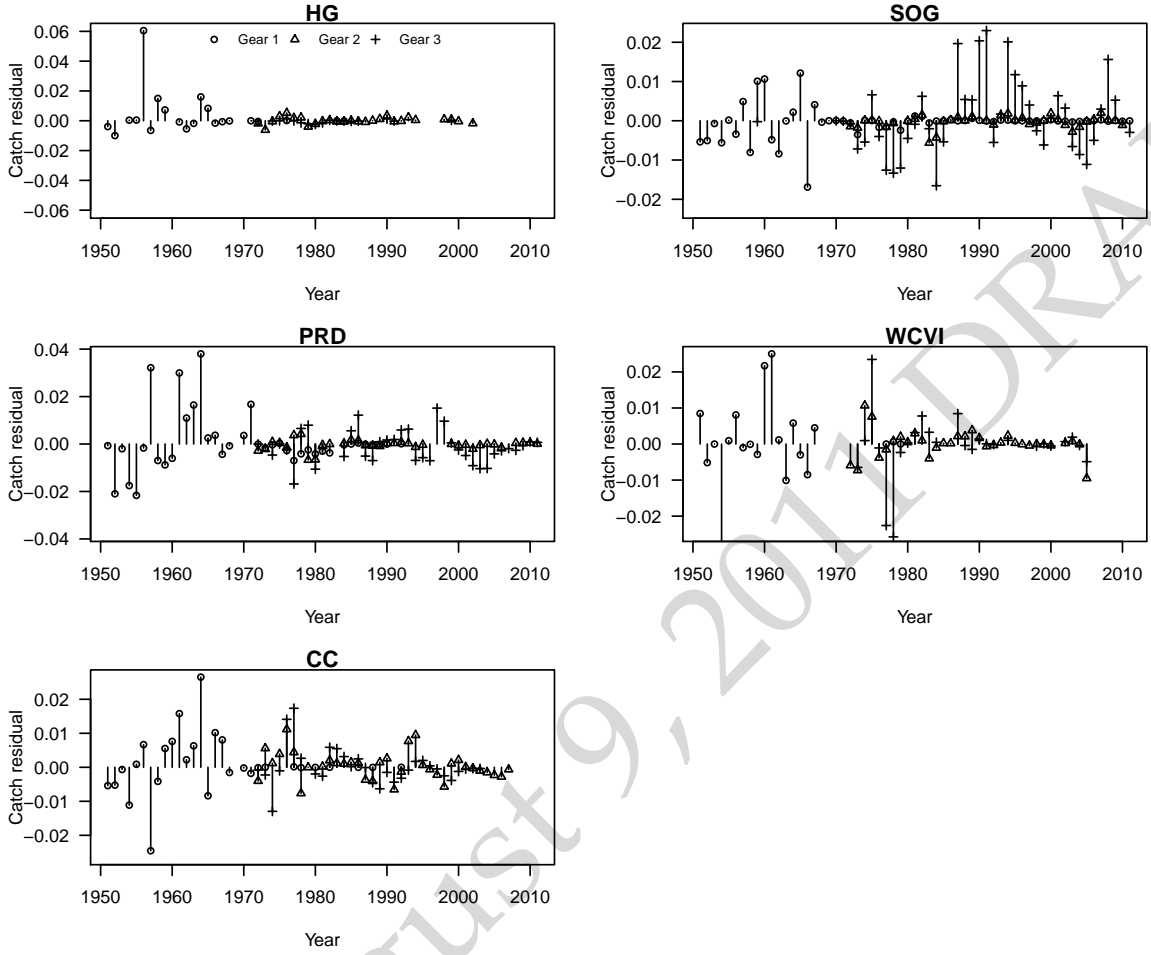


Figure 2.10: Residual for the log difference between observed and predicted catch for the five major SARs for each gear type (Gear 1 = winter seine fishery, Gear 2 = seine-roe fishery, Gear 3 = gillnet fishery).

2.7.1 Maximum likelihood fits to the data

Although the maximum likelihood estimates are not explicitly used for constructing the catch advice, we do present the MLE estimates of the residual patterns and fits to the data for comparisons.

Catch residuals

Residuals between the observed and predicted catch are largely determined by the user specified standard deviation in each of the control files. In this assessment, the assumed variance for all regions (including minor regions) was set at 0.005, which corresponds to a standard deviation of approximately 0.0707. Overall the residuals for each fishery in each stock assessment region are unremarkable (Fig. 2.10), with exception of a major outlier in the Haida Gwaii in the mide 1950s. In 1956, the reported catch in Haida Gwaii was extremely large ($> 60,000$ mt) and the model has a difficult time explaining this large catch. In order to explain this large catch in a single year, a large biomass in the region is required.

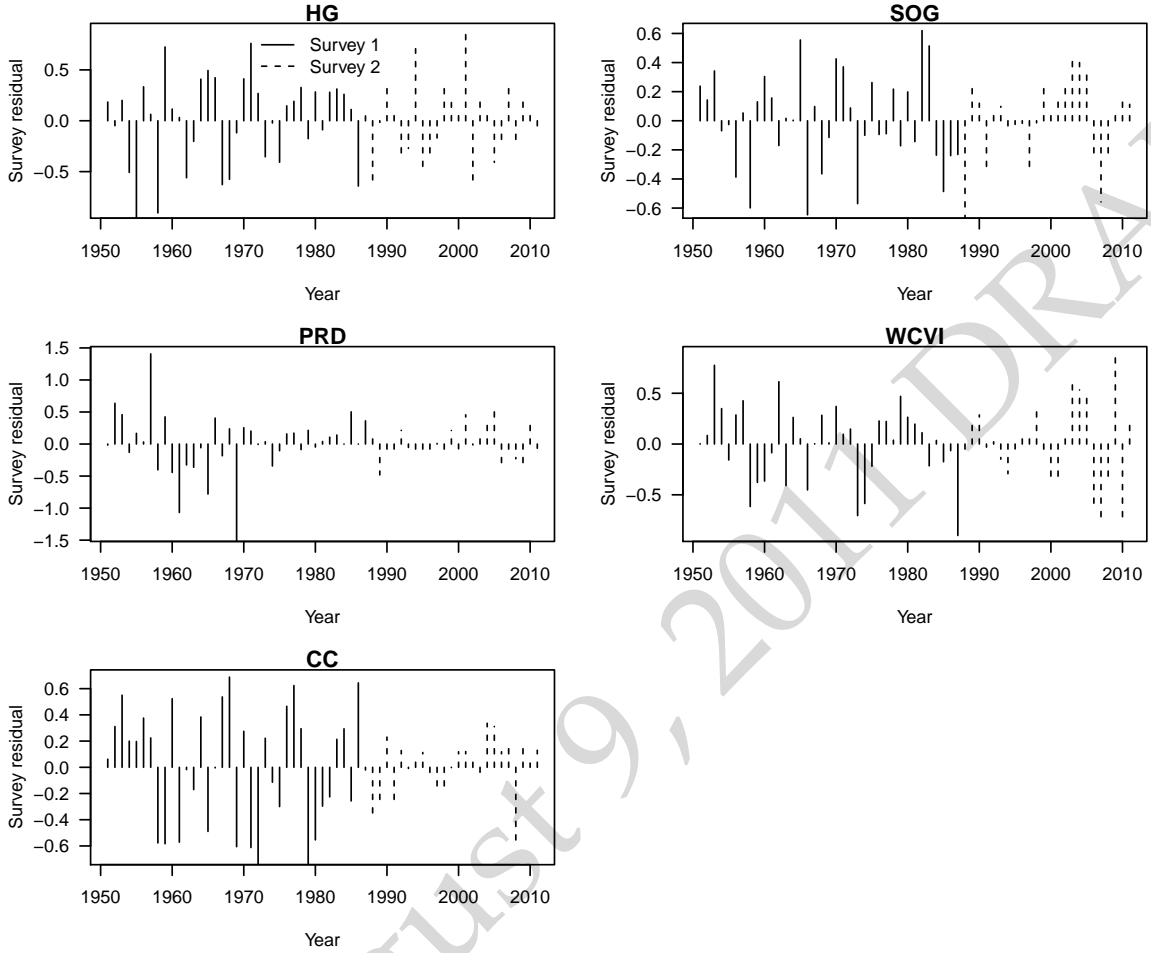


Figure 2.11: Residual patterns for the log difference between observed and predicted spawn survey abundance for the five major SARs. Spawn survey data based on surface estimates are shown as solid lines and data based on diver surveys is shown as dashed lines.

Fits to the spawn survey data

The residuals between the observed and predicted spawn survey index (on a log scale) are shown in Figure 2.11. Recall that the spawn survey data are treated as two independent time series where data between 1951–1987 were based on surface estimates of spawn area and data post 1988 are based on diver surveys of spawn area. More weight was assigned to the contemporary data.

For most areas, there is little pattern in the residuals between the observed and predicted survey data (Fig 2.11). For the HG, PRD and CC regions, there is very good correspondence between the observed and predicted survey data post 1988. In the SOG, there is a period of positive residuals between 1999 and 2005 where the predicted spawn biomass fails to increase as much as indicated by the survey. Similarly 3–4 year trends also exist in the WCVI spawn survey data after the year 2000.

In comparison to the previous assessment for Pacific herring using the HCAM model, estimates of the catchability coefficient are very different (HCAM assumed $q=1$ for post 1988 data). In each of the five major assessment regions (and the two minor regions) a less informative prior for the catchability coefficient was used (see Appendix C.3). Maximum Likelihood Estimates (MLE) of the catchability coefficients are

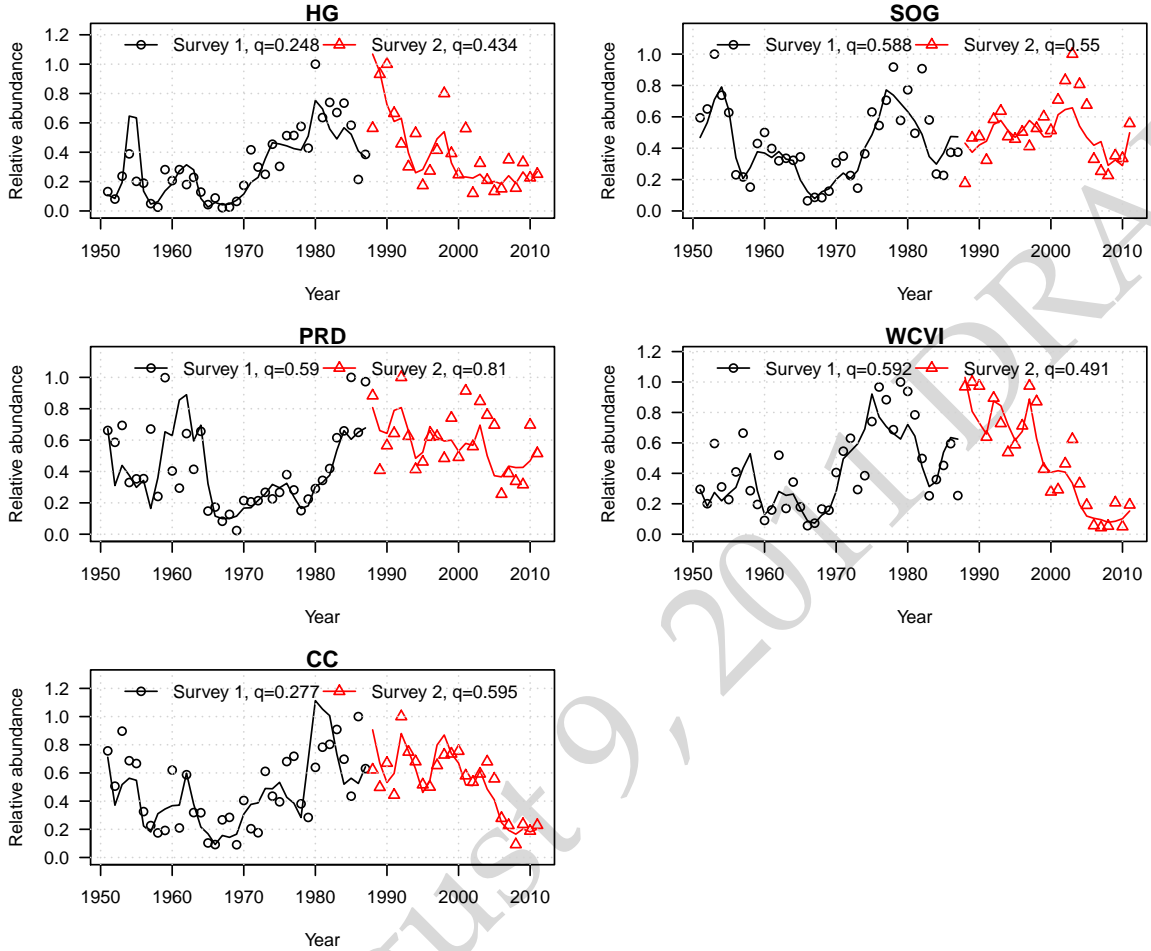


Figure 2.12: Observed (points) and predicted (lines) relative abundance data (spawn survey data) for each of the five major SARs. In each panel, the corresponding scaler (q) is presented for each of the surveys.

presented for each region in Fig. 2.12 along with the observed and predicted trends in the spawn index. Estimates of q in both time periods are less than 1.0 for all regions. The interpretation of $q = 1$ is that the spawn survey data is an absolute measure of spawn abundance, $q < 1$ implies that the survey under-estimates the spawn abundance and $q > 1$ implies an over-estimate. For example, in the HG region the MLE values for q are 0.248 and 0.434 for the pre- and post-1988 data, respectively. This could be interpreted as the spawn survey, on average, sees 24.8% and 43.4% of the deposited spawn each year. This interpretation however is conditional on the specification of mature biomass in the stock assessment model and the methods used to extrapolate egg density to spawning biomass.

Age composition residuals

The assumed error distribution for the age-composition data has changed in this assessment from a multinomial distribution implemented in HCAM to a multivariate-logistic distribution. In the former implementation the age-composition data were weighted by the annual samples sizes in each region for each age and year. In the *iSCAM* implementation the age-composition data for all years is given the same weight (i.e., we assume the observation errors is homogenous) based on the conditional maximum likelihood estimate of

the variance (see Appendix A.1 for full details). We further pool age-proportions that are less than 2% into the adjacent younger year class to reduce the influence of small outliers and weak cohorts.

In HG the MLE estimates of the variance for each gear is 0.102, 0.106 and 0.306, for the winter seine, seine-roe and gillnet fleets, respectively (Fig. 2.13). In general there is fairly good agreement between the observed and predicted age-composition data in this region, with poorer fits to the gillnet age-composition data. There is no persistent pattern in the residuals.

For the PRD region, the fits to the age-composition data are slightly poorer, with MLE estimates of the variance ranging from 0.164 to 0.269 for the gillnet and winter seine fleets (Fig. 2.14). There is no remarkable pattern in the winter seine fishery, the seine-roe fishery tends to have positive residuals for age-3 and age 7+ fish, and negative residuals for ages 5-6 fish. Residuals in the gillnet fishery are mostly negative for age-4 fish post 1988. The gillnet gear tends to catch older fish than both seine gears.

For the Central Coast (CC) region, there is also good correspondence between the observed and predicted age-composition data, with MLE estimates of the variance ranging from 0.135 to 0.201 (Fig. 2.15). There is no striking temporal pattern in the residuals for any of the fishing fleets. There is a tendency to overestimate the proportion-at-age 4 in the seine-roe fishery.

For the Strait of Georgia, there is also very good correspondence between the observed and predicated age-composition data for all three gears (Fig 2.16). The MLE estimates of the variance range from 0.089 to 0.263 for the seine-roe and winter seine fleets, respectively. In the gillnet fleet there has been a tendency to under-estimate the proportions-at-age 6-7 between the 1996 to 2011. Recall that selectivity for the gillnet fishery can be influenced by the empirical weight-at-age data, which has been trending to small fish in recent years. In this case, the age-composition data do not suggest that changes in mean weight-at-age has influenced the selectivity patterns (see results for selectivities).

In the case of WCVI, there is good correspondence between the observed and predicted age composition data for the seine fisheries and less so for the gillnet fishery (Fig 2.17). The MLE estimates of the variance range fro 0.092 to 0.237 for the seine-roe and gillnet fisheries, respectively. Residual patterns in the seine fisheries and gillnet fisheries are unremarkable. The size of the residuals are fairly homogenous over time for all gears.

2.7.2 Biomass estimates & reference points

Maximum likelihood estimates of total biomass (age 2+) and the spawning stock biomass for each of the five major assessment regions in summarized in Figure 2.18. Estimates of spawning stock depletion (B_t/B_0) for the five major regions is summarized in Figure 2.19 along with estimates of the sustainable fisheries framework reference points. With the exceptions of CC and WCVI, estimates of spawning stock depletion in 2011 are all currently at or above 40% of their estimated unfished state. In the CC and WCVI, spawning stock depletion is estimated to be 25% and 25% of their unfished state, respectively (Fig 2.19).

Maximum likelihood estimates of spawning stock biomass in 2011 were as follows: HG – 16,723 tonnes, PRD – 27,288 tonnes, CC – 14,624 tonnes, SOG – 129,070 tonnes, and WCVI – 14,909 tonnes (Table 2.1). These estimates are considerably higher in comparison to last years HCAM estimates; the difference largely owes to the substantial change in spawn survey scaling coefficient (q).

In addition to the current estimates of spawning biomass, Table 2.1 also summarizes estimates of reference points and the total number of estimated parameters for each of the five major stock assessment regions. Each region contained data from 1951 to 2010, and the number of estimated parameters ranges from 159 in HG to 235 in SOG. The difference in the number of estimated parameters owes to the difference in the number of years of catch data for each region.

Estimates of unfished spawning biomass for each region is as follows: HG – 40,684 tonnes, PRD – 68,761 tonnes, CC – 59,365 tonnes, SOG – 135,523 tonnes, and WCVI – 57,462 tonnes. Applying the same cutoff rule used in previous assessments (25% of B_0), the results in a substantial change in the cutoff levels for PRD, CC, SOG, and WCVI. The previous cutoff level for HG was estimated at 10,700 tonnes, and in this assessment there is a minor downward revision to 10,171 tonnes. In the case of PRD, the previous cutoff was 12,100 tonnes and in this assessment is now 17,190 tonnes. For the CC, the previous cutoff was 17,600 tonnes and now 14,841 tonnes. For the SOG, the previous cutoff was 21,200 tonnes, and in this assessment it has been revised upwards to 33,881 tonnes. Lastly, for the WCVI the cutoff has decreased

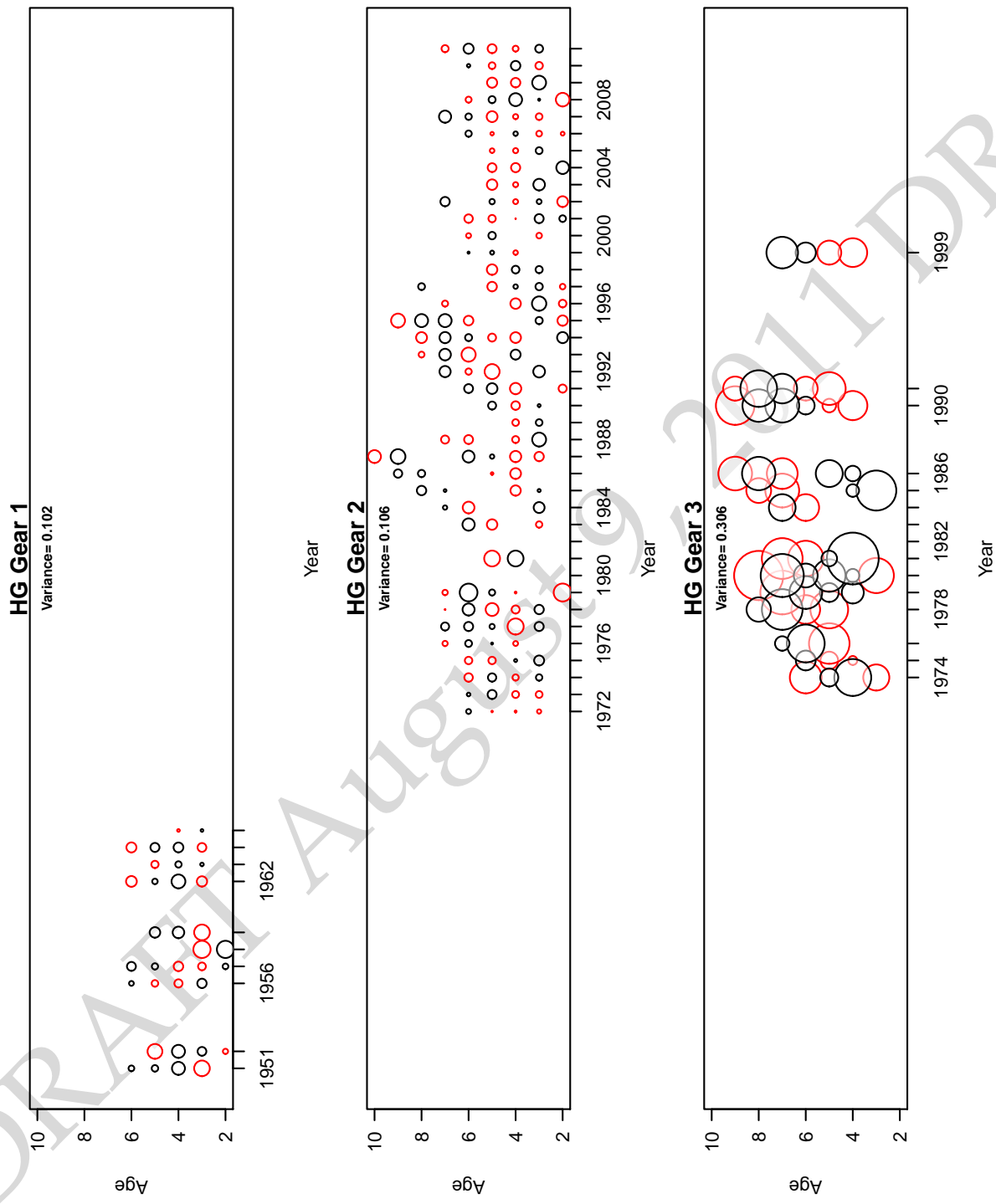


Figure 2.13: Residual difference between the observed and predicted proportions-at-age for HG for each of the three gear types (Gear 1 = winter seine, Gear 2 = seine-roe, Gear 3 = gillnet). The area of each circle is proportional to the residuals, black is positive, and red is negative. The corresponding MLE estimates of the residual variance is displayed in each panel.

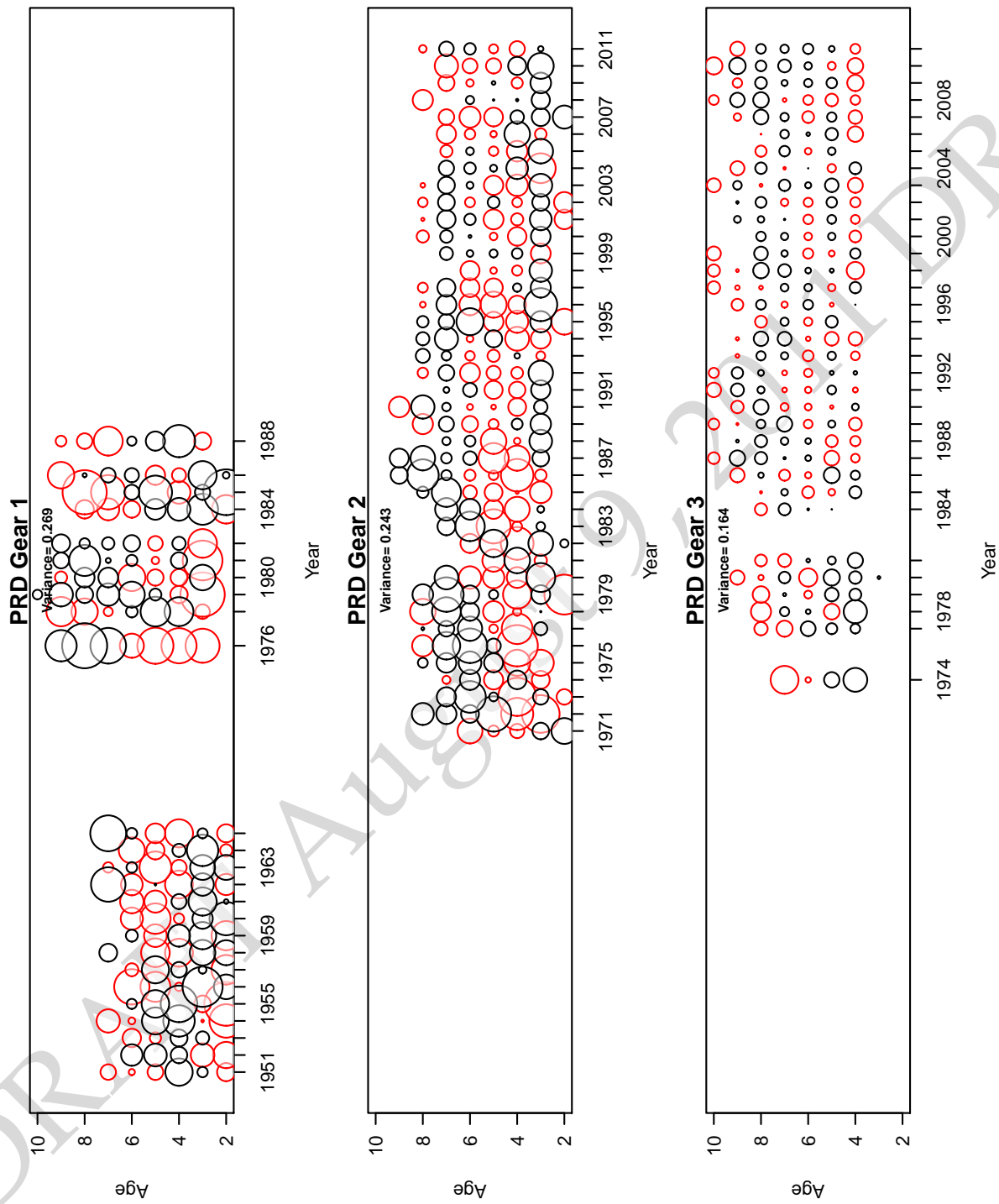


Figure 2.14: Residual difference between the observed and predicted proportions-at-age for PRD for each of the three gear types (Gear 1 = winter seine, Gear 2 = seine-roe, Gear 3 = gillnet). The area of each circle is proportional to the residua, black is positive, and red is negative. The corresponding MLE estimates of the residual variance is displayed in each panel.



Figure 2.15: Residual difference between the observed and predicted proportions-at-age for CC for each of the three gear types (Gear 1 = winter seine, Gear 2 = seine-roe, Gear 3 = gillnet). The area of each circle is proportional to the residua, black is positive, and red is negative. The corresponding MLE estimates of the residual variance is displayed in each panel.

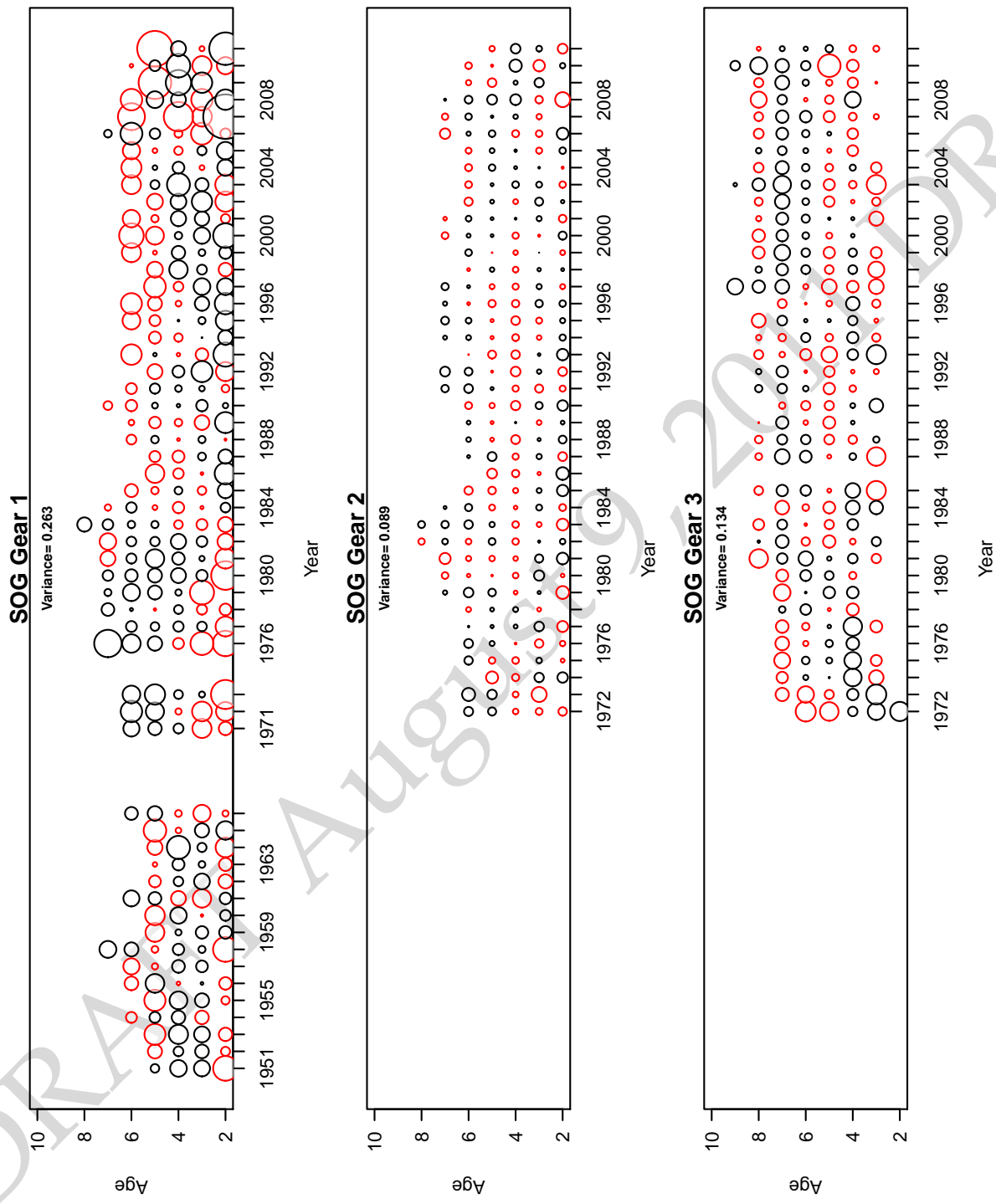


Figure 2.16: Residual difference between the observed and predicted proportions-at-age for SOG for each of the three gear types (Gear 1 = winter seine, Gear 2 = seine-roe, Gear 3 = gillnet). The area of each circle is proportional to the residua, black is positive, and red is negative. The corresponding MLE estimates of the residual variance is displayed in each panel.

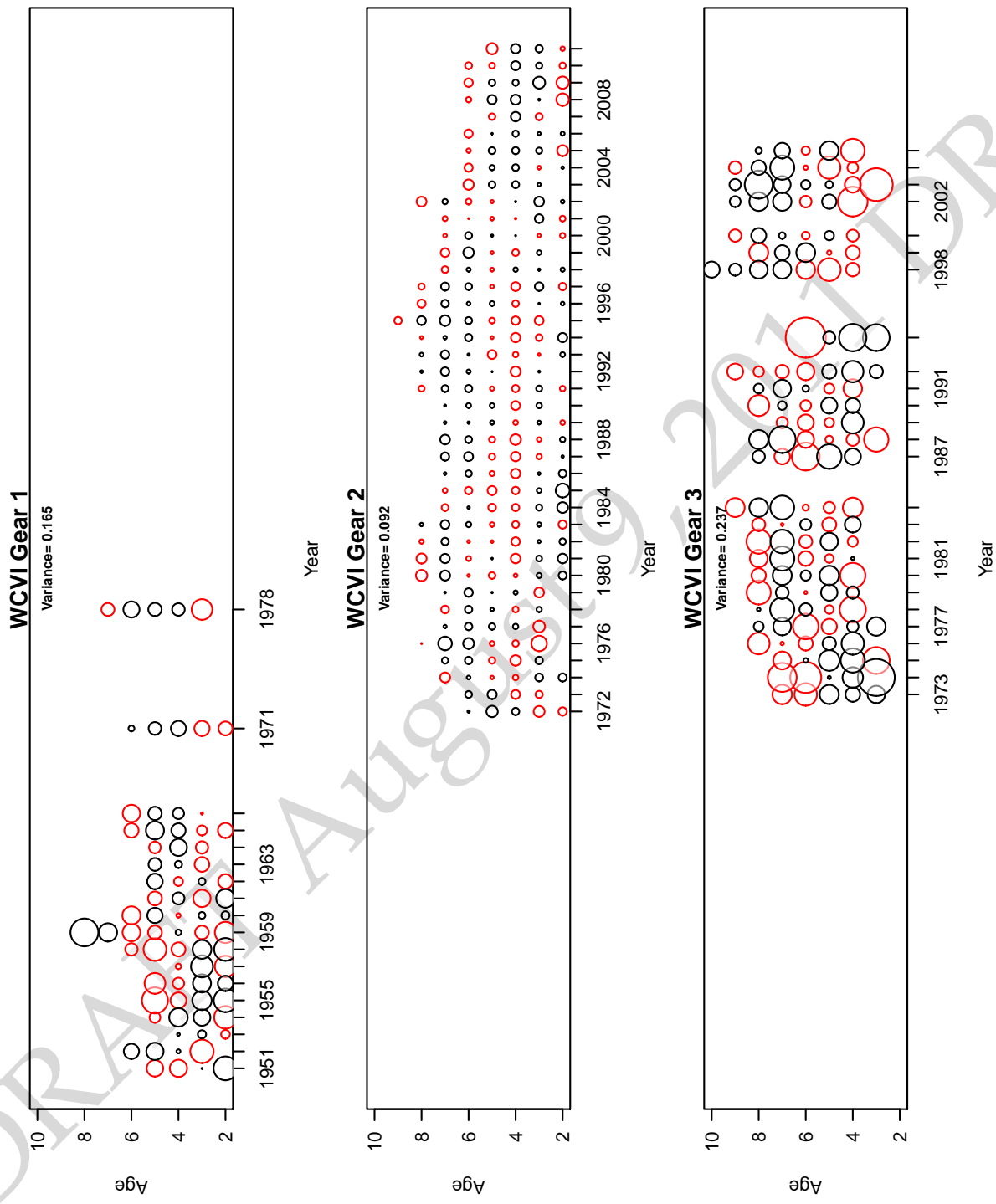


Figure 2.17: Residual difference between the observed and predicted proportions-at-age for WCVI for each of the three gear types (Gear 1 = winter seine, Gear 2 = seine-roe, Gear 3 = gillnet). The area of each circle is proportional to the residua, black is positive, and red is negative. The corresponding MLE estimates of the residual variance is displayed in each panel.

Table 2.1: Summary of maximum likelihood estimates for each of the five major stock areas. No. is the total number of estimated parameters, F_{MSY} the average instantaneous fishing rate to achieve the maximum sustainable yield (MSY), B_0 is the unfished spawning biomass, B_{MSY} is the spawning biomass that achieves maximum sustainable yield, B_t is the spawning biomass at the end of the 2011 fishing season, and B_t/B_0 is the spawning depletion level at the end of the 2011 fishing season.

Stock	HG	PRD	CC	SOG	WCVI
No.	159	206	190	235	174
F_{MSY}	2.36	0.54	1.31	1.4	0.98
MSY	8,761	6,669	9,104	27,442	10,260
B_0	40,684	68,761	59,365	135,523	57,462
$0.25B_0$	10,171	17,190	14,841	33,881	14,366
B_{MSY}	8,708	18,600	11,514	28,211	11,281
$0.8B_{MSY}$	6,966	14,880	9,211	22,568	9,025
$0.4B_{MSY}$	3,483	7,440	4,605	11,284	4,512
B_t	16,723	27,288	14,624	129,070	14,909
B_t/B_0	0.41	0.4	0.25	0.95	0.26

from 18,800 tonnes to 14,366 tonnes. Note however, that these revised B_0 's and cutoffs are Maximum Likelihood Estimates (MLE) and not median values from the joint posterior distribution (see section 2.7.10)

2.7.3 Estimates of mortality

The most recent HCAM assessment model allowed for annual estimates of M_t where natural mortality was modelled as a random walk process. The same random walk model has been adopted in this *iSCAM* implementation; however, a reduced number of parameters (12 nodes instead of 60 annual deviations) was estimated and interpolated using a bicubic spline. The number of estimated nodes does have minor influences on the various trends in natural mortality; we came to arrive at estimating 12 nodes by ensuring the estimated trends were very similar to trends in M when estimating 60 annual natural mortality rate deviations (NB. the use of formal model selection criterion should be used to determine the optimal number of nodes).

For all of the five major stock assessment regions, estimates of natural mortality rates have trended upwards since the 1950s (Figure 2.20). Trends in estimates of natural mortality are also consistent with the trends in natural mortality from last years HCAM model (see Figure 18 in Cleary and Schweigert, 2010). In the mid to late 1970s, estimates of natural mortality rates were very low during a time when most of the stocks were recovering from the earlier reduction fishery. In the last decade, estimates of natural mortality rates for herring have been at an all time high, and in all locations there is indication that natural mortality rates may be starting to decline. Estimates of M_t in the most recent years, however, are highly suspect because there are incomplete cohorts to infer estimates of total mortality rates and M_t is also confounded with selectivity.

Estimates of fishing mortality rates in each of the regions, between 1951 and 1970 were very high due to the reduction fishery by the winter purse seine (Gear 1). After the fishery re-opened in the early 1970s fishing mortality rates have been greatly reduced and periodic since the early 1990s due to the implementation of a harvest control rule with target escapements (cutoffs). Of notable exceptions are the fishing mortality rates for the gillnet fishery in PRD and SOG have been substantially higher than other regions and consistently open each and every year (Fig. 2.20). Note that fishing mortality rates for each gear in Fig. 2.20 reflect the average fishing mortality over all age-classes and are not comparable among gears due to differences in gear selectivity. Fishing mortality rates for the gillnet fishery tend to be higher than the seine-roe fishery because recruitment to the gillnet gear is much older in comparison to the seine-roe gear.

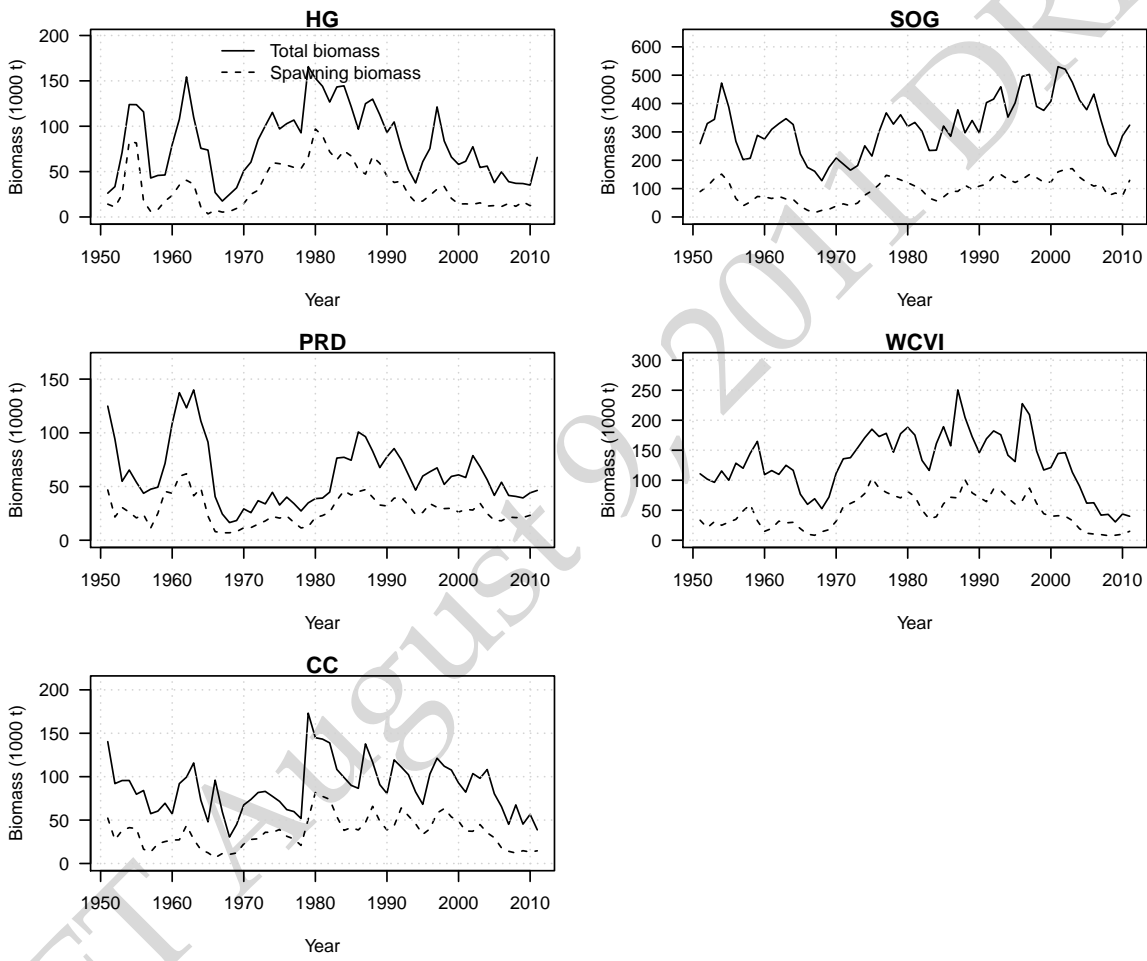


Figure 2.18: Estimates of total biomass at the start of the year (numbers times empirical weight-at-age) and spawning stock biomass (post fishery) for the five major SARs.

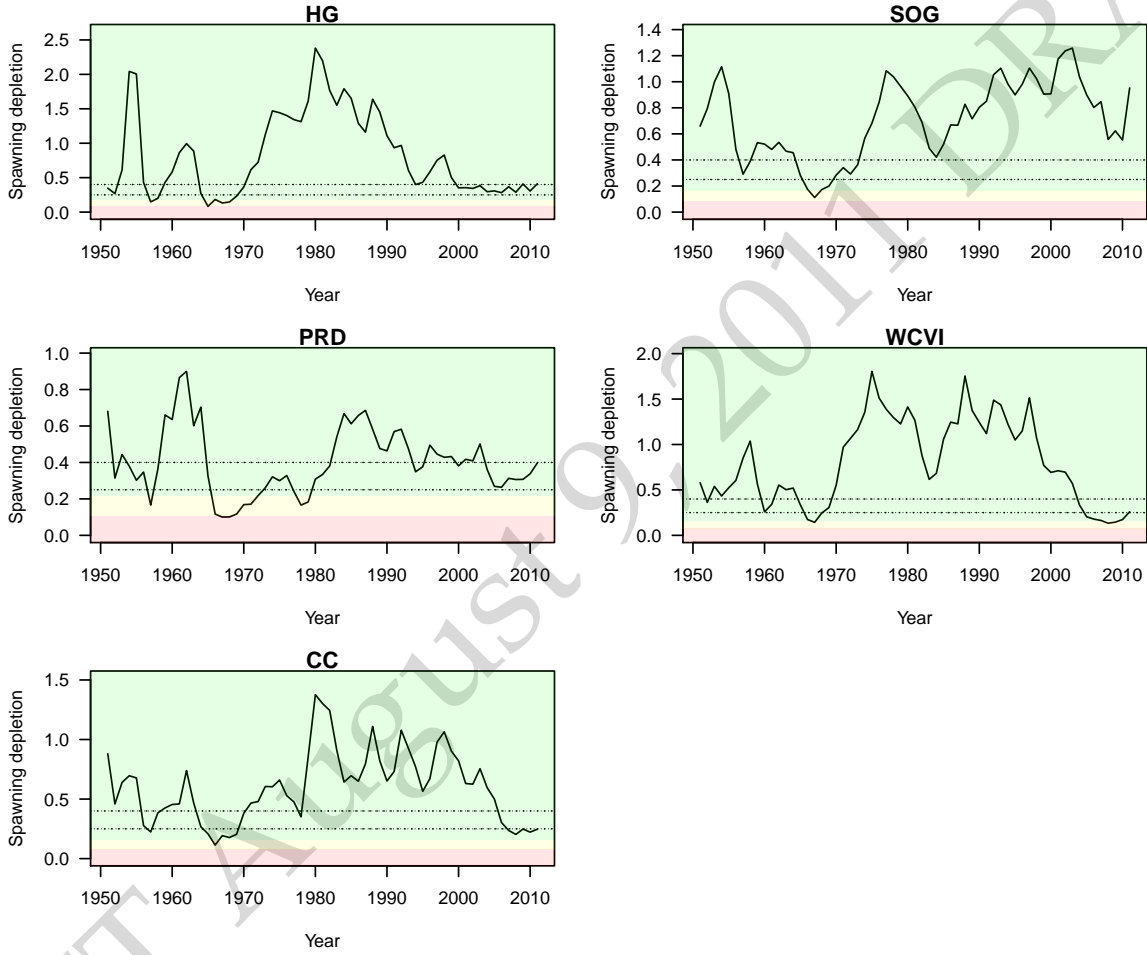


Figure 2.19: Estimates of spawning biomass depletion (B_t/B_0) for each of the five major stock areas. Horizontal dotted lines represent 25% and 40% depletion levels, and the shaded regions demarcate reference points based on $<40\%$ B_{MSY}/B_0 (critical zone) and $40\text{--}80\%$ B_{MSY}/B_0 (cautious zone) and $>80\%$ B_{MSY}/B_0 (healthy zone).

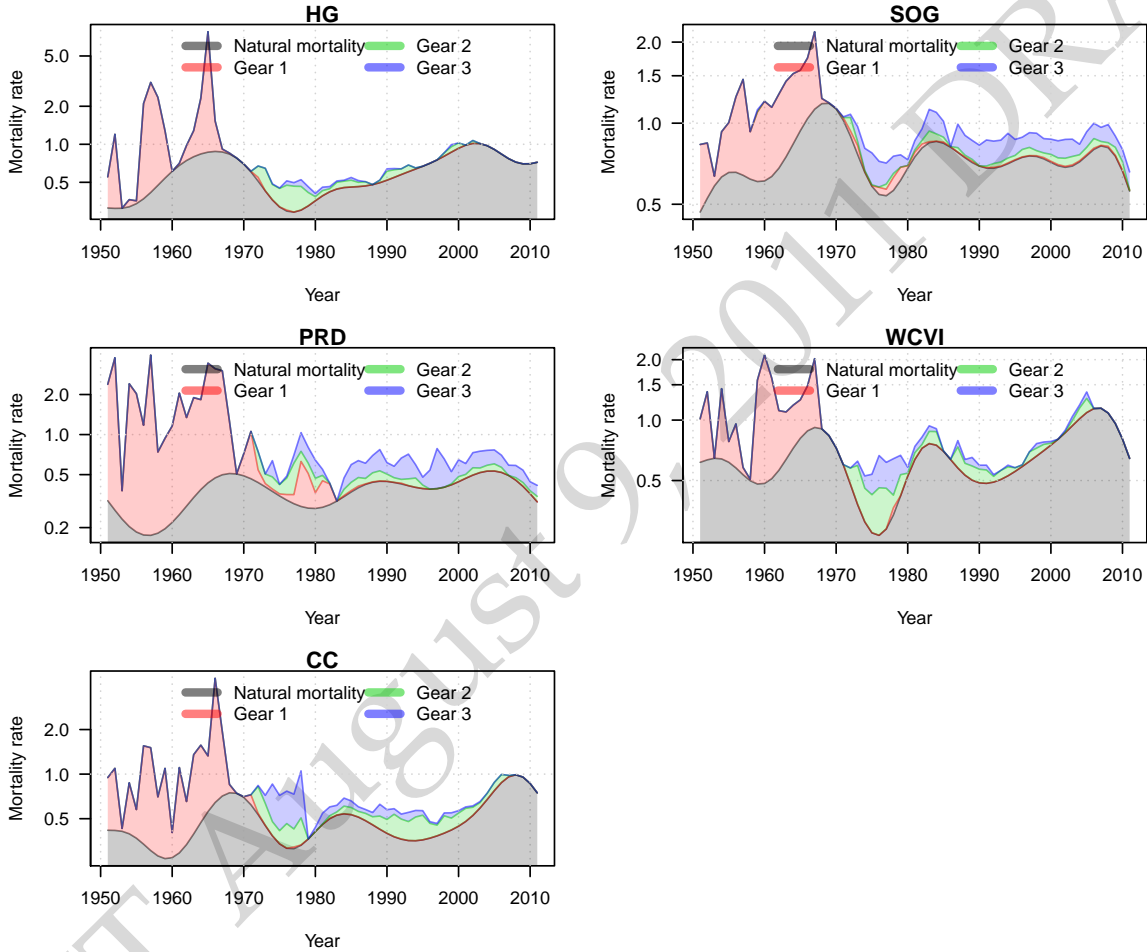


Figure 2.20: Maximum likelihood estimates of the components of average total mortality for each of the five major stock assessment regions. Note that the y-axis is plotted on a log scale, natural mortality (grey) is age-independent, fishing mortality is age-specific and the average fishing mortality rate over all age-classes is plotted here.

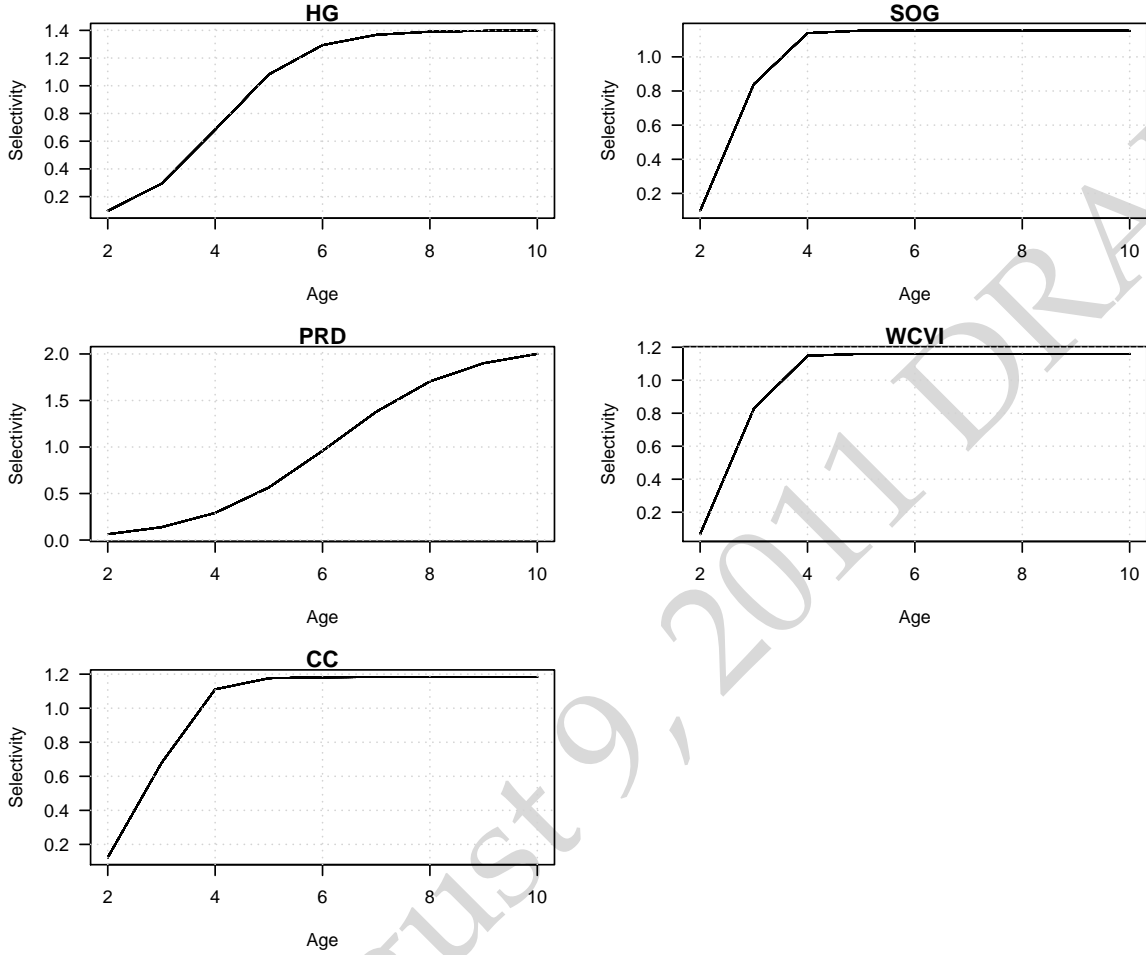


Figure 2.21: Maximum likelihood estimates of age-specific selectivity coefficients for the winter seine fishery for each of the major stock areas.

2.7.4 Selectivity

Maximum likelihood estimates of selectivity for the winter seine fishery, seine-roe fishery and the gillnet fishery for each of the five major SARs are shown in Figures 2.21, 2.22, and 2.23, respectively. Selectivities for the seine fisheries were assumed time-invariant, and selectivity for the gillnet fishery varies over time due to changes in the mean weight-at-age data.

For the winter seine fishery, age-specific selectivity coefficients were somewhat variable among the assessment regions (Fig. 2.21). The age at which herring were fully recruited to the gear was roughly age 5 for CC, SOG, and WCVI. Age at full recruitment for HG and PRD was much older, 9- and 10-years, respectively.

For the seine-roe fishery, maximum likelihood estimates of selectivity were much more consistent among regions than the winter seine fishery (Fig. 2.22). Age at full recruitment to this gear type was roughly 5-6 years, and roughly the age at 50% vulnerability was roughly 3-4 years, with a tendency to recruit to the fishery at a younger age in the southern regions.

In the case of the gill net fishery, selectivity was allowed to vary over time according to variation in the empirical weight-at-age data (Fig. 2.23). Recall that selectivity for the gillnet fishery was modelled as a logistic function of age with the addition of age-specific deviations where selectivity can increase if the

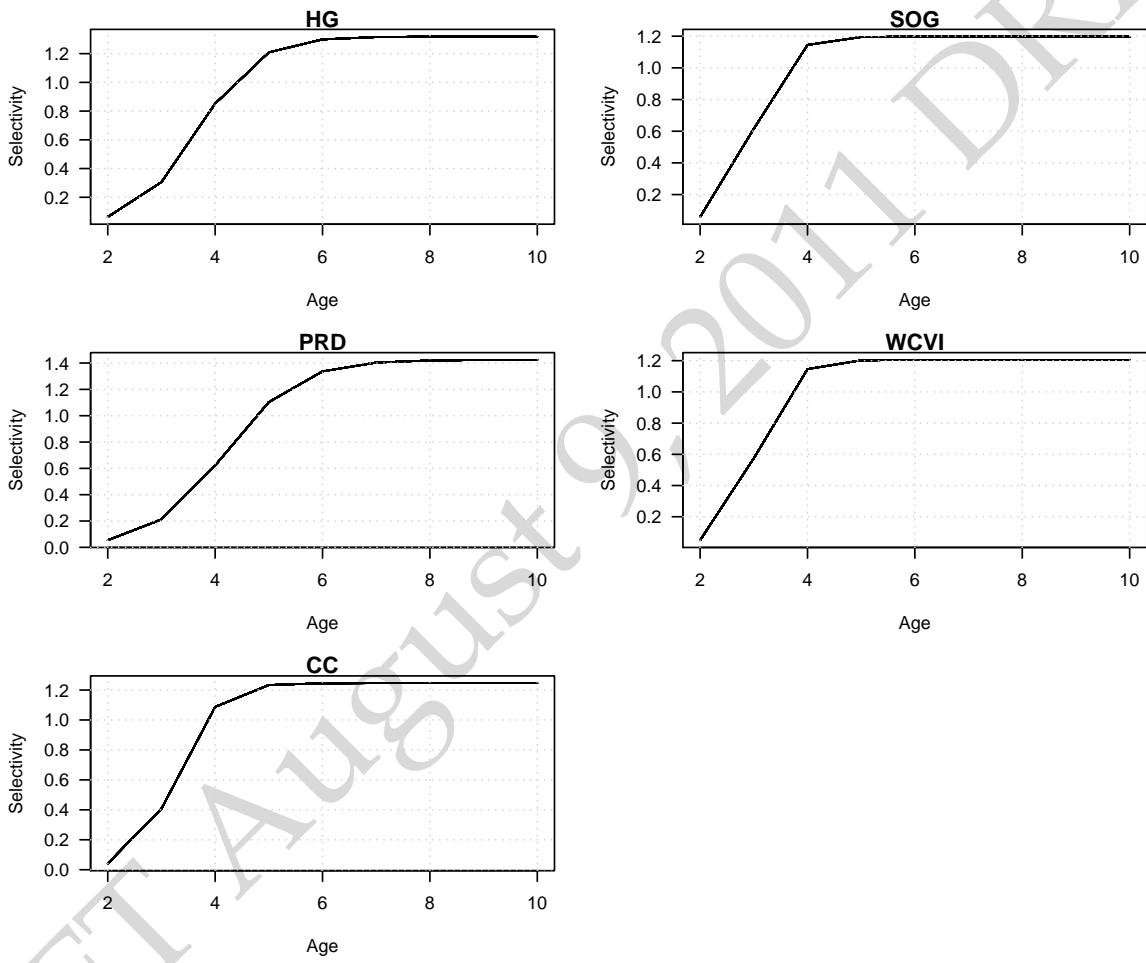


Figure 2.22: Maximum likelihood estimates of age-specific selectivity coefficients for the seine-roe fishery for each of the major stock areas.



Figure 2.23: Estimates of selectivity for the gillnet fleet for each of the five major stock assessment regions. In this case selectivity is a logistic function of the empirical weight-at-age data; due to declining growth there is a tendency for selectivity to shift to older ages.

weight-at-age is above average for that year. This selectivity function consists of three latent variables: two that describe the age-at-50% vulnerability and standard deviation in vulnerability-at-age, and a third parameter that describes the influence of variation in weight-at-age on departures from the logistic selectivity function ($\lambda^{(a)}$). Maximum likelihood estimates for these parameters for the gillnet fishery are presented in Table 2.2. With the exception of PRD and WCVI, estimates of $\lambda^{(a)}$ are negative and close to 0 implying no affect of variation in weight-at-age on selectivity or a slight negative effect (i.e., vulnerability to the gear declines for fish that are larger than the average weight). In the case of PRD and WCVI, the variation in weight-at-age explains approximately 4.1% and 8.7% of the residual variation in the age-composition data (Table 2.2).

2.7.5 Recruitment and stock-recruitment relationships

Recruitment to each stock is defined as the number of age-2 fish entering the population at the beginning of each year. Age-2 recruitment is estimated as a free parameter within $i\text{SCA}_M$, subject to the constraint that annual estimates vary around a Beverton-Holt stock recruitment relationship with an estimated standard

Table 2.2: Maximum likelihood estimates of gillnet selectivity parameters, where μ_a is the age-at-50% vulnerability, σ_a is the standard deviation in selectivity, and $\lambda^{(a)}$ is the coefficient that describes the influence of growth on selectivity ($\lambda^{(a)}=0$ implies no effect, $\lambda^{(a)} > 0$ implies a positive effect).

Stock	$\ln(\mu_a)$	$\ln(\sigma_a)$	$\lambda^{(a)}$
HG	1.598	-0.68125	-0.030581
PRD	1.727	-0.66217	0.040988
CC	1.604	-0.8050	-0.019404
SOG	1.540	-0.9797	-0.02835
WCVI	1.608	-0.6647	0.08677

deviation. Maximum likelihood estimates of age-2 recruits are shown in Figure 2.24 along with horizontal lines that demarcate the 0.33 and 0.66 quantiles that was traditionally used to categorize recruitment as poor, average, and good in previous assessments.

Estimates of age-2 recruits for 2010 and 2011 were average and good in HG, average in PRD, good and average in CC, good in SOG, and average and poor in the WCVI region.

The underlying stock-recruitment relationship is key for determining reference points for this stock. Maximum likelihood estimates of the age-2 recruits versus spawning biomass, along with the corresponding Beverton-Holt stock recruitment model are shown in Figure 2.25. The Beverton-Holt stock recruitment model was jointly fitted to these data by estimating the steepness of the stock recruitment relationship (h) and the unfished age-2 recruits (R_0). The unfished spawning biomass was determined by using the average fecundity and average natural mortality rates (from 1951-2011) to calculate the average spawning biomass per recruit. Alternative stock-recruitment models (e.g., Ricker model) were not explored to determine if they provided a better fit.

Between 1951 and 2011, four of the five major stock areas have fluctuated above the estimate of unfished spawning biomass; the exception is the PRD area. In HG, age-2 recruitment has been remarkably stable over a very wide range of spawner abundance. This is also the case for CC and WCVI. In PRD and SOG, variation in recruitment appears to be lower at low spawning abundance and the average recruitment rate tends to drop. Maximum likelihood estimates for steepness for these five stocks are as follows: HG – 0.81, PRD – 0.66, CC – 0.82, SOG – 0.76, WCVI – 0.77.

The log residual differences between the estimated age-2 recruits and that predicted by the estimated spawning-biomass and Beverton-Holt model for each of the major stock areas is shown in Figure 2.26. There is no strong autocorrelation in recruitment, except perhaps 5-8 year periods of poor and good recruitment in SOG. There is good correspondence between the standard deviations of the residuals and the estimated standard deviation of the process error variance (τ).

2.7.6 Retrospective analysis

Four of the five major regions contained little to no retrospective bias in the estimates of spawning stock biomass when fitting the data back to 2001 (10 years, Figure 2.27). The PRD region does show a strong retrospective biomass; as each year of data is removed estimates of the terminal spawning biomass that year increase. This pattern of declining estimates of biomass as data are added is persistent for all of the years in which the retrospective estimates were examined.

2.7.7 Marginal posterior distributions

Marginal posterior distributions for estimated model parameters were constructed using AD Model Builders built in Metropolis-Hastings algorithm (Gelman, 2004). For each of the major and minor assessment areas, a systematic sample of 2,000 points from a chain of length 1,000,000 and is intended to represent a random sample from the joint posterior distribution. These samples were then used to construct marginal distributions for derived quantities (e.g., B_0). All areas with the exception of the SOG used the inverse Hessian

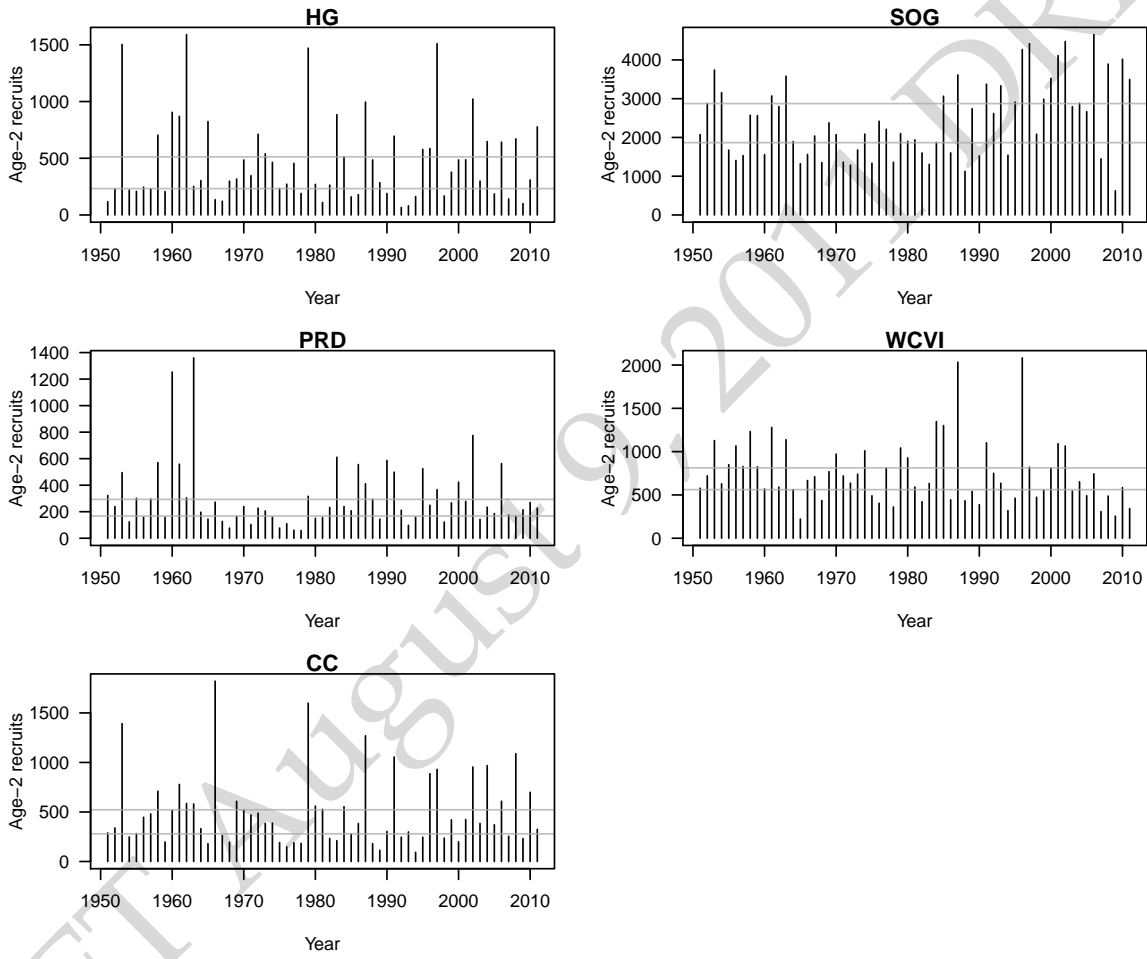


Figure 2.24: Maximum likelihood estimates of age-2 recruits for each of the five major stock areas. The horizontal divisions demarcate the 0.33 and 0.66 quantiles that define poor, average, and good recruitment.

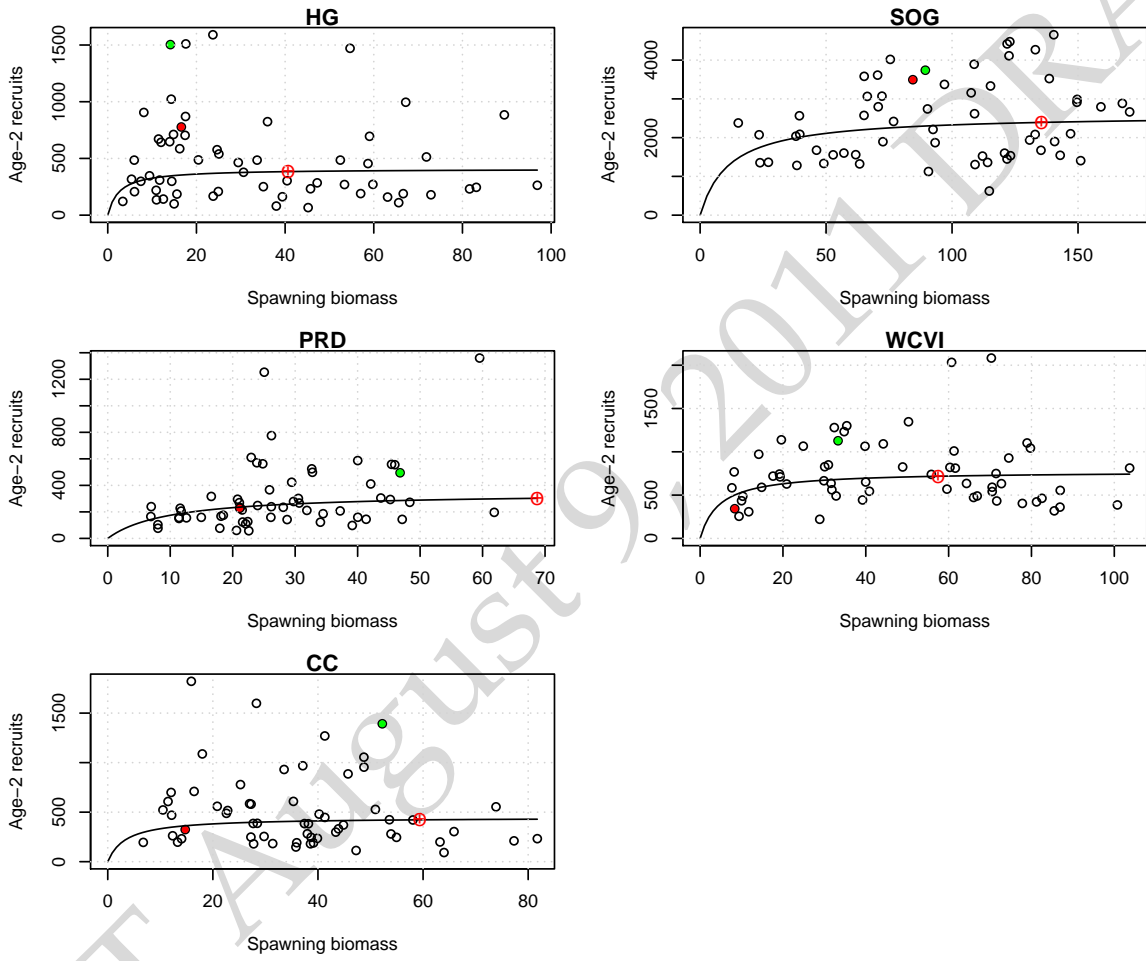


Figure 2.25: Maximum likelihood estimates of age-2 recruits versus estimated spawning stock biomass in each of the five major assessment regions. The green and red circles indicate the start (recruits in 1952) and end (recruits in 2011) of the series, the circle plus (red) corresponds to the maximum likelihood estimate of unfished spawning biomass (B_0) and unfished age-2 recruitment R_0 , the line is the Beverton-Holt stock recruitment model fitted to these data.

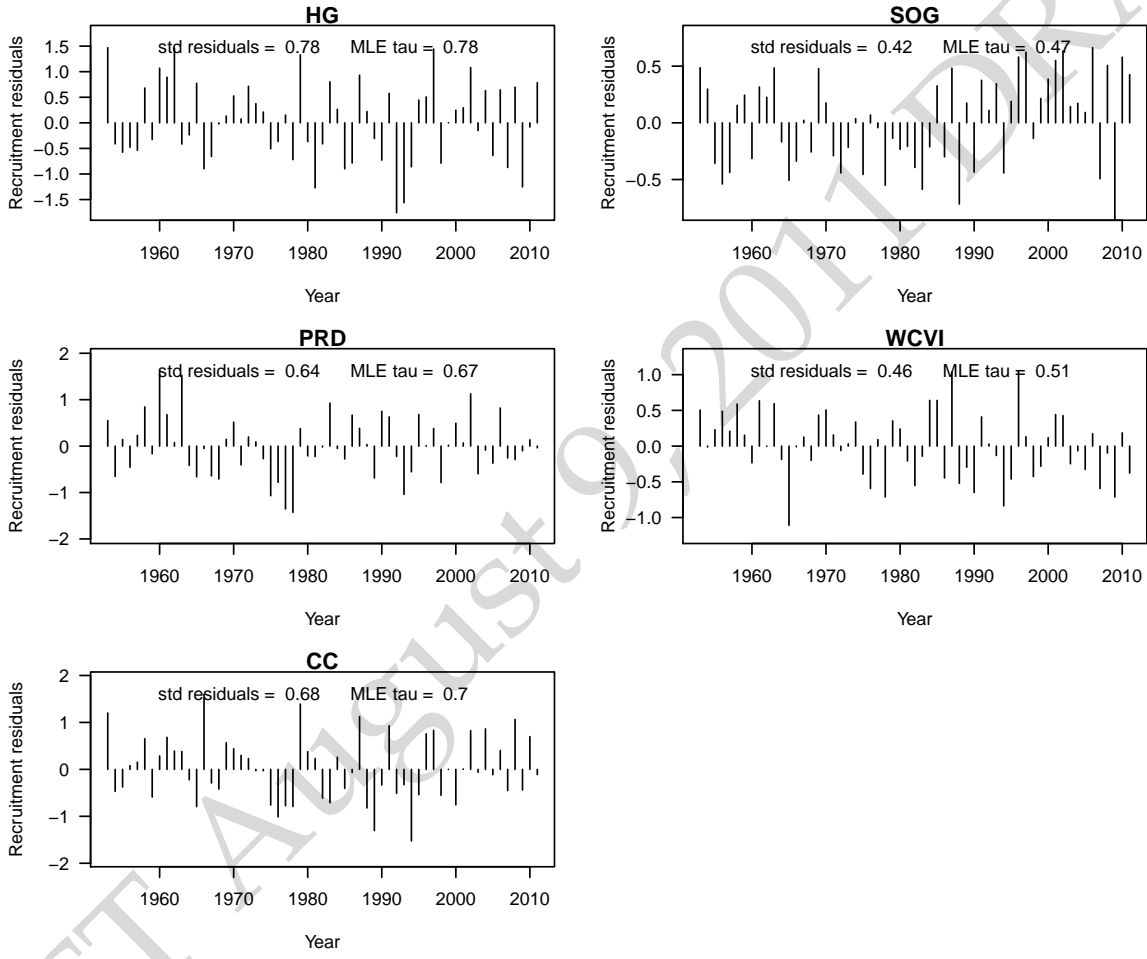


Figure 2.26: Log residual differences between estimated age-2 recruits and the recruitment predicted by the Beverton-Holt model and estimated spawning stock biomass. The standard deviations of the residuals along with the MLE estimate of the process error standard deviations are displayed at the top of each panel.

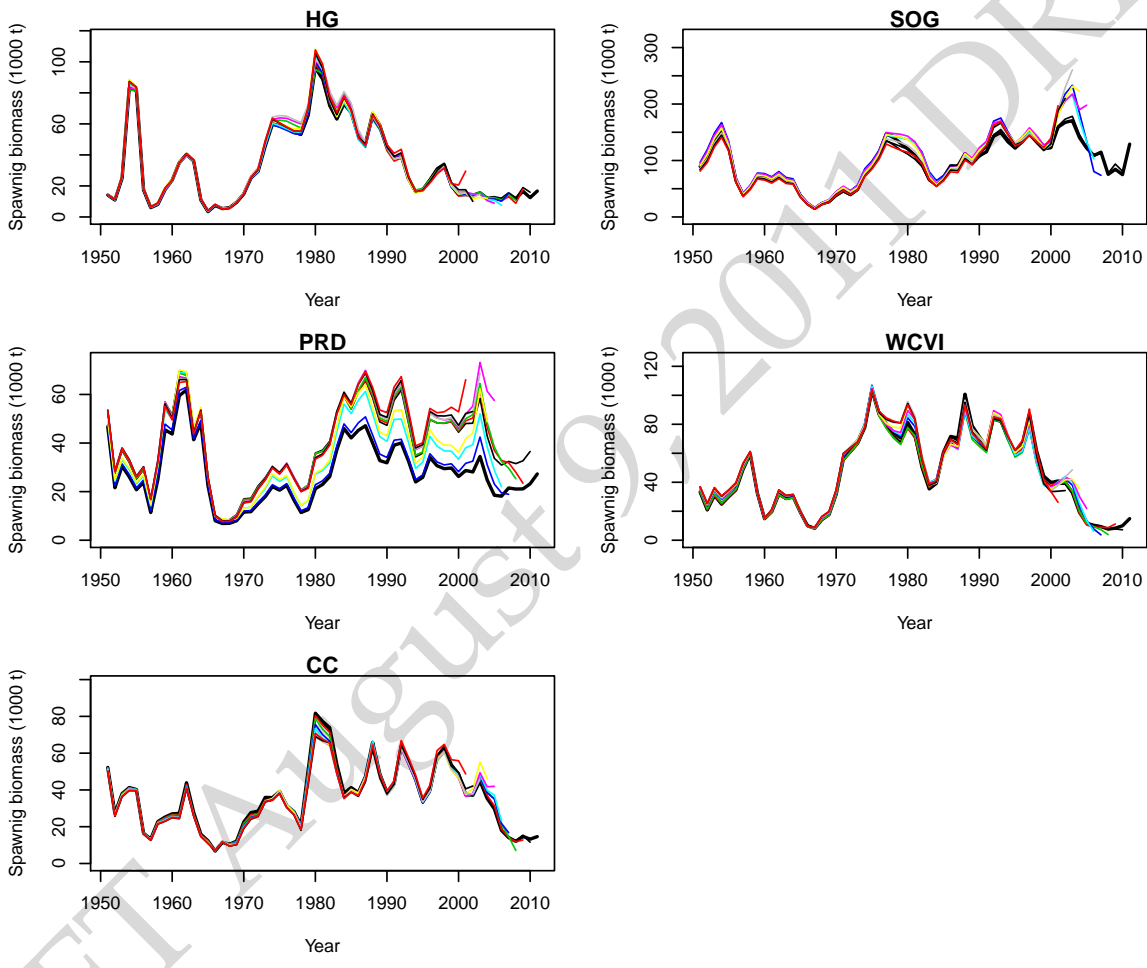


Figure 2.27: Retrospective estimates of spawning stock biomass for each of the five major stock assessment areas. The model was sequentially fitted to the full data set, then from 1951:2010, 1951:2009, ... 1951:2001.

matrix as the jumping distribution. In the case of SOG, the hessian matrix had to be re-scaled (using the `-mcmult 2.0` option in ADMB) in order to invert the Hessian matrix.

Diagnostic trace plots

No formal statistical tests were carried out to determine if the samples from the joint posterior distribution were taken from a converged distribution. Visual inspection was used to determine overall convergence and the trace plots for each of the five major regions are shown in Figures 2.28–2.32.

2.7.8 Parameter confounding

To examine the level of confounding among the estimated parameters, 200 randomly selected points from the joint posterior distribution for the seven leading parameters were plotted against each other in a pairs plot (e.g., Fig. 2.33). Only 200 points were plotted to reduce the file size. Among the seven leading estimated parameters ($R_0, h, M, \bar{R}, \ddot{R}, \rho, \vartheta$) there was very little confounding (Figures 2.33 – 2.37).

There is, however, some strong confounding between the estimated parameters and a few of the derived reference points. In all major areas, there was a strong positive correlation between steepness (h) and F_{MSY} ; similarly there is a strong positive correlation between B_0 and R_0 . Among the reference points alone, there is a negative correlation between B_{MSY} and F_{MSY} , and a positive correlation between F_{MSY} and MSY . This level of confounding among the derived variables is not cause for concern from a parameter estimation standpoint; it does, however, highlight the tradeoffs that must be made from a decision makers perspective.

2.7.9 Marginal posterior distributions

Marginal posterior distributions along with the prior densities for the seven leading parameters are shown in Figure 2.38. In all cases, the steepness parameter, followed by the instantaneous natural mortality rate appears to be the most influenced by the prior density. Uniform prior distributions were assumed for the scaling parameters (R_0, \bar{R} , and \ddot{R}). There were good posterior updates for the total variance and variance portioning parameters (ϑ, ρ).

2.7.10 Forecast and catch advice based on the joint posterior distribution

Catch advice has historically been provided in the form of a decision table based on median values of the joint posterior distribution. The decision table contains columns specifying the 2011 SSB the age 4+ total biomass, estimates of age-3 recruit biomass for poor, average, and good recruitment, cutoff levels, and the available harvest under poor, average, and good recruitment scenarios. Moving towards DFO's sustainable fisheries framework (SFF) is a necessary next step.

Cutoff levels for the BC herring stocks is defined as $0.25B_0$. The historical cutoff levels have not been updated for the over 10 years now (1996/1997). Recent stock assessments for BC herring have assumed $q = 1$ for the spawn survey data (the lead author is unaware if the historical estimates of B_0 were based on the same $q = 1$ assumption). In this assessment we have relaxed this assumption and as a consequence estimates of herring biomass have increased substantially. Due to significant changes in population scaling it would not make sense to continue to use the previous cutoff levels as this may lead to policies that would result in overfishing or under utilization of the resource. We therefore present catch advice based on both the old cutoffs and the new cutoffs in Tables 2.3-2.4

2.8 Stock assessments for minor stock areas

Abundance estimates for the minor stock areas, Area 2W and Area 27 were also obtained using the $iSCA_M$ model. For these minor areas, there were some minor differences in the treatment of the data and model assumptions. Also, the gillnet selectivity in area 27 was not allowed to vary over time due to the sparse amount of information (and presumably biological samples) available to reliably estimate minor changes

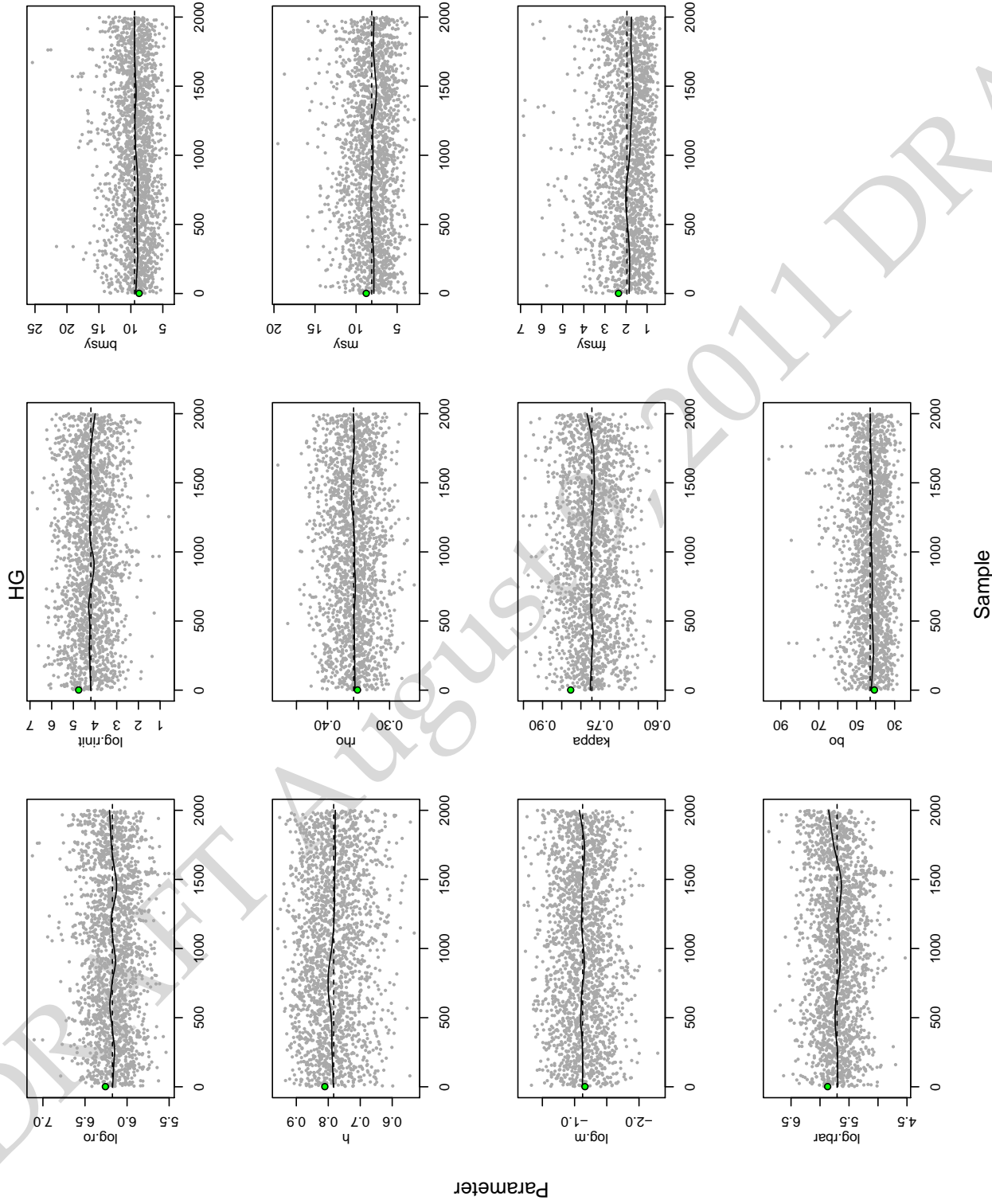


Figure 2.28: A systematic sample of 2,000 from an MCMC chain of length 1,000,000 of leading parameters and derived variables used in reference point calculations for HG. Green circle corresponds to the MLE estimates and the solid line is a lowess smooth fit to the data ($f=1/4$), and the dashed line is the mean of the distribution.

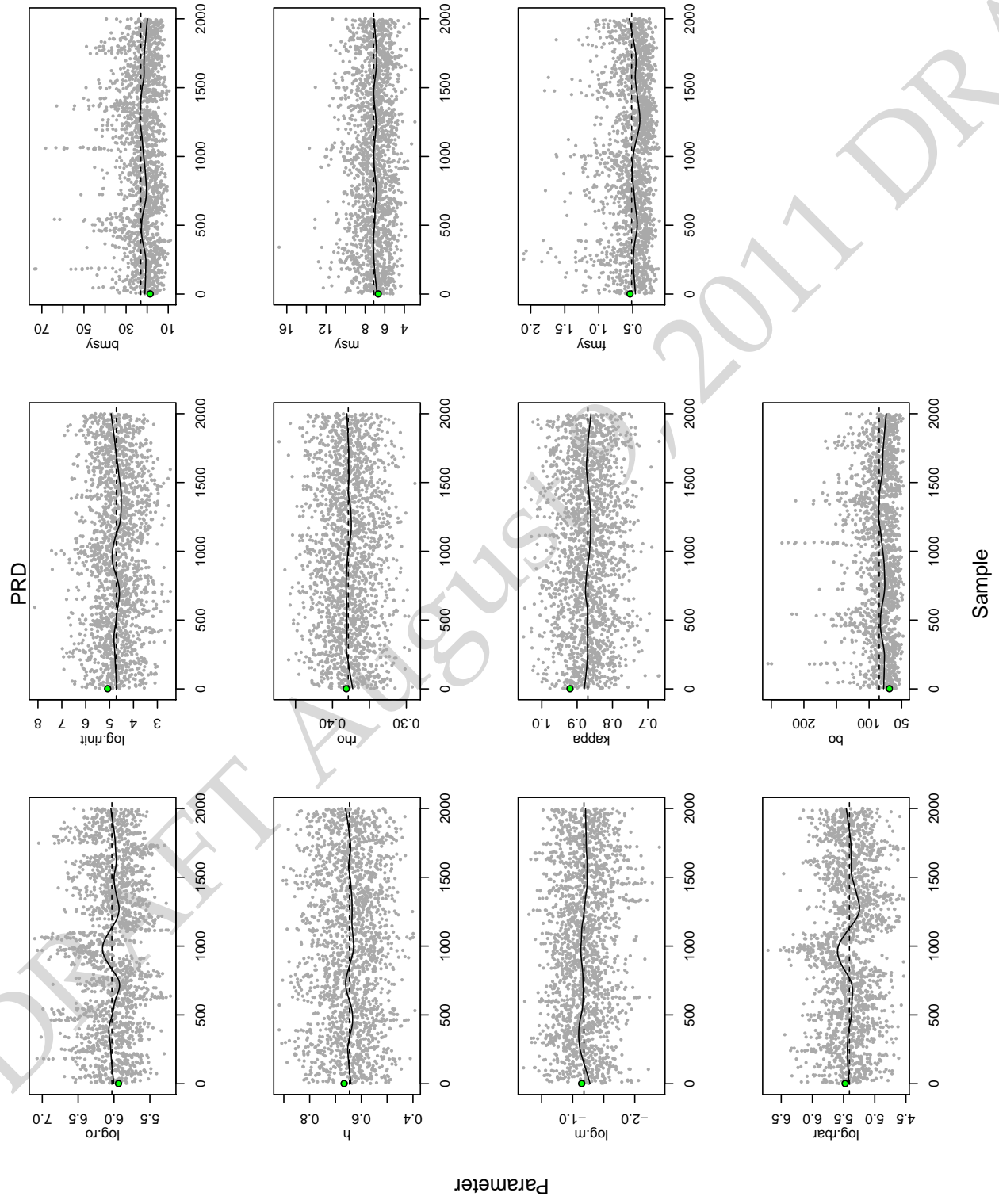


Figure 2.29: A systematic sample of 2,000 from an MCMC chain of length 1,000,000 of leading parameters and derived variables used in reference point calculations for PRD. Green circle corresponds to the MLE estimates and the solid line is a lowess smooth fit to the data ($f=1/4$), and the dashed line is the mean of the distribution.

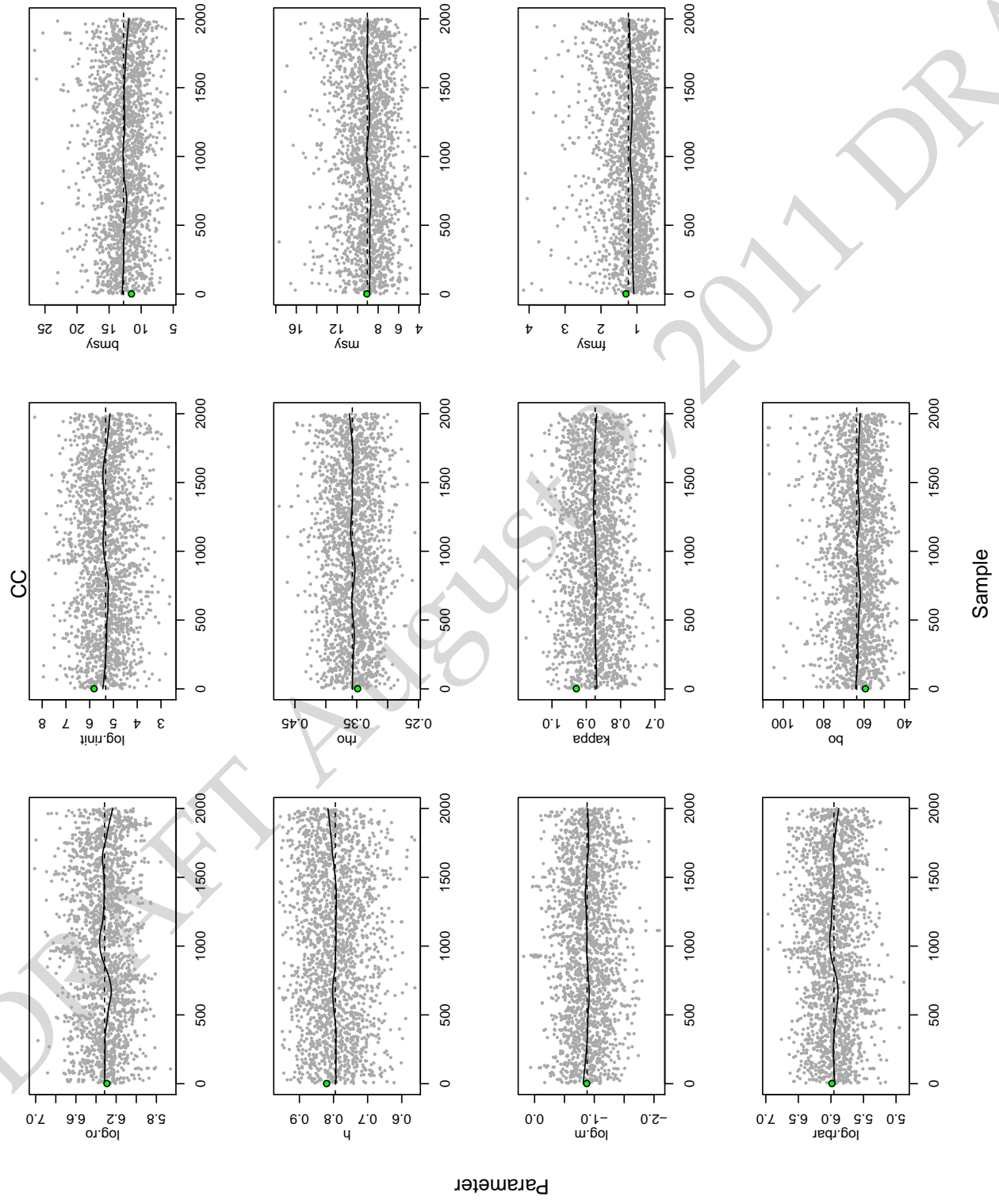


Figure 2.30: A systematic sample of 2,000 from an MCMC chain of length 1,000,000 of leading parameters and derived variables used in reference point calculations for CC. Green circle corresponds to the MLE estimates and the solid line is a lowess smooth fit to the data ($f=1/4$), and the dashed line is the mean of the distribution.

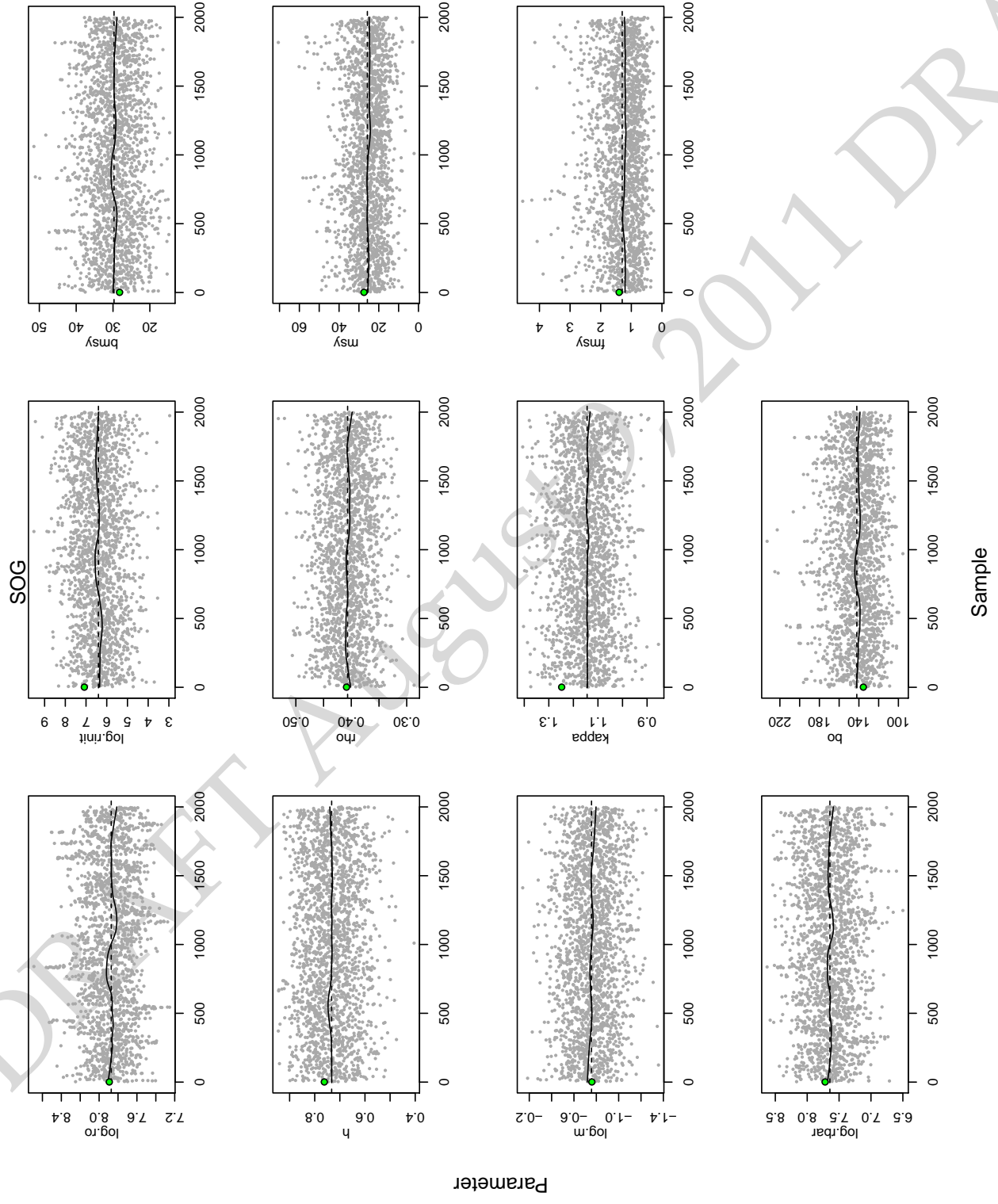


Figure 2.31: A systematic sample of 2,000 from an MCMC chain of length 1,000,000 of leading parameters and derived variables used in reference point calculations for SOG. Green circle corresponds to the MLE estimates and the solid line is a lowess smooth fit to the data ($f=1/4$), and the dashed line is the mean of the distribution.

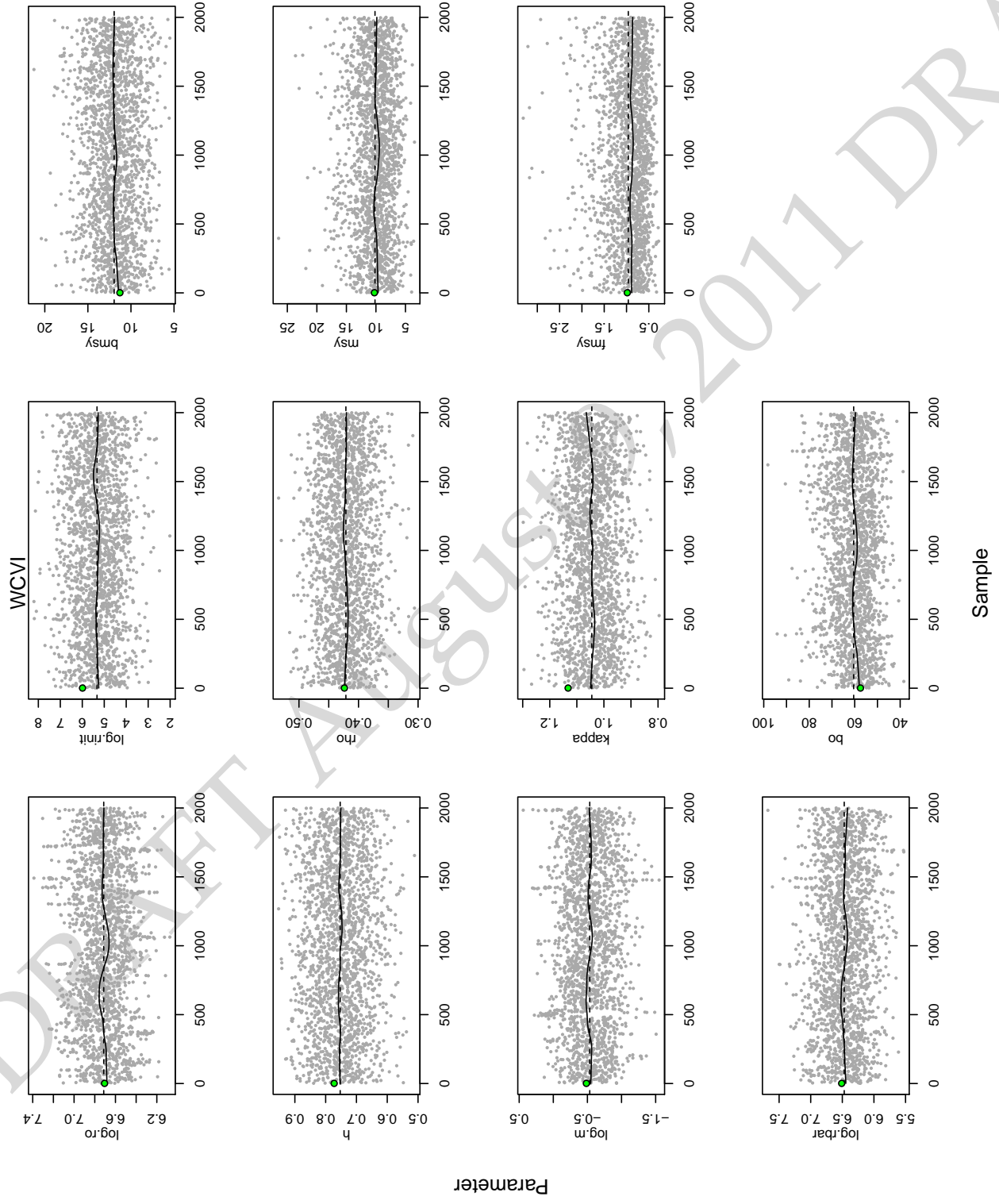


Figure 2.32: A systematic sample of 2,000 from an MCMC chain of length 1,000,000 of leading parameters and derived variables used in reference point calculations for WCVI. Green circle corresponds to the MLE estimates and the solid line is a lowess smooth fit to the data ($f=1/4$), and the dashed line is the mean of the distribution.

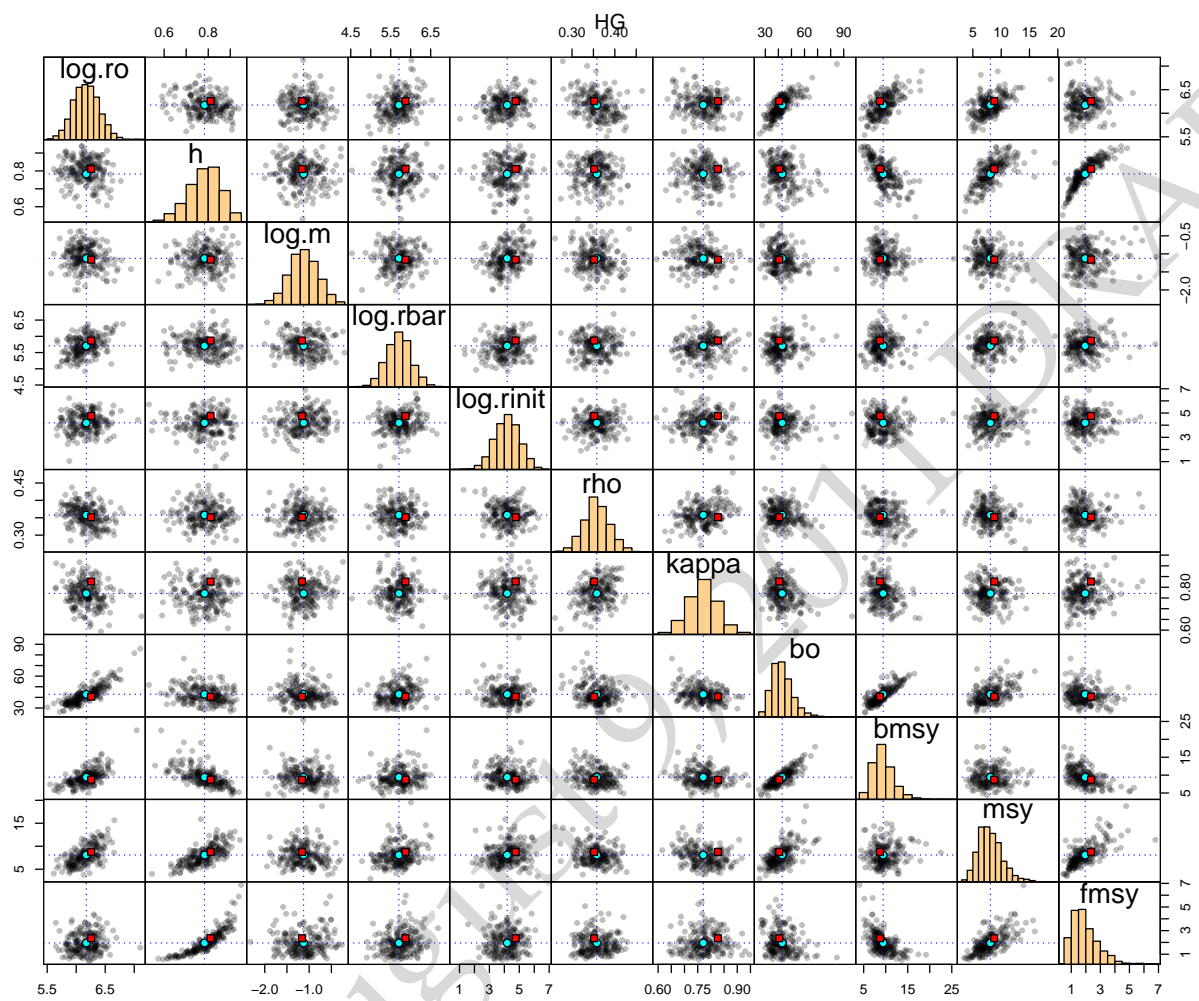


Figure 2.33: Pairs plot and marginal distributions for leading parameters in HG region (200 random samples). The dotted lines correspond to the means of the distributions, circle is the mean, and the red square is the mode of the distribution.

Table 2.3: Estimated spawning stock biomass, age-4+ biomass and pre-fishery biomass for poor average and good recruitment, old cutoffs, and available harvest based on median values from the joint posterior distribution.

Stock	SSB	4+ Biomass	Pre-fishery forecast biomass			Cutoff	Available harvest		
			Poor	Average	Good		Poor	Average	Good
HG	16,579	7,089	9,618	12,892	21,478	10,700	0	2,192	4,296
PRD	27,046	20,593	24,150	27,492	37,286	12,100	4,830	5,498	7,457
CC	14,666	7,809	11,357	14,709	22,883	17,600	0	0	4,577
SOG	125,261	72,937	94,703	112,856	138,448	21,200	18,941	22,571	27,690
WCVI	14,679	8,267	15,321	20,906	31,130	18,800	0	2,106	6,226

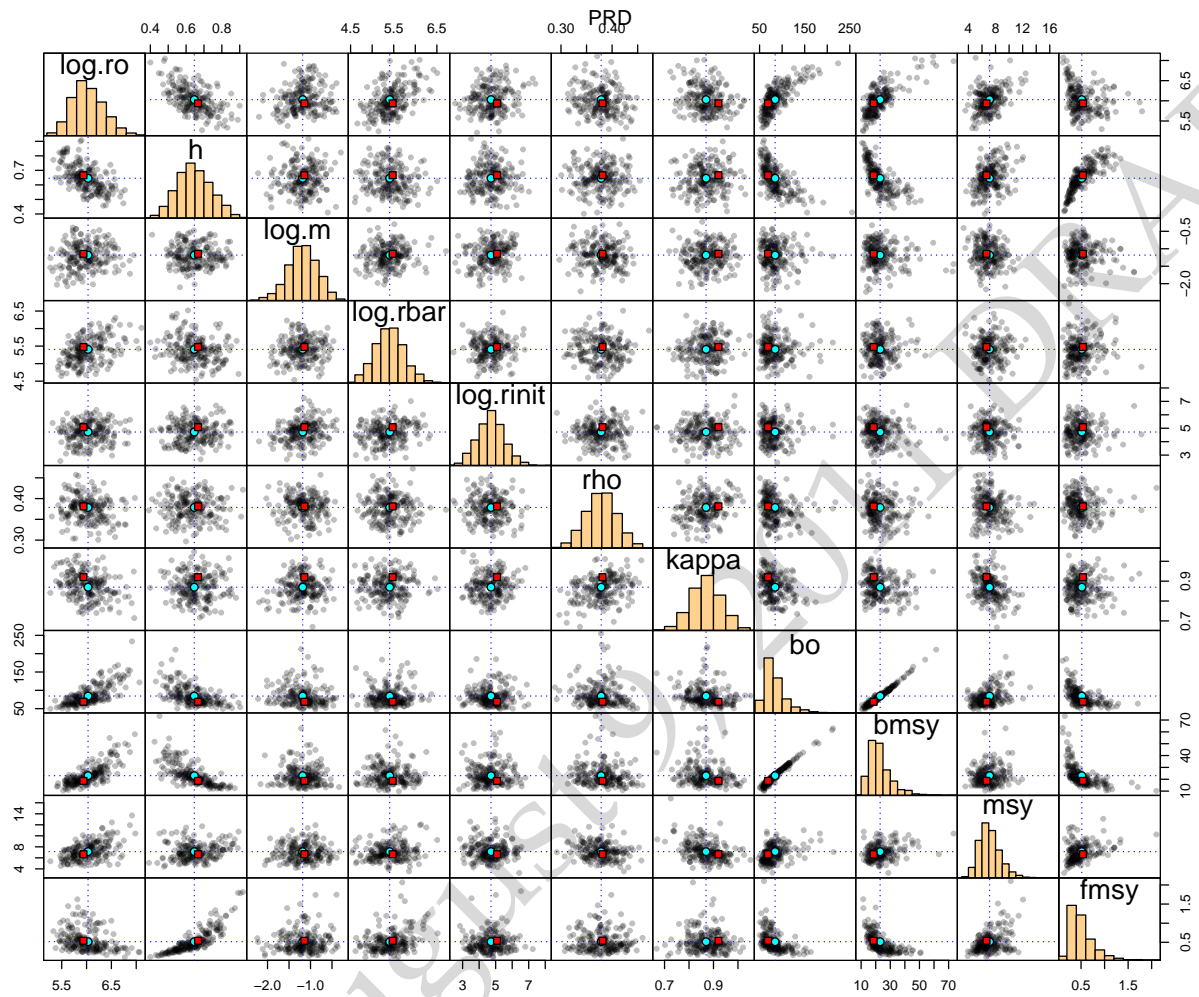


Figure 2.34: Pairs plot and marginal distributions for leading parameters in PRD region (200 random samples). The dotted lines correspond to the means of the distributions, circle is the mean, and the red square is the mode of the distribution.

Table 2.4: Estimated spawning stock biomass, age-4+ biomass and pre-fishery biomass for poor average and good recruitment, new cutoffs (based on median value of $0.25B_0$ estimated within the $i\text{SCA}_M$ model), and available harvest based on the median values from the joint posterior distribution.

Stock	SSB	4+ Biomass	Pre-fishery forecast biomass			Cutoff	Available harvest		
			Poor	Average	Good		Poor	Average	Good
HG	16,579	7,089	9,618	12,892	21,478	10,436	0	2,456	4,296
PRD	27,046	20,593	24,150	27,492	37,286	19,641	4,510	5,498	7,457
CC	14,666	7,809	11,357	14,709	22,883	15,600	0	0	4,577
SOG	125,261	72,937	94,703	112,856	138,448	35,013	18,941	22,571	27,690
WCVI	14,679	8,267	15,321	20,906	31,130	14,894	427	4,181	6,226

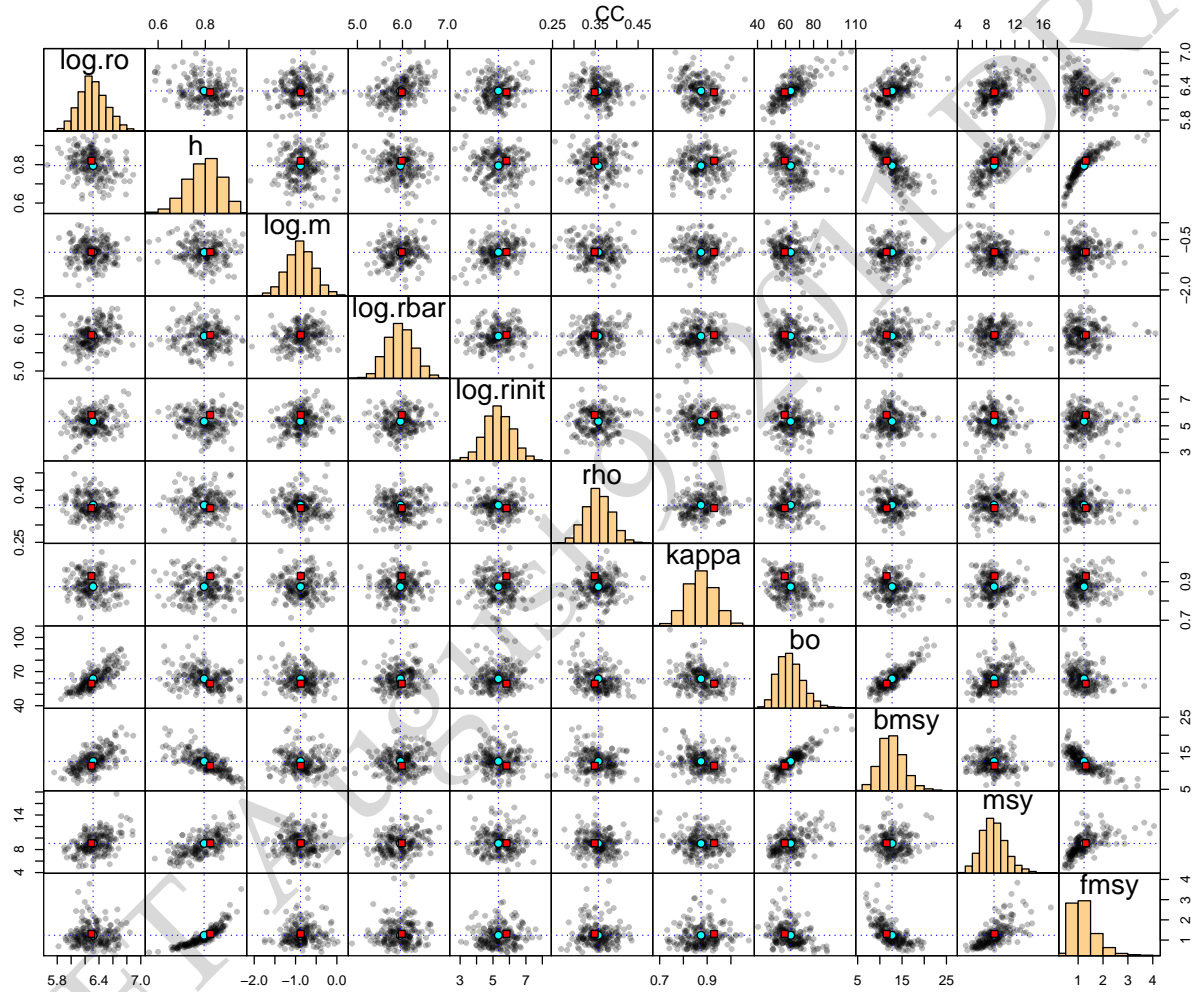


Figure 2.35: Pairs plot and marginal distributions for leading parameters in CC region (200 random samples). The dotted lines correspond to the means of the distributions, circle is the mean, and the red square is the mode of the distribution.

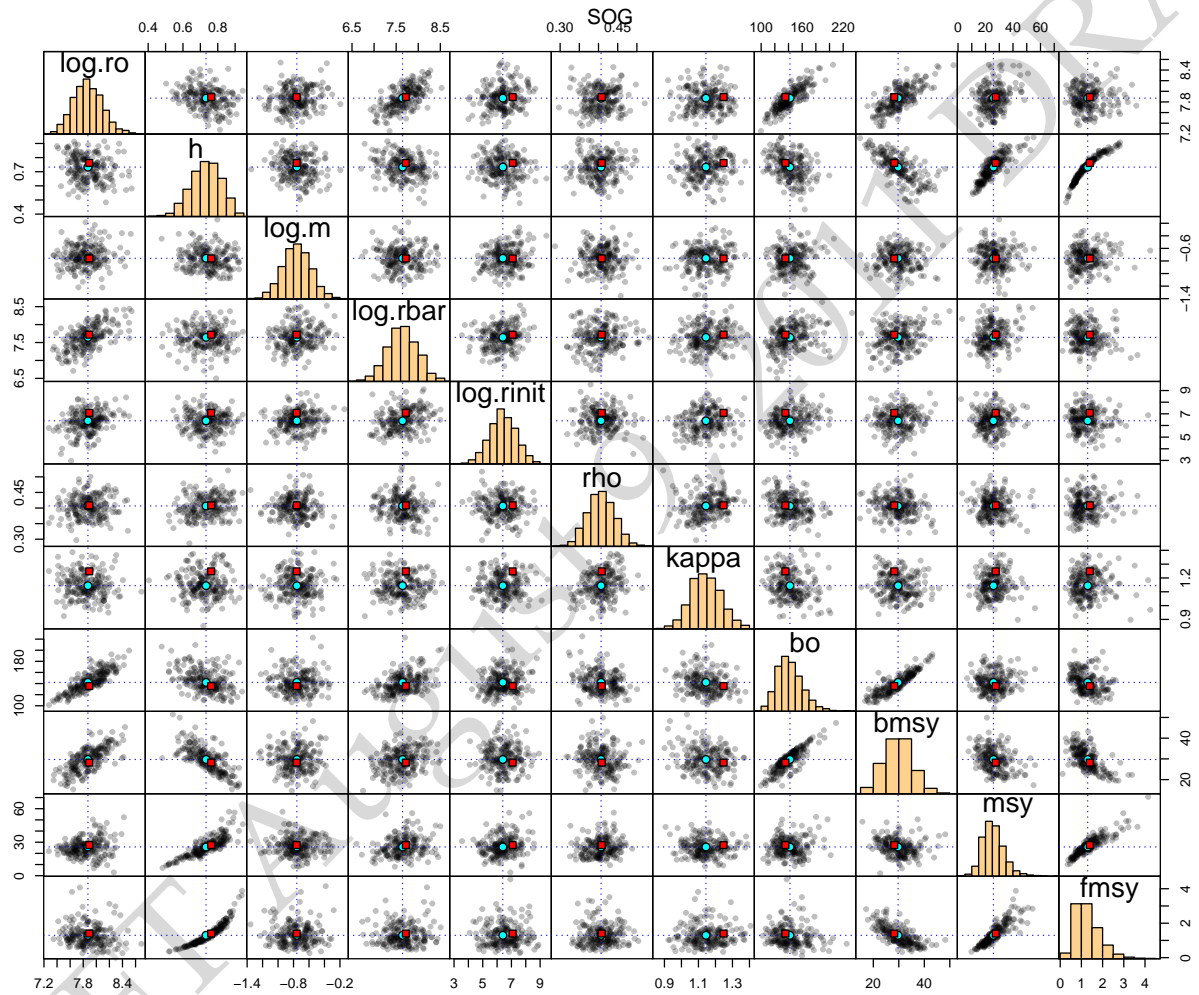


Figure 2.36: Pairs plot and marginal distributions for leading parameters in SOG region (200 random samples). The dotted lines correspond to the means of the distributions, circle is the mean, and the red square is the mode of the distribution.

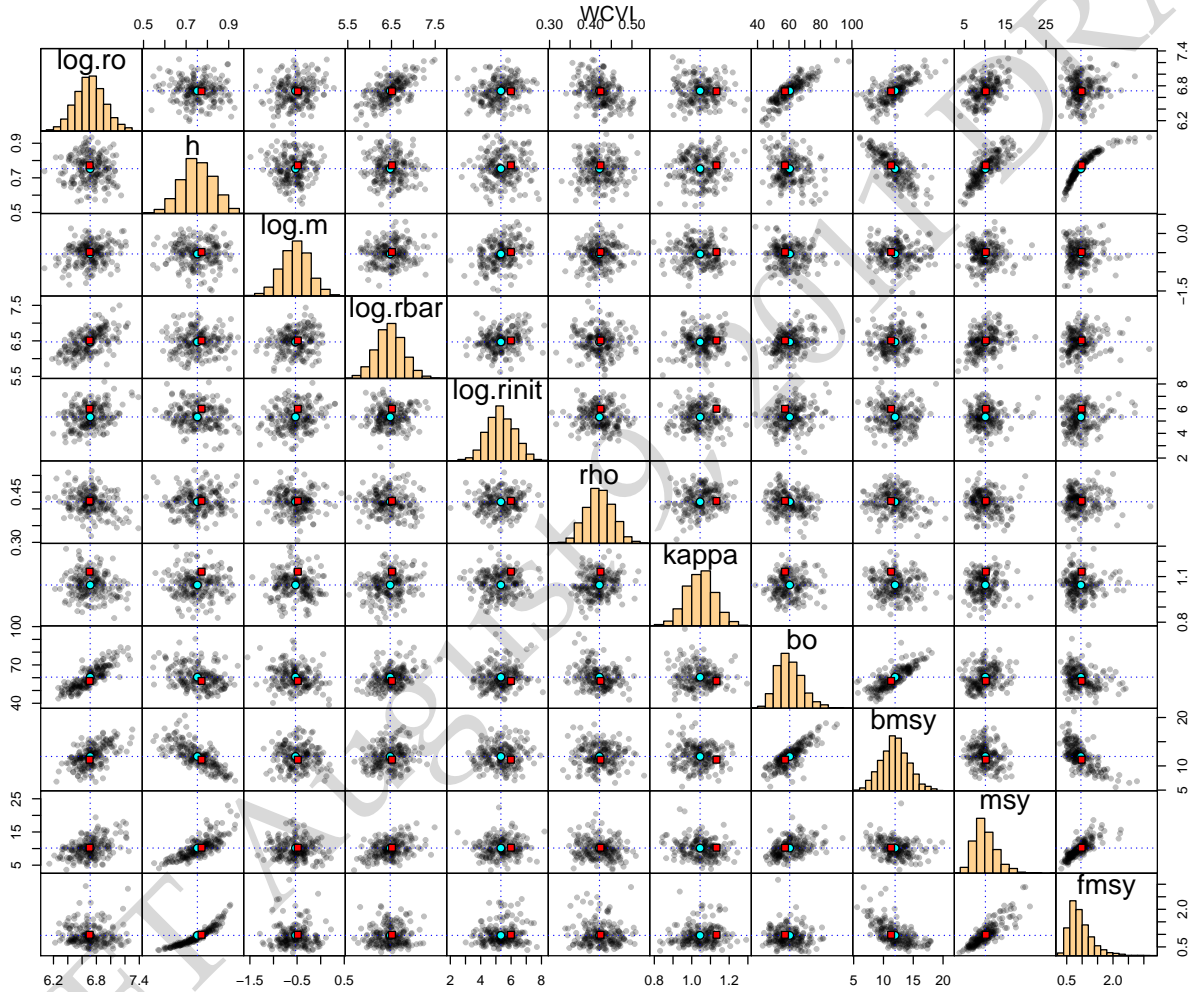


Figure 2.37: Pairs plot and marginal distributions for leading parameters in WCVI region (200 random samples). The dotted lines correspond to the means of the distributions, circle is the mean, and the red square is the mode of the distribution.

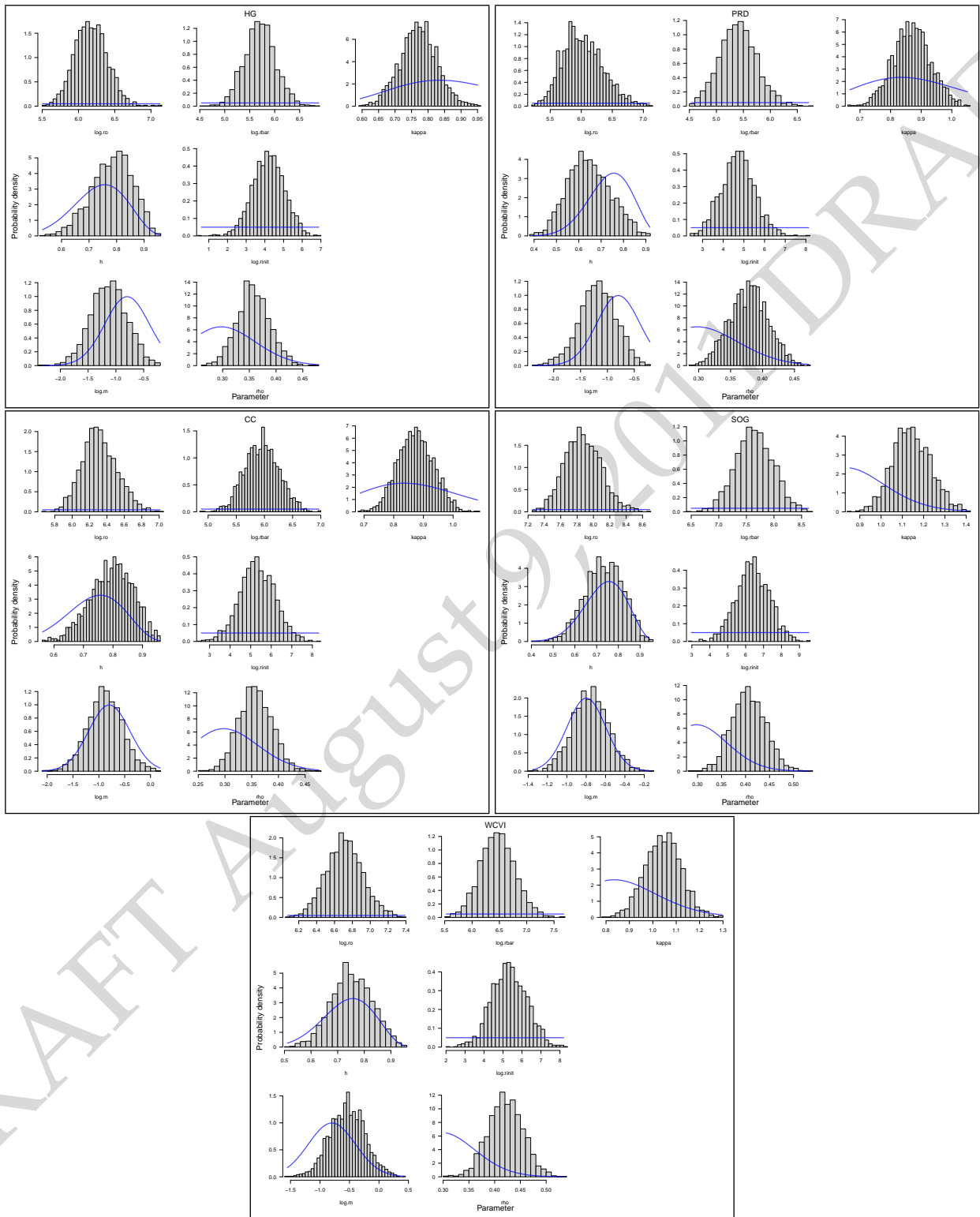


Figure 2.38: Marginal posterior densities (histograms) and prior densities (lines) for the seven leading parameters for each of the five major assessment regions.

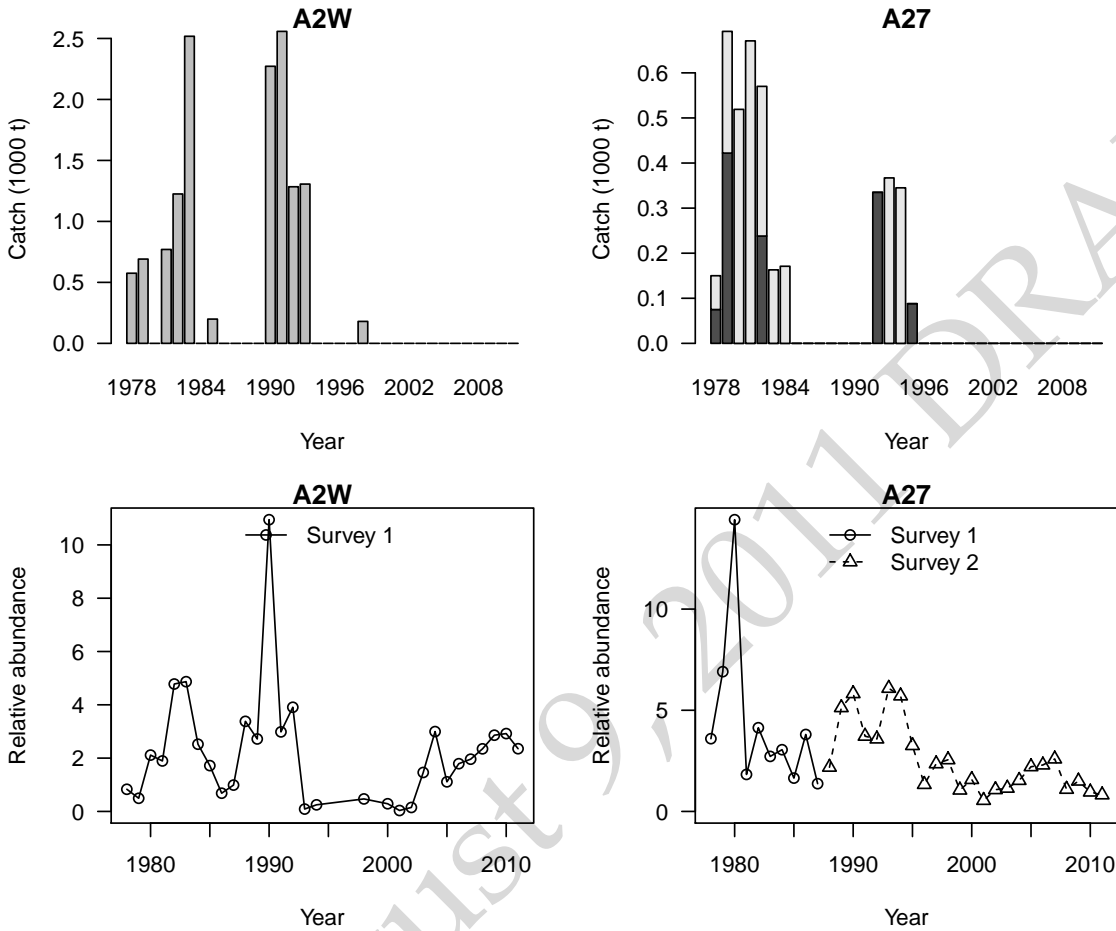


Figure 2.39: Catch and survey data for minor stock Areas 2W and Area 27.

in selectivity for this fishery. Selectivity for area 27 gillnet fishery was assumed to be a logistic function of age and invariant over time.

The input data (Catch and relative abundance) for the minor areas is shown in Figure 2.39. As in the previous assessments of Area 2W, the spawn survey data is treated as a single continuous series from 1978 to 2011. Area 27 however, the time series is split into two series between 1978-1987 and 1988-2011. The age-composition data used in fitting the model is shown in Figure 2.40.

2.8.1 Maximum likelihood estimates of biomass

Spawning biomass in 2011 for Area 2W and Area 27 was estimated at 4,671 tonnes and 928 tonnes, respectively (Table 2.5). The time series of total biomass and spawning biomass for these two areas is presented in Figure 2.41

2.8.2 Estimates of recruitment and reference points

Maximum likelihood estimates of age-2 recruitment, stock-recruitment relationships and residuals in the stock-recruitment model is shown in Figure 2.42. Estimates of age-2 recruits in area 2W have been poor-

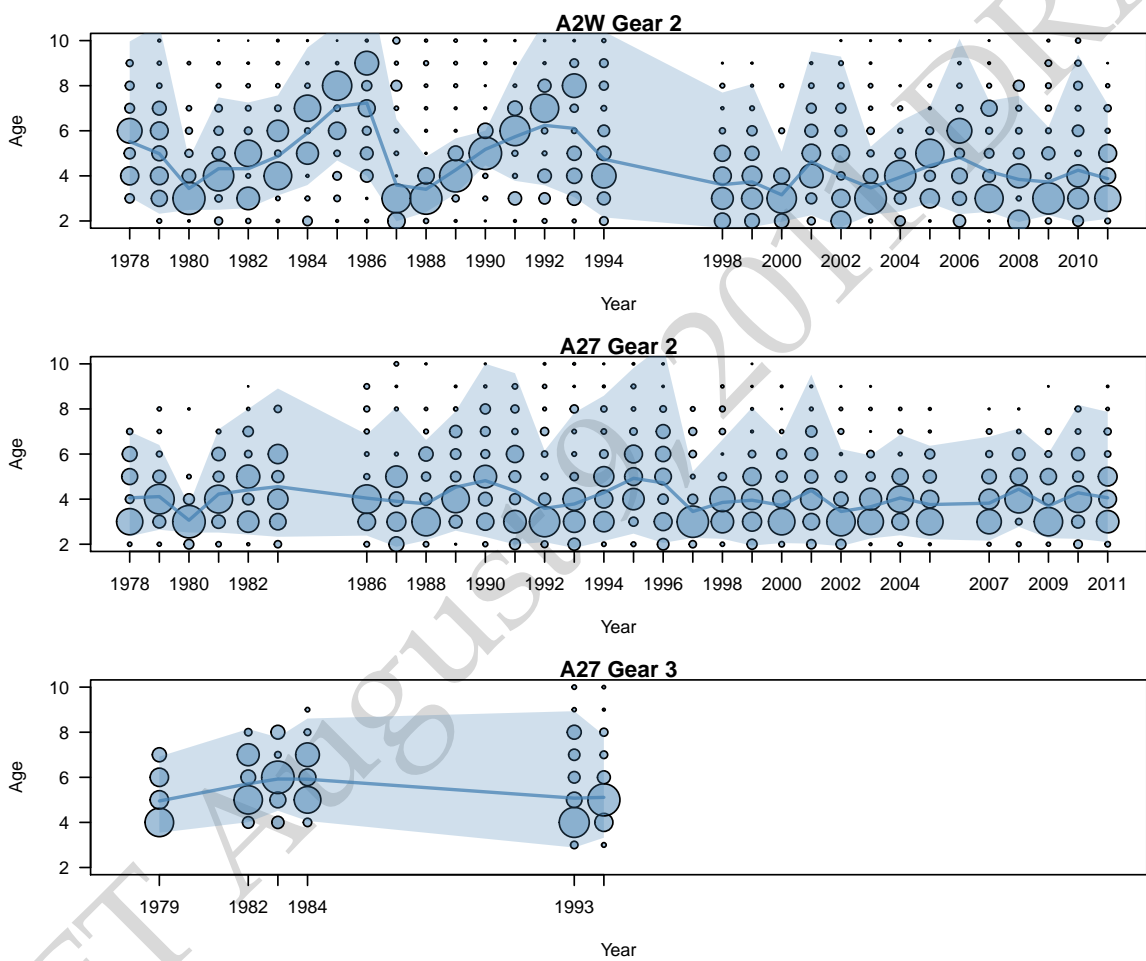


Figure 2.40: Age composition data for Area 2W and Area 27 for the seine-roe fishery (Gear 2) and the gillnet fishery (Gear 3).

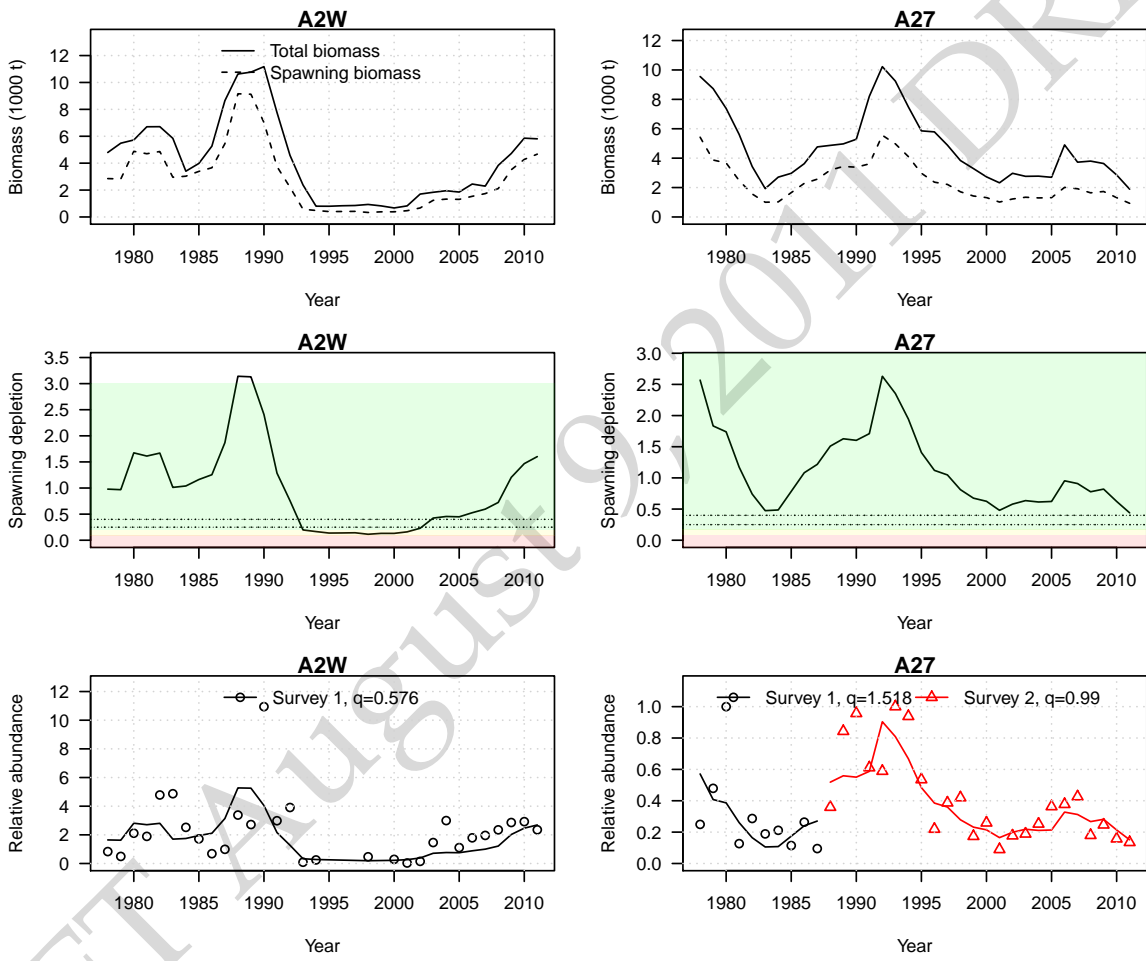


Figure 2.41: Maximum likelihood estimates of total biomass, spawning biomass, spawning depletion and fits to the spawn survey data for the two minor stock areas.

Table 2.5: Summary of maximum likelihood estimates for the two minor stock areas. No. is the total number of estimated parameters, F_{MSY} the average instantaneous fishing rate to achieve the maximum sustainable yield (MSY), B_0 is the unfished spawning biomass, B_{MSY} is the spawning biomass that achieves maximum sustainable yield, B_t is the spawning biomass at the end of the 2011 fishing season, and B_t/B_0 is the spawning depletion level at the end of the 2011 fishing season.

Stock	A2W	A27
No.	74	80
F_{MSY}	0.34	1.81
MSY	265	290
B_0	2,915	2,112
$0.25B_0$	729	528
B_{MSY}	705	448
$0.8B_{MSY}$	564	358
$0.4B_{MSY}$	282	179
B_t	4,671	928
B_t/B_0	1.6	0.44

to average for much of the time-series. There have been 4 periods of above average recruitment for area 2W (late 1970s, mid 1980s, 2002, and 2008–2010). Recruitment in area 27 has been much more consistent by comparison. Estimates of unfished spawning biomass for areas 2W and 27 are 2,915 tonnes and 2,112 tonnes.

2.8.3 Retrospective analysis

There is almost no retrospective bias for the estimates of spawning stock biomass in area 27 using data between 1951:2001 and 1951:2011 (Fig. 2.43). In Area 2W, there is a slight retrospective bias in the estimates of spawning stock biomass. As the more recent data are fit in the model estimates of spawning biomass in the mid 2000s are revised downwards.

2.8.4 Marginal posterior distributions and trace plots

Information for the catch advice for the two minor areas is based on the median values of the joint posterior distribution. Therefore, it is important to show posterior samples to ensure proper convergence and the marginal posterior distributions for the leading parameter estimates and derived variables that are of management interest.

The trace plots for the two minor areas are summarized in Figure 2.44, and the marginal distributions for the leading parameters is shown in Figure 2.45. Again, no formal convergence statistics were examined to determine if MCMC chain converged to a stable distribution. Visual inspection of the trace plots appear to have a homogenous distribution over the course of the 2000 samples. In both of the statistical areas, the posterior updates did occur (Figure 2.45). The marginal posterior for steepness in area 27 does appear to be influenced considerably by the assumed prior distribution.

2.8.5 Catch advice

Catch advice for the minor areas differs from that of the major areas in that there are not cutoffs for these two areas and the reference exploitation rate is reduced from 20% to 10%. The same decision table format is provided with catch advice based on poor, average, and good recruitment. Catch advice for the two minor areas is summarized in Table 2.6.

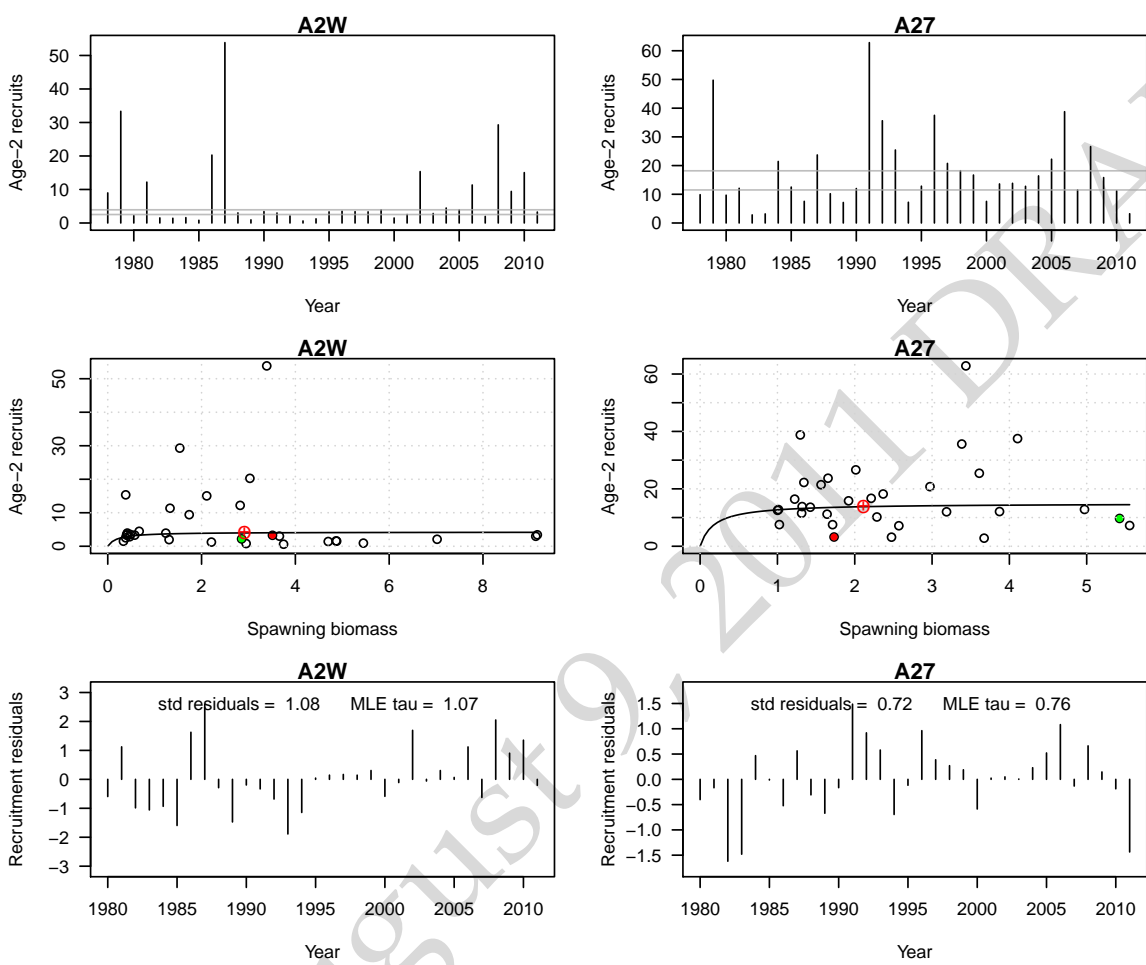


Figure 2.42: Maximum likelihood estimates of age-2 recruits, spawner-recruit relationships with the fitted Beverton Holt model and unfished reference points (B_o, R_o), and the residuals between the estimated age-2 recruits and that predicted by the Beverton-Holt model.

Table 2.6: Estimated spawning stock biomass, age-4+ biomass and pre-fishery biomass for poor average and good recruitment, cutoffs, and available harvest based on median values of the joint posterior distribution for the two minor areas. All units are in tonnes.

Stock	Pre-fishery forecast biomass						Available harvest		
	SSB	4+ Biomass	Poor	Average	Good	Cutoff	Poor	Average	Good
A2W	5,448	5,204	5,294	5,398	6,141	0	529	540	614
A27	1,077	692	909	1,124	1,736	0	91	112	174

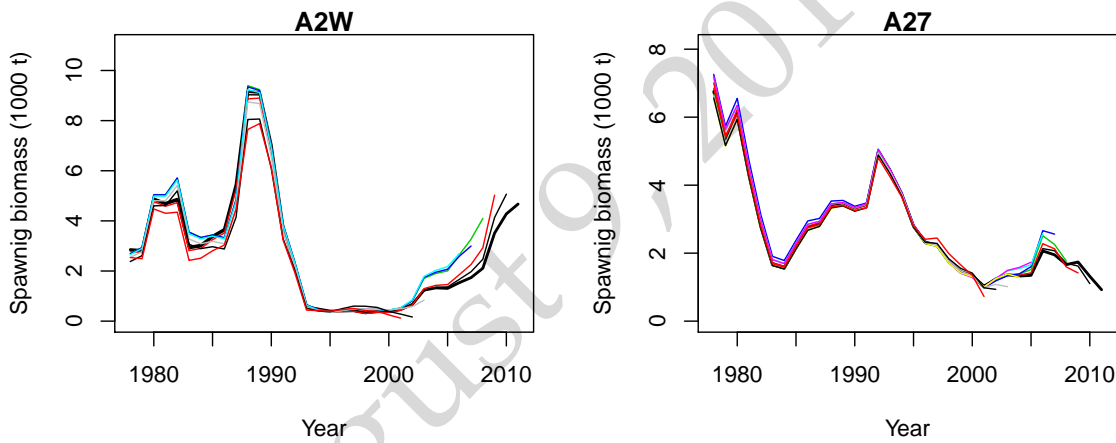


Figure 2.43: Retrospective estimates of spawning stock biomass for each of the minor stock assessment areas. The model was sequentially fitted to the full data set, then from 1951:2010, 1951:2009, ... 1951:2001.

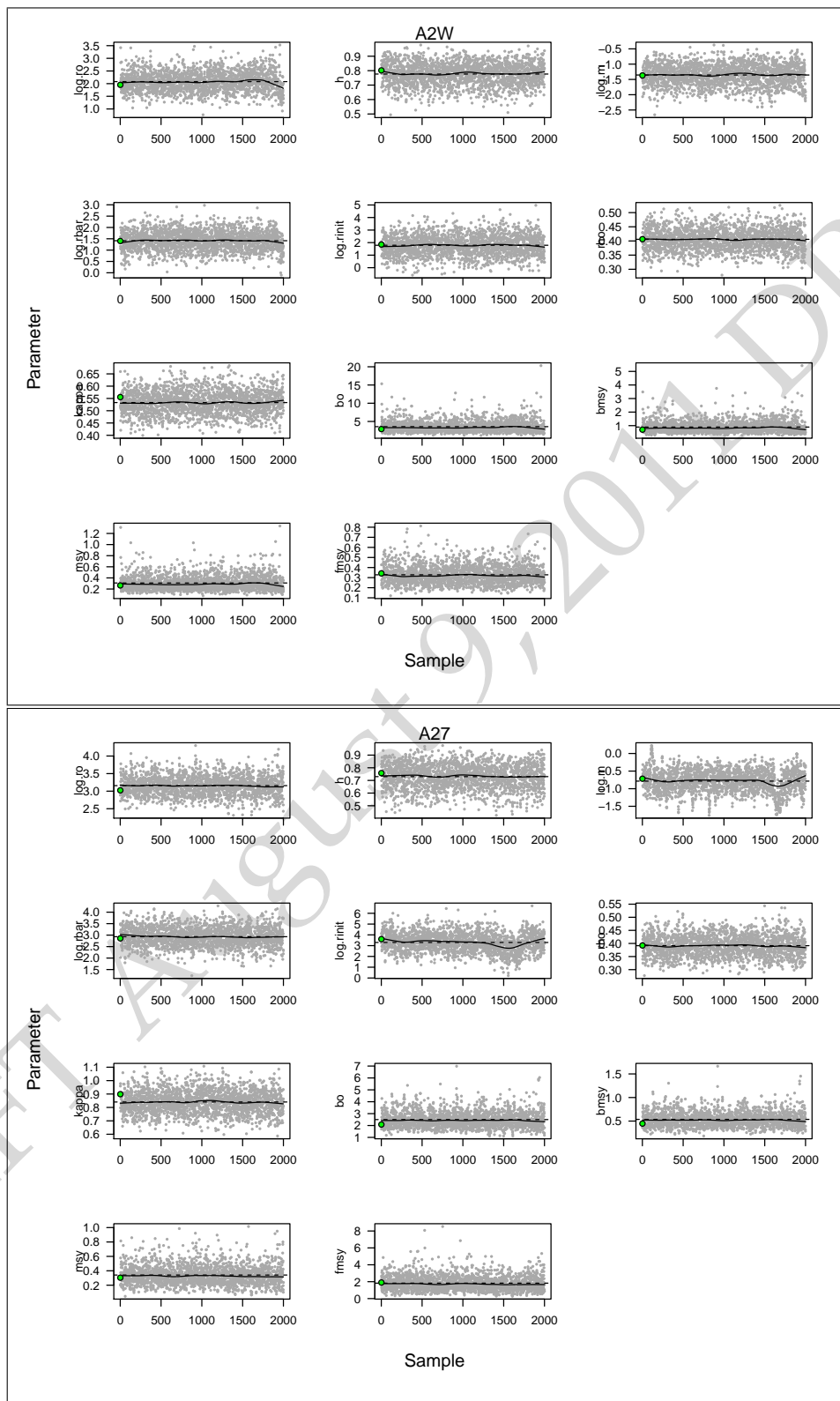


Figure 2.44: A systematic sample of 2000 points from a chain of length 1,000,000 from the joint posterior distribution for areas 2W and area 27.

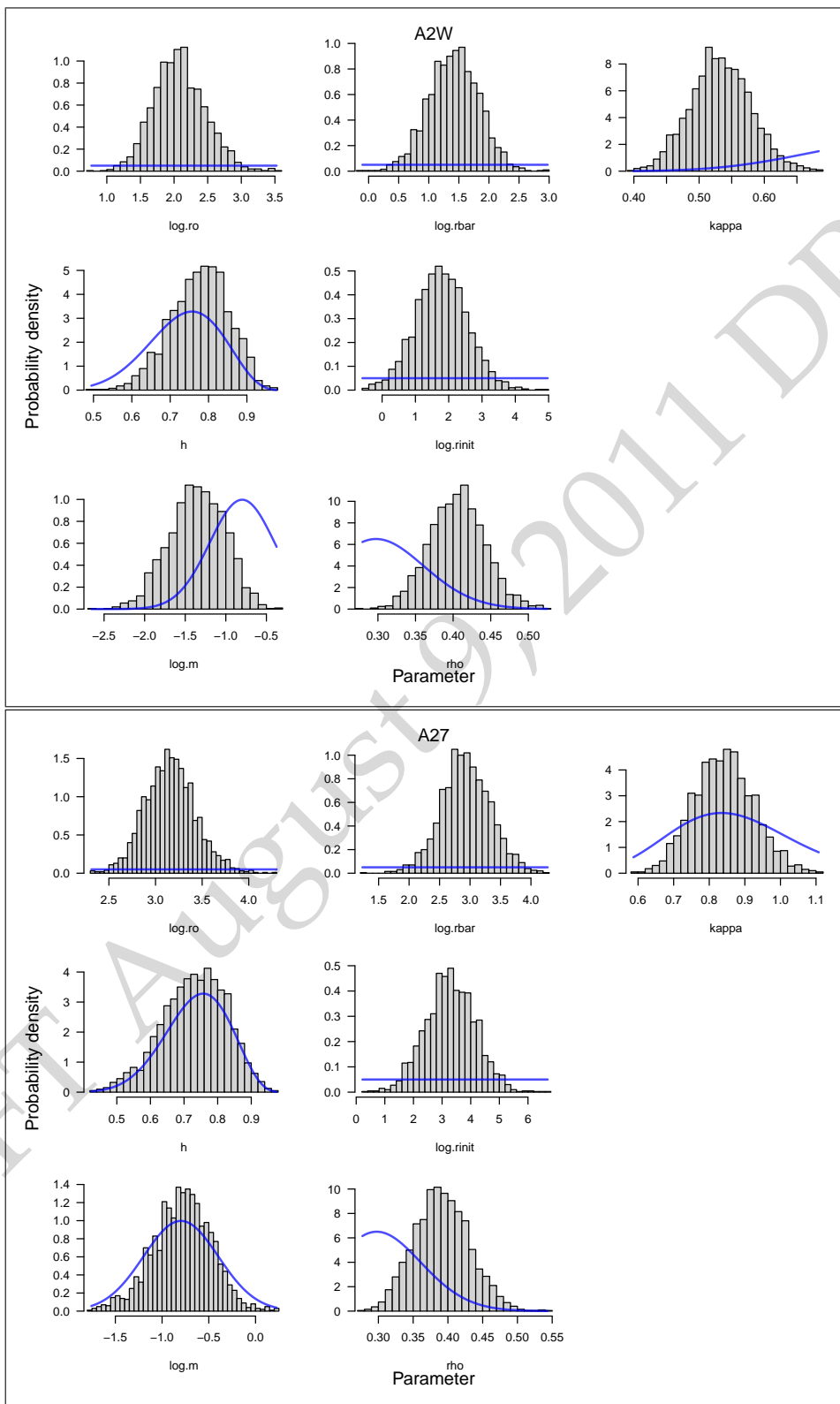


Figure 2.45: Marginal distributions for the leanding parameters based on a systematic sample of 2000 points from a chain of length 1,000,000 from the joint posterior distribution for areas 2W and area 27.

2.9 Acknowledgements

The authors would like to thank Charles Fort and Kristen Daniel for their continued efforts in error checking, reviewing and updating the catch, spawn survey and biological sampling databases. We would also like to acknowledge Howard Stiff for providing programming support for the MS Access database used to summarize the assessment data time series.

Funding for the test fishing and spawn survey programs was provided by DFO through Larocque relief funds through a contract to the HCRS. The herring industry provided additional biological samples for the SOG and PRD stock areas through a modified roe testing program.

We also extend our thanks to Jim Ianelli for ideas and help with the cubic splines for selectivity and time varying natural mortality rates. Also, our huge appreciation to the members of the ADMB Foundation for continued development and support of AD Model Builder.

Bibliography

- ADMB Project (2009). 2009 AD Model Builder: Automatic Differentiation Model Builder. Developed by David Fournier and freely available from admb-project.org.
- Bishop, M. and Green, S. (2001). Predation on pacific herring (*clupea pallasi*) spawn by birds in prince william sound, alaska. *Fisheries Oceanography*, 10:149–158.
- Cleary, J. and Schweigert, J. (2010). Stock Assessment and Management Advice for the British Columbia Herring Stocks: 2010 Assessment and 2011 Forecasts. *Canadian Science Advisory Secretariat*, 2010:90.
- Conn, P., Williams, E., and Shertzer, K. (2010). When can we reliably estimate the productivity of fish stocks? *Canadian Journal of Fisheries and Aquatic Sciences*, 67(3):511–523.
- Cordue, P. L. (in prep, 2006). Prior distributions for trawl and acoustic survey proportionality constants used in the 2006 orange roughy stock assessments. *New Zealand Fisheries Assessment Report*, Draft:22p.
- Fisheries and Oceans Canada (2006). A harvest strategy compliant with the precautionary approach. *Canadian Science Advisory Secretariat Sci. Adv. Rep. No. 2006/023*.
- Fournier, D. and Archibald, C. (1982). A general theory for analyzing catch at age data. *Canadian Journal of Fisheries and Aquatic Sciences*, 39(8):1195–1207.
- Gavaris, S. and Ianelli, J. (2002). Statistical Issues in Fisheries' Stock Assessments*. *Scandinavian Journal of Statistics*, 29(2):245–267.
- Gelman, A. (2004). *Bayesian data analysis*. CRC press.
- Haegele, C. and Schweigert, J. (1989). Egg loss from pacific herring spawns in barkley sound in 1988. *Canadian Manuscript Report Fish. Aquat. Sci.*
- Haegele, C. and Schweigert, J. (1991). Egg loss in herring spawns in georgia strait, british columbia. In *Proceedings of the international herring symposium. University of Alaska, Alaska Sea Grant Report*, pages 91–01.
- Haist, V., Schweigert, J., Stocker, M., Station, P., of Fisheries, C. D., and Oceans (1986). *Stock assessments for British Columbia herring in 1985 and forecasts of the potential catch in 1986*. Fisheries and Oceans, Canada.
- Hardwick, J. (1973). Biomass estimates of spawning herring, *clupea harengus pallasi*, herring eggs, and associated vegetation in tomales bay. *Calif. Fish Game*, 59(1):36–61.
- Hay, D. (1985). Reproductive biology of pacific herring (*clupea harengus pallasi*). *Canadian Journal of Fisheries and Aquatic Sciences*, 42(S1):111–126.
- Hay, D., Fort, C., Schweigert, J. F., Hamer, L., and McCarter, P. B. (in press, 2011). Investigating changes in pacific herring spawn intensity (layers). *Canadian Stock Advisory Secretariat*, 2011(xx).
- McAllister, M. K. and Ianelli, J. (1997). Bayesian stock assessment using catch-age data and the sampling: importance resampling algorithm. *Canadian journal of fisheries and aquatic sciences(Print)*, 54(2):284–300.
- Midgley, P. (2003). Definitions and codings of localities, herring sections, stock assessment regions for british columbia herring data. *Can. MS Rep. Fish. Aquat. Sci.*, 2634:113.

- Outram, D. (1958). The magnitude of herring spawn losses due to bird predation on the west coast of vancouver island. *Fisheries Research Board of Canada, Progress Reports of Pacific Biological Stations*, 111:9–13.
- Palsson, W. (1984). *Egg mortality upon natural and artificial substrata within Washington state spawning grounds of Pacific herring (Clupea harengus pallasi)*. PhD thesis, University of Washington.
- Richards, L., Schnute, J., and Olsen, N. (1997). Visualizing catch-age analysis: a case study. *Canadian Journal of Fisheries and Aquatic Sciences*, 54(7):1646–1658.
- Rooper, C., Haldorson, L., and Quinn, T. (1999). Habitat factors controlling pacific herring (clupea pallasi) egg loss in prince william sound, alaska. *Canadian journal of fisheries and aquatic sciences*, 56(6):1133–1142.
- Schnute, J. and Richards, L. (1995). The influence of error on population estimates from catch-age models. *Canadian Journal of Fisheries and Aquatic Sciences*, 52(10):2063–2077.
- Schweigert, J. (2002). Herring size-at-age variation in the North Pacific. *PICES-GLOBEC INTERNATIONAL PROGRAM ON CLIMATE CHANGE AND CARRYING CAPACITY*, page 47.
- Schweigert, J., Christensen, L., Haist, V., and Secretariat, C. S. A. (2009). *Stock Assesment for British Columbia Herring in 2008 and Forecasts of the Potential Catch in 2009*. Canadian Science Advisory Secretariat=Secrétariat canadien de consultation scientifique.
- Schweigert, J., Secretariat, C. S. A., of Fisheries, C. D., and Oceans (2001). Stock assessment for british columbia herring in 2001 and forecasts of the potential catch in 2002. *Can. Sci. Adv. Secr.*, 2001(140):84.
- Walters, C. and Ludwig, D. (1994). Calculation of Bayes posterior probability distributions for key population parameters. *Canadian Journal of Fisheries and Aquatic Sciences*, 51(3):713–722.

Part III

Appendices

A.1 Technical description of $i\text{SCAM}$

A.1.1 Analytic methods

The section contains the documentation in mathematical form of the underlying age structured model, and its steady state version that is used to calculate MSY-based reference points, the observation models used in predicting observations, and the components of the objective function that formulate the statistical criterion that is used to estimate model parameters. All of the model equations are laid out in tables and are intended to represent the order of operations, or pseudocode, in which to implement the model. $i\text{SCAM}$ was implemented in AD Model Builder version 10.1 [ADMB Project \(2009\)](#). This appendix also describes some of the optional features in $i\text{SCAM}$ for estimating nonparametric selectivities.

A.1.2 Equilibrium considerations

Steady-state conditions are presented in Table A-1, in here we assume the parameter vector Θ in (T1.1) is unknown and would eventually be estimated by fitting $i\text{SCAM}$ to time series data. For a given set of growth parameters and maturity-at-age parameters defined by (T1.3), growth is assumed to follow the von Bertalanffy model (T1.4), mean weight-at-age is given by the allometric relationship in (T1.5), and the age-specific vulnerability is given by a logistic function (T1.6). Note, however, there are alternative selectivity functions implemented in $i\text{SCAM}$, the logistic function used here is simply for demonstration purposes. Mean fecundity-at-age is assumed to be proportional to the mean weight-at-age of mature fish, where maturity at age is specified by the parameters a and γ for the logistic function.

Survivorship for unfished and fished populations is defined by (T1.8) and (T1.9), respectively. It is assumed that all individuals ages A and older (i.e., the plus group) have the same total mortality rate. The incidence functions refer to the life-time or per-recruit quantities such as spawning biomass per recruit (ϕ_E) or vulnerable biomass per recruit (ϕ_b). Note that upper and lower case subscripts denote unfished and fished conditions, respectively. Spawning biomass per recruit is given by (T1.10), the vulnerable biomass per recruit is given by (T1.11) and the per recruit yield to the fishery is given by (T1.12). Unfished recruitment is given by (T1.13) and the steady-state equilibrium recruitment for a given fishing mortality rate F_e is given by (T1.14). Note that in (T1.14) we assume that recruitment follows a Beverton-Holt model of the form:

$$R_e = \frac{s_o R_e \phi_e}{1 + \beta R_e \phi_e}$$

where

$$\begin{aligned} s_o &= \kappa / \phi_E, \\ \beta &= \frac{(\kappa - 1)}{R_o \phi_E}, \end{aligned}$$

which simplifies to (T1.14). The equilibrium yield for a given fishing mortality rate is (T1.15). These steady-state conditions are critical for determining various reference points such as F_{MSY} and B_{MSY} .

A.1.3 MSY based reference points

$i\text{SCAM}$ calculates MSY-based reference points by finding the value of F_e that results in the zero derivative of the steady-state catch equation (T1.15). This is accomplished numerically using a Newton-Raphson method where an initial guess for F_{MSY} is set equal to 1.5M, then use (A.1) to iteratively find F_{MSY} . Note that the partial derivatives in (A.1) can be found in Table A-2.

Table A-1: Steady-state age-structured model assuming unequal vulnerability-at-age, age-specific natural mortality, age-specific fecundity and Beverton-Holt type recruitment.

Parameters	
$\Theta = (B_o, \kappa, M_a, \hat{a}, \dot{\gamma})$	(T1.1)
$B_o > 0; \kappa > 1; M_a > 0$	(T1.2)
$\Phi = (l_\infty, k, t_o, a, b, \dot{a}, \dot{\gamma})$	(T1.3)
Age-schedule information	
$l_a = l_\infty(1 - \exp(-k(a - t_o)))$	(T1.4)
$w_a = a(l_a)^b$	(T1.5)
$v_a = (1 + \exp(-(\hat{a} - a)/\gamma))^{-1}$	(T1.6)
$f_a = w_a(1 + \exp(-(\dot{a} - a)/\dot{\gamma}))^{-1}$	(T1.7)
Survivorship	
$\iota_a = \begin{cases} 1, & a = 1 \\ \iota_{a-1}e^{-M_{a-1}}, & a > 1 \\ \iota_{a-1}/(1 - e^{-M_a}), & a = A \end{cases}$	(T1.8)
$\hat{\iota}_a = \begin{cases} 1, & a = 1 \\ \hat{\iota}_{a-1}e^{-M_{a-1}-F_e v_{a-1}}, & a > 1 \\ \hat{\iota}_{a-1}e^{-M_{a-1}-F_e v_{a-1}}/(1 - e^{-M_a - F_e v_a}), & a = A \end{cases}$	(T1.9)
Incidence functions	
$\phi_E = \sum_{a=1}^{\infty} \iota_a f_a, \quad \phi_e = \sum_{a=1}^{\infty} \hat{\iota}_a f_a$	(T1.10)
$\phi_B = \sum_{a=1}^{\infty} \iota_a w_a v_a, \quad \phi_b = \sum_{a=1}^{\infty} \hat{\iota}_a w_a v_a$	(T1.11)
$\phi_q = \sum_{a=1}^{\infty} \frac{\hat{\iota}_a w_a v_a}{M_a + F_e v_a} \left(1 - e^{(-M_a - F_e v_a)}\right)$	(T1.12)
Steady-state conditions	
$R_o = B_o/\phi_B$	(T1.13)
$R_e = R_o \frac{\kappa - \phi_E/\phi_e}{\kappa - 1}$	(T1.14)
$C_e = F_e R_e \phi_q$	(T1.15)

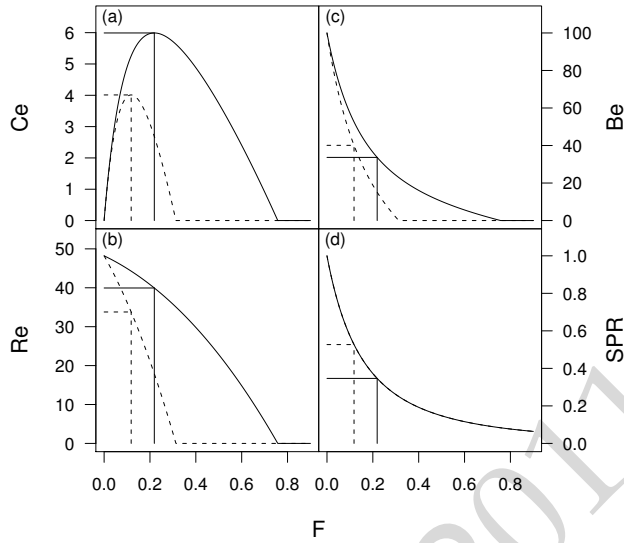


Figure A.46: Equilibrium yield (a), recruits (b), biomass (c) and spawner per recruit (ϕ_e/ϕ_E) (d) versus instantaneous fishing mortality F_e for two different values of the recruitment compensation ratio ($\kappa = 12$ solid lines, $\kappa = 4$ dashed lines). Vertical lines in each panel correspond to F_{MSY} and horizontal lines correspond to various reference points that would achieve MSY.

$$F_{e+1} = F_e - \frac{\frac{\partial C_e}{\partial F_e}}{\frac{\partial^2 C_e}{\partial F_e}} \quad (A.1)$$

where

$$\begin{aligned} \frac{\partial C_e}{\partial F_e} &= R_e \phi_q + F_e \phi_q \frac{\partial R_e}{\partial F_e} + F_e R_e \frac{\partial \phi_q}{\partial F_e} \\ \frac{\partial^2 C_e}{\partial F_e} &= \phi_q \frac{\partial R_e}{\partial F_e} + R_e \frac{\partial \phi_q}{\partial F_e} \end{aligned}$$

The algorithm usually converges in less than 10 iterations depending on how close the initial guess of F_{MSY} is to the true value. A maximum of 20 iterations are allowed in $iSCA_M$, however, if $\frac{\partial C_e}{\partial F_e} < 10^{-5}$ the algorithm stops. Note also, that this is only performed on data type variables and not differentiable variables within AD Model Builder.

Given an estimate of F_{MSY} , other reference points such as MSY are calculated use the equations in Table A-1 where each of the expressions is evaluated at F_{MSY} . A graphical representation of MSY based reference points for two alternative values of the recruitment compensation parameter κ is show in Figure A.46.

There are some additional technical details about calculating MSY based reference points when considering multiple fishing gears with different selectivities. The maximum sustainable yield summed over all fishing gears is a function of the selectivities of each gear type and what fraction of the total catch is allocated to each gear. In the Pacific herring fishery, there are three distinct fleets that all have different selectivities; the purse-seine gears tend to catch smaller younger fish, while the gill net fishery tends to target larger mature females. The optimum fishing mortality rate for each gear that would maximize the yield depends on what the other gears are removing; this in itself is another optimization problem that fisheries management must contend with. For the purposes of this assessment, $iSCA_M$ requires an allocation of the total catch (summed across gear type) to each gear before it proceeds with calculating reference points.

Table A-2: Partial derivatives, based on components in Table A-1, required for the numerical calculation of F_{MSY} using (A.1).

Mortality & Survival	
$Z_a = M_a + F_e v_a$	(T2.1)
$S_a = 1 - e^{-Z_a}$	(T2.2)
Partial for survivorship	
$\frac{\partial \hat{t}_a}{\partial F_e} = \begin{cases} 0, & a = 1 \\ e^{-Z_{a-1}} \left(\frac{\partial \hat{t}_{a-1}}{\partial F_e} - \hat{t}_{a-1} v_{a-1} \right), & 1 < a < A \\ \frac{\partial \hat{t}_{a-1}}{\partial F_e} - \frac{\hat{t}_{a-1} e^{-Z_{a-1}} v_a e^{-Z_a}}{(1 - e^{-Z_a})^2}, & a = A \end{cases}$	(T2.3)
Partials for incidence functions	
$\frac{\partial \phi_e}{\partial F_e} = \sum_{a=1}^{\infty} f_a \frac{\partial \hat{t}_a}{\partial F_e}$	(T2.4)
$\frac{\partial \phi_q}{\partial F_e} = \sum_{a=1}^{\infty} \frac{w_a v_a S_a}{Z_a} \frac{\partial \hat{t}_a}{\partial F_e} + \frac{\hat{t}_a w_a v_a^2}{Z_a} \left(e^{-Z_a} - \frac{S_a}{Z_a} \right)$	(T2.5)
Partial for recruitment	
$\frac{\partial R_e}{\partial F_e} = \frac{R_o}{\kappa - 1} \frac{\phi_E}{\phi_e^2} \frac{\partial \phi_e}{\partial F_e}$	(T2.6)

For this herring assessment, the average catch over the past 20 years was arbitrarily used to determine the allocation scheme for each of the stock assessment regions. For the Strait of Georgia this corresponds to 6.9% for the winter seine fishery, 41.4% for the seine roe fishery, and 51.8% for the gill net fishery. We further assume that 100% of the total mortality takes place prior to spawning.

A.1.4 Dynamic age-structured model

The estimated parameter vector in ${}^i\text{SCAM}$ is defined in (T3.1), where R_0 , κ and M are the leading unknown population parameters that define the overall population scale in the form of unfished recruitment and productivity in the form of recruitment compensation and natural mortality. The total variance ϑ^2 and the proportion of the total variance that is associated with observation errors ρ are also estimated, then the variance is partitioned into observation errors (σ^2) and process errors (τ^2) using (T3.2).

The unobserved state variables (T3.3) include the numbers-at-age year t ($N_{t,a}$), the spawning stock biomass (B_t) and the total age-specific total mortality rate ($Z_{t,a}$).

The initial numbers-at-age in the first year (T3.4) and the annual recruits (T3.5) are treated as estimated parameters and used to initialize the numbers-at-age matrix. Age-specific selectivity for gear type k is a function of the selectivity parameters γ_k (T3.6), and the annual fishing mortality for each gear k in year t ($F_{k,t}$). The vector of log fishing mortality rate parameters $F_{k,t}$ is a bounded vector with a minimum value of -30 and an upper bound of 3.0. In arithmetic space this corresponds to a minimum value of 9.36e-14 and a maximum value of 20.01 for annual fishing mortality rates. In years where there are 0 reported catches for a given fleet, no corresponding fishing mortality rate parameter is estimated and the implicit assumption is there was no fishery in that year.

There is an option to treat natural mortality as a random walk process (T3.7), where the natural mortality rate in the first year is the estimated leading parameter (T3.1) and in subsequent years the mortality rate

Table A-3: Statistical catch-age model using the Baranov catch equation and C^* and F^* as leading parameters.

Estimated parameters	
$\Theta = \left(R_0, \kappa, M, \bar{R}, \ddot{R}, \rho, \vartheta, \vec{\gamma}_k, F_{k,t}, \{\ddot{\omega}_a\}_{a=\dot{a}+1}^{a=A}, \{\omega_t\}_{t=1}^{t=T}, \{\varphi_t\}_{t=2}^T \right)$	(T3.1)
$\sigma = \rho/\vartheta, \quad \tau = (1 - \rho)/\vartheta$	(T3.2)
Unobserved states	
$N_{t,a}, B_t, Z_{t,a}$	(T3.3)
Initial states ($t = \dot{t}$)	
$N_{t,a} = \ddot{R} e^{\ddot{\omega}_a} \exp(-M_t)^{(a-\dot{a})}; \quad t = \dot{t}; \dot{a} \leq a \leq A$	(T3.4)
$N_{t,a} = \bar{R} e^{\omega_t}; \quad \dot{t} \leq t \leq T; a = \dot{a}$	(T3.5)
$v_{k,a} = f(\vec{\gamma}_k)$	(T3.6)
$M_t = M_{t-1} \exp(\varphi_t), \quad t > 1$	(T3.7)
$F_{k,t} = \exp(F_{k,t})$	(T3.8)
State dynamics ($t > \dot{t}$)	
$B_t = \sum_a N_{t,a} f_a$	(T3.9)
$Z_{t,a} = M_t + \sum_k F_{k,t} v_{k,t,a}$	(T3.10)
$\hat{C}_{k,t} = \sum_a \frac{N_{t,a} w_a F_{k,t} v_{k,t,a} (1 - e^{-Z_{t,a}})^{\eta_t}}{Z_{t,a}}$	(T3.11)
$N_{t,a} = \begin{cases} N_{t-1,a-1} \exp(-Z_{t-1,a-1}) & a > \dot{a} \\ N_{t-1,a} \exp(-Z_{t-1,a}) & a = A \end{cases}$	(T3.12)
Recruitment models	
$R_t = \frac{s_o B_{t-k}}{1 + \beta B_{t-k}} e^{\delta_t - 0.5\tau^2} \quad \text{Beverton-Holt}$	(T3.13)
$R_t = s_o B_{t-k} e^{-\beta B_{t-k} + \delta_t - 0.5\tau^2} \quad \text{Ricker}$	(T3.14)

deviates from the previous year based on the estimated deviation parameter φ_t . If the mortality deviation parameters are not estimated, then M is assumed to be time invariant.

State variables in each year are updated using equations T3.9–T3.12, where the spawning biomass is the product of the numbers-at-age and the mature biomass-at-age (T3.9). The total mortality rate is given by (T3.10), and the total catch (in weight) for each gear is given by (T3.11) assuming that both natural and fishing mortality occur simultaneously throughout the year. The numbers-at-age are propagated over time using (T3.12), where members of the plus group (age A) are all assumed to have the same total mortality rate.

Recruitment to age k can follow either a Beverton-Holt model (T3.13) or a Ricker model (T3.14) where the maximum juvenile survival rate (s_o) in either case is defined by $s_o = \kappa/\phi_E$. For the Beverton-Holt model, β is derived by solving (T3.13) for β conditional on estimates of κ and R_o :

$$\beta = \frac{\kappa - 1}{R_o \phi_E},$$

Table A-4: An incomplete list of symbols, constants and description for variables used in $i\text{SCA}_M$.

Symbol	Constant value	Description
<u>Indexes</u>		
a		index for age
t		index for year
k		index for gear
<u>Model dimensions</u>		
\acute{a}, A	2, 10	youngest and oldest age class (A is a plus group)
\acute{t}, T	1951, 2010	first and last year of catch data
K	5	Number of gears including survey gears
<u>Observations (data)</u>		
$C_{k,t}$		catch in weight by gear k in year t
$I_{k,t}$		relative abundance index for gear k in year t
$p_{k,t,a}$		observed proportion-at-age a in year t for gear k
<u>Estimated parameters</u>		
R_o		Age- \acute{a} recruits in unfished conditions
κ		recruitment compensation
M		instantaneous natural mortality rate
\bar{R}		average age- \acute{a} recruitment from year \acute{t} to T
\ddot{R}		average age- \acute{a} recruitment in year $\acute{t} - 1$
ρ		fraction of the total variance associated with observation error
ϑ		total precision (inverse of variance) of the total error
$\vec{\gamma}_k$		vector of selectivity parameters for gear k
$F_{k,t}$		logarithm of the instantaneous fishing mortality for gear k in year t
$\ddot{\omega}_a$		age- \acute{a} deviates from \ddot{R} for year \acute{t}
ω_t		age- \acute{a} deviates from \ddot{R} for years \acute{t} to T

and for the Ricker model this is given by:

$$\beta = \frac{\ln(\kappa)}{R_o \phi_E}$$

A.1.5 Options for selectivity

At present, there are eight alternative age-specific selectivity options in $i\text{SCA}_M$. The simplest of the selectivity options is a simple logistic function with two parameters where it is assumed that selectivity is time-invariant. The more complex selectivity options assume that selectivity may vary over time and may have as many as $(A-1)\cdot T$ parameters. For time-varying selectivity, cubic and bicubic splines are used to reduce the number of estimated parameters. The last two options consider how selectivity may vary over time based on changes in mean weight-at-age. Prior to parameter estimation, $i\text{SCA}_M$ will determine the exact number of selectivity parameters that need to be estimated based on which selectivity option was chosen for each gear type. It is not necessary for all gear types to have the same selectivity option. For example it is possible to have a simple two parameter selectivity curve for say a survey gear, and a much more complicated selectivity option for a commercial fishery.

Logistic selectivity The logistic selectivity option is a two parameter model of the form

$$v_a = \frac{1}{1 + \exp(-(a - \mu_a)/\sigma_a)}$$

where μ_a and σ_a are the two estimated parameters representing the age-at-50% vulnerability and the standard deviation, respectively.

Age-specific selectivity coefficients The second option also assumes that selectivity is time-invariant and estimates a total of $A-1$ selectivity coefficients, where the plus group age-class is assumed to have the same selectivity as the previous age-class. For example, if the ages in the model range from 1 to 15 years, then a total of 14 selectivity parameters are estimated, and age-15+ animals will have the same selectivity as age-14 animals.

When estimating age-specific selectivity coefficients, there are two additional penalties that are added to the objective function that control how much curvature there is and limit how much dome-shaped can occur. To penalize the curvature, the square of the second differences of the vulnerabilities-at-age are added to the objective function:

$$\lambda_k^{(1)} \sum_{a=2}^{A-1} (v_{k,a} - 2v_{k,a-1} + v_{k,a-2})^2 \quad (\text{A.2})$$

The dome-shaped term penalty as:

$$\begin{cases} \lambda_k^{(2)} \sum_{a=1}^{A-1} (v_{k,a} - v_{k,a+1})^2 & (\text{if } v_{k,a+1} < v_{k,a}) \\ 0 & (\text{if } v_{k,a+1} \geq v_{k,a}) \end{cases} \quad (\text{A.3})$$

For this selectivity option the user must specify the relative weights $(\lambda_k^{(1)}, \lambda_k^{(2)})$ to add to these two penalties.

Cubic spline interpolation The third option also assumes time-invariant selectivity and estimates a selectivity coefficients for a series age-nodes (or spline points) and uses a natural cubic spline to interpolate between these nodes (Figure A.47). Given $n + 1$ distinct knots x_i , selectivity can be interpolated in the intervals defined by

$$S(x) = \begin{cases} S_0(x) & x \in [x_0, x_1] \\ S_1(x) & x \in [x_1, x_2] \\ \dots \\ S_{n-1}(x) & x \in [x_{n-1}, x_n] \end{cases}$$

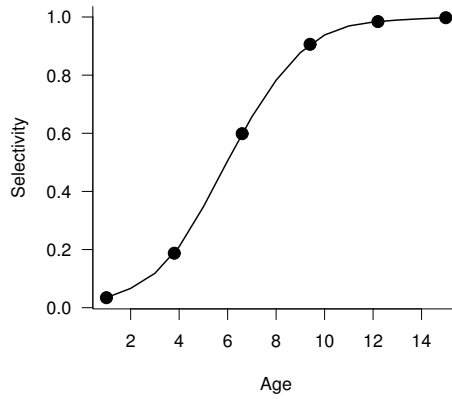


Figure A.47: Example of a natural cubic spline interpolation for estimating selectivity coefficients. In $i\text{SCA}_M$ the user specifies the number of nodes (circles) to estimate; then age-specific selectivity coefficients are interpolated using a natural cubic spline.

where $S''(x_0) = S''(x_n) = 0$ is the condition that defines a natural cubic spline.

The same penalty functions for curvature and dome-shaped selectivity are also invoked for the cubic spline interpolation of selectivity.

Time-varying selectivity with cubic spline interpolation A fourth option allows for cubic spline interpolation for age-specific selectivity in each year. This option adds a considerable number of estimated parameters but the most extreme flexibility. For example, given 40 years of data and estimated 5 age nodes, this amounts 200 (40 years times 5 ages) estimated selectivity parameters. Note that the only constraints at this time are the dome-shaped penalty and the curvature penalty; there is no constraint implemented for say a random walk (first difference) in age-specific selectivity. As such this option should only be used in cases where age-composition data is available for every year of the assessment.

Bicubic spline to interpolate over time and ages The fifth option allows for a two-dimensional interpolation using a bicubic spline (Figure A.48). In this case the user must specify the number of age and year nodes. Again the same curvature and dome shaped constraints are implemented. It is not necessary to have age-composition data each and every year as in the previous case, as the bicubic spline will interpolate between years. However, it is not advisable to extrapolate selectivity back in time or forward in time where there are no age-composition data unless some additional constraint, such as a random-walk in age-specific selectivity coefficients is implemented (as of August 9, 2011, this has not been implemented).

Selectivity as a logistic function of weight-at-age The seventh option for selectivity is to parameterize a logistic function in terms of the weight-at-age in year t ($w_{a,t}$). In this case changes in weight-at-age over time allow for changes in selectivity. Such a weight-based function may be appropriate for size selective gears such as gill nets.

$$v_{a,t} = \frac{1}{1 + \exp(-(w_{a,t} - \mu_a)/\sigma_a)}$$

Using weight as a covariate The eighth option for selectivity is to use a logistic function based on age, but allow selectivity to vary based on deviations in the mean weight-at-age over time. In this case:

$$v_{a,t} = \frac{1}{1 + \exp(-(a - \mu_a)/\sigma_a)} \exp(\lambda^{(a)} \delta_{a,t})$$

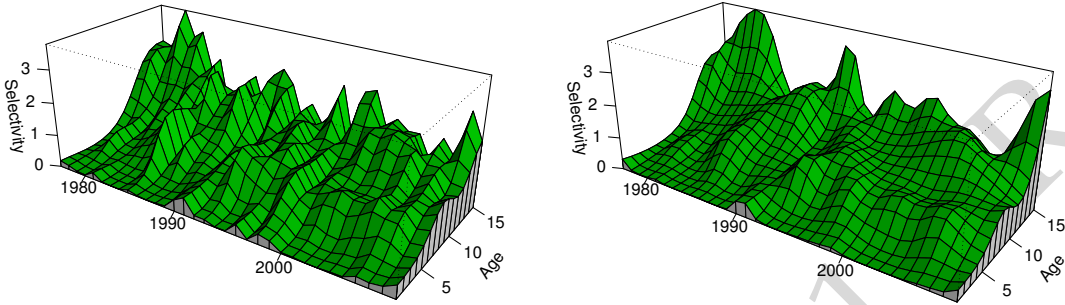


Figure A.48: Example of a time-varying cubic spline (left) and bicubic spline (right) interpolation for selectivity. The panel on the left contains 165 estimated selectivity parameters and the bicubic interpolation estimates 85 selectivity parameters, or 5 age nodes and 17 year nodes. There are 495 actual nodes (selectivity parameters) being interpolated.

where $\lambda^{(a)}$ is a latent variable that describes the residual variation in the age-composition data that is due to changes in selectivity, and $\delta_{a,t}$ is a standardized ($\mu = 0, \sigma = 1$) annual age-specific deviation in mean weight-at-age. In this case, estimates of $\lambda^{(a)} = 0$ imply that variation in the empirical weight-at-age data explain none of the residual variation in the age-composition data. Values of $\lambda^{(a)} \neq 0$ imply a positive or negative affect of variation in growth on selectivity.

A.1.6 Options for natural mortality

There is an option in $i\text{SCAM}$ to estimate a time series of deviations in natural mortality rates (φ_t). If not estimated, natural mortality M is assumed to be invariant over time and age. If, however, M is thought to vary over time, then $i\text{SCAM}$ models natural mortality as a random walk process (T3.7). In such cases where M is allowed to freely vary over time, the user must specify two additional components in the control file. First, the phase in which the vector of deviations φ_t is estimated must be specified (use a -ve phase to turn off the estimation), and the user must also specify a standard deviation in the deviation parameters. If estimated, then an additional component is added to the objective function to constrain the first differences in the deviation parameters. This first difference constraint only limits how quickly M may increase or decrease over time and does not penalize deviations from an underlying mean. Thus it is possible for M to drift (increase or decrease) away from some central tendency. This drifting can have profound effects on reference point calculations as it also allows for non-stationarity in the underlying production function.

A.1.7 Residuals, likelihoods & objective function value components

There are 3 major components to the overall objective function that are minimized. These components consist of the likelihood of the data, prior distributions and penalty functions that are invoked to regularize the solution during intermediate phases of the non-linear parameter estimation. This section discusses each of these in turn, starting first with the residuals between observed and predicted states followed by

the negative loglikelihood that is minimized for the catch data, relative abundance data, age-composition, and stock-recruitment relationships.

A.1.8 Catch data

It is assumed that the measurement errors in the non-zero catch observations are log-normally distributed, and the residuals is given by:

$$\eta_{k,t} = \ln(C_{k,t}) - \ln(\hat{C}_{k,t}), \quad (\text{A.4})$$

The residuals are assumed to be normally distributed with a user specified standard deviation σ_C . At present, it is assumed that observed catches for each gear k is assumed to have the same standard deviation. To aid in parameter estimation, two separate standard deviations are specified in the control file: the first is the assumed standard deviation used in the first, second, to N-1 phases, and the second is the assumed standard deviation in the last phase. The negative loglikelihood (ignoring the scaling constant) for the catch data is given by:

$$\ell_C = \sum_k \left[T_k \ln(\sigma_C) + \frac{\sum_{t \in \hat{C}_{k,t} \neq 0} (\eta_{k,t})^2}{2\sigma_C^2} \right], \quad (\text{A.5})$$

where T_k is the total number of non-zero catch observations for gear type k .

A.1.9 Relative abundance data

The relative abundance data are assumed to be proportional to biomass that is vulnerable to the sampling gear:

$$V_{k,t} = \sum_a N_{t,a} e^{-\lambda_{k,t} Z_{t,a}} v_{k,a} w_{a,t}, \quad (\text{A.6})$$

where $v_{k,a}$ is the age-specific selectivity of gear k , and w_a is the mean-weight-at-age. A user specified fraction of the total mortality $\lambda_{k,t}$ adjusts the numbers-at-age to correct for survey timing. In the case of Pacific herring spawn surveys, the vulnerability is fixed to the assumed maturity ogive and the empirical weight-at-age data are used to construct the predicted relative abundance. Also, it was assumed that all the mortality (post-fishing) had occurred during the time the survey took place (i.e., $\lambda_{k,t} = 1$). The residuals between the observed and predicted relative abundance index is given by:

$$\epsilon_{k,t} = \ln(I_{k,t}) - \ln(q_k) - \ln(V_{k,t}), \quad (\text{A.7})$$

where $I_{k,t}$ is the observed relative abundance index, q_k is the catchability coefficient for index k , and $V_{k,t}$ is the predicted vulnerable biomass at the time of sampling. The catchability coefficient q_k is evaluated at its conditional maximum likelihood estimate:

$$q_k = \frac{1}{N_k} \sum_{t \in I_{k,t}} \ln(I_{k,t}) - \ln(V_{k,t}),$$

where N_k is the number of relative abundance observations for index k (see [Walters and Ludwig, 1994](#), for more information). The negative loglikelihood for relative abundance data is given by:

$$\ell_I = \sum_k \sum_{t \in I_{k,t}} \ln(\sigma_{k,t}) + \frac{\epsilon_{k,t}^2}{2\sigma_{k,t}^2} \quad (\text{A.8})$$

where

$$\sigma_{k,t} = \frac{\rho\varphi^2}{\omega_{k,t}},$$

where $\rho\varphi^2$ is the proportion of the total error that is associated with observation errors, and $\omega_{k,t}$ is a user specified relative weight for observation t from gear k . The $\omega_{k,t}$ terms allow each observation to be weighted relative to the total error $\rho\varphi^2$; for example, to omit a particular observation, set $\omega_{k,t} = 0$, or to give 2 times

the weight, then set $\omega_{k,t} = 2.0$. To assume all observations have the same variance then simply set $\omega_{k,t} = 1$. Note that if $\omega_{k,t} = 0$ then equation (A.8) is undefined; therefore, $i\text{SCAM}$ adds a small constant to $\omega_{k,t}$ (1.e-10, which is equivalent to assuming an extremely large variance) to ensure the likelihood can be evaluated.

In the case of the Pacific herring assessment, the spawn survey data post-1988 were assumed to be twice as precise as the pre-dive survey data (1951-1987). To implement this, weights for the 1951-1987 data were set equal to $\omega_{k,t} = 1.0$ and the contemporary data was assigned $\omega_{k,t} = 2.0$. The standard deviation in the observation errors is conditional on estimated values of ρ and φ^2 .

A.1.10 Age composition data

Sampling theory suggest that age composition data are derived from a multinomial distribution (Fournier and Archibald, 1982); however, $i\text{SCAM}$ assumes that age-proportions are obtained from a multivariate logistic distribution (Schnute and Richards, 1995; Richards et al., 1997). The main reason $i\text{SCAM}$ departs from the traditional multinomial model has to do with how the age-composition data are weighted in the objective function. First, the multinomial distribution requires the specification of an effective sample size; this may be done arbitrarily or through iterative re-weighting (McAllister and Ianelli, 1997; Gavaris and Ianelli, 2002), and in the case of multiple and potentially conflicting age-proportions this procedure may fail to converge properly. The assumed effective sample size can have a large impact on the overall model results.

A nice feature of the multivariate logistic distribution is that the age-proportion data can be weighted based on the conditional maximum likelihood estimate of the variance in the age-proportions. Therefore, the contribution of the age-composition data to the overall objective function is “self-weighting” and is conditional on other components in the model.

Ignoring the subscript for gear type for clarity, the observed and predicted proportions-at-age must satisfy the constraint

$$\sum_{a=1}^A p_{t,a} = 1$$

for each year. The multivariate logistic residuals between the observed ($p_{t,a}$) and predicted proportions ($\widehat{p}_{t,a}$) is given by:

$$\eta_{t,a} = \ln(p_{t,a}) - \ln(\widehat{p}_{t,a}) - \frac{1}{A} \sum_{a=1}^A [\ln(p_{t,a}) - \ln(\widehat{p}_{t,a})]. \quad (\text{A.9})$$

The conditional maximum likelihood estimate of the variance is given by

$$\widehat{\tau}^2 = \frac{1}{(A-1)T} \sum_{t=1}^T \sum_{a=1}^A \eta_{t,a}^2,$$

and the negative loglikelihood evaluated at the conditional maximum likelihood estimate of the variance is given by:

$$\ell_A = (A-1)T \ln(\widehat{\tau}^2). \quad (\text{A.10})$$

In short, the multivariate logistic likelihood for age-composition data is just the log of the residual variance weighted by the number observations over years and ages.

There is also a technical detail in (A.9), where observed and predicted proportions-at-age must be greater than 0. It is not uncommon in catch-age data sets to observe 0 proportions for older, or young, age classes. $i\text{SCAM}$ adopts the same approach described by Richards et al. (1997) where the definition of age-classes is altered to require that $p_{t,a} \geq 0.02$ for every age in each year. This is accomplished by grouping consecutive ages, where $p_{t,a} < 0.02$, into a single age-class and reducing the effective number of age-classes in the variance calculation ($\widehat{\tau}^2$) by the number of groups created. The choice of 2% is arbitrary and the user can specify the minimum proportion (including 0) to consider when pooling age-proportion data. In the case of an exact 0 in the observed age-proportions the pooling of the adjacent age-class still occurs, this ensures that (A.9) is defined.

In the Strait of Georgia herring example, we set the minimum proportion to 2% to reduce the influence of the large numbers of 0 proportions in the purse-seine fleets, especially prior to 1970 during the reduction fishery.

A.1.11 Stock-recruitment

There are two alternative stock-recruitment models available in $i\text{SCAM}$: the Beverton-Holt model and the Ricker model. Annual recruitment and the initial age-composition are treated as latent variables in $i\text{SCAM}$, and residuals between estimated recruits and the deterministic stock-recruitment models are used to estimate unfished spawning stock biomass and recruitment compensation. The residuals between the estimated and predicted recruits is given by

$$\delta_t = \ln(\bar{R}e^{w_t}) - f(B_{t-k}) \quad (\text{A.11})$$

where $f(B_{t-k})$ is given by either (T3.13) or (T3.14), and k is the age at recruitment. Note that a bias correction term for the lognormal process errors is included in (T3.13) and (T3.14).

The negative log likelihood for the recruitment deviations is given by the normal density (ignoring the scaling constant):

$$\ell_\delta = n \ln(\tau) + \frac{\sum_{t=1+k}^T \delta_t^2}{2\tau^2} \quad (\text{A.12})$$

Equations (A.11) and (A.12) are key for estimating unfished spawning stock biomass and recruitment compensation via the recruitment models. The relationship between (s_o, β) and (B_o, κ) is defined as:

$$s_o = \kappa/\phi_E \quad (\text{A.13})$$

$$\beta = \begin{cases} \frac{\kappa-1}{B_o} & \text{Beverton-Holt} \\ \frac{\ln(\kappa)}{B_o} & \text{Ricker} \end{cases} \quad (\text{A.14})$$

where s_o is the maximum juvenile survival rate, β is the density effect on recruitment, and B_o is the unfished spawning stock biomass. Unfished steady-state spawning stock biomass per recruit is given by ϕ_E , which is the sum of products between age-specific survivorship and relative fecundity. In cases where the natural mortality rate is allowed to vary over time, the calculation of ϕ_E , and the corresponding unfished spawning stock biomass (B_o) is based on the average natural mortality rate over the entire time period. This subtle calculation has implications for reference point calculations in cases where there are increasing or decreasing trends in natural mortality rates over time; as estimates of natural mortality rates trend upwards, estimates of B_o decrease.

For the Strait of Georgia Pacific herring example, only the Beverton-Holt recruitment model was considered. The description of the Ricker model is included here for the sake of completely documenting the features in the $i\text{SCAM}$ platform.

A.1.12 Parameter Estimation and Uncertainty

Parameter estimation and quantifying uncertainty was carried out using the tools available in AD Model Builder (ADMB Project, 2009). AD Model Builder (ADMB) is a software for creating computer programs to estimate the parameters and associated probability distributions for nonlinear statistical models. The software is freely available from <http://admb-project.org/>. This software was used to develop $i\text{SCAM}$, and the source code and documentation for $i\text{SCAM}$ is freely available from <https://sites.google.com/site/iscamproject/>, or from a subversion repository at <http://code.google.com/p/iscam-project/>.

Suffice it to say that there is a lot more going on in the $i\text{SCAM}$ software than just minimizing the sum of the four negative loglikelihood functions defined in the previous section. There are actually five distinct components that make up the objective function that ADMB is minimizing:

$$f = \text{negative loglikelihoods} + \text{constraints} + \text{priors for parameters} + \text{survey priors} + \text{convergence penalties}.$$

The purpose of this section is to completely document all of the components that make up the objective function. Such transparency is absolutely necessary to better understand estimation performance, as well as, to ensure the results are repeatable.

A.1.13 Negative loglikelihoods

The negative loglikelihoods pertain specifically elements that deal with the data and variance partitioning and have already been described in detail in section A.1.7. There are four specific elements that make up the vector of negative loglikelihoods:

$$\vec{\ell} = \ell_C, \ell_I, \ell_A, \ell_\delta. \quad (\text{A.15})$$

To reiterate, these are the likelihood of the catch data ℓ_C , likelihood of the survey data ℓ_I , the likelihood of the age-composition data ℓ_A and the likelihood of the stock-recruitment residuals ℓ_δ . Each of these elements are expressed in negative log-space, and ADMB attempts to estimate model parameters by minimizing the sum of these elements.

A.1.14 Constraints

There are two specific constraints that are described here: 1) parameter bounds, and 2) constraints to ensure that a parameter vector sums to 0. In $i\text{SCA}_M$ the user must specify the lower and upper bounds for the leading parameters defined in the control file ($\ln(R_o)$, h , $\ln(M)$, $\ln(\bar{R})$, ρ , ϑ). All estimated selectivity parameters $\vec{\gamma}_k$ are estimated in log space and have a minimum and maximum values of -5.0 and 5.0, respectively. These values are hard-wired into the code, but should be sufficiently large/small enough to capture a wide range of selectivities. Estimated fishing mortality rates are also constrained (in log space) to have a minimum value of -30, and a maximum value of 3.0. Log annual recruitment deviations are also constrained to have minimum and maximum values of -15.0 and 15.0 and there is an additional constraint to ensure the vector of deviations sums to 0. This is necessary in order to be able to estimate the average recruitment \bar{R} . Finally, the annual log deviations in natural mortality rates are constrained to lie between -2.0 and 2.0.

An array of selectivity parameters (i.e., `init_bounded_matrix_vector`) is estimated within $i\text{SCA}_M$ where each matrix corresponds to a specific gear type, and the number of rows and columns of each depends on the type of selectivity function assumed for the gear and if that selectivity changes over time. In cases where the nodes of a spline are estimated these nodes also have an additional constraint to sum to 0. This is effectively implemented by adding to the objective function:

$$1000 \left(\frac{1}{N_{\vec{\lambda}_k}} \sum \vec{\lambda}_k \right)^2.$$

This additional constraint is necessary to ensure the model remains separable and the annual fishing mortality rates are less confounded with selectivity parameters.

A.1.15 Priors for parameters

Each of the six leading parameters specified in the control file ($\ln(R_o)$, h , $\ln(M)$, $\ln(\bar{R})$, ρ , ϑ) are declared as bounded parameters and in addition the user can also specify an informative prior distribution for each of these parameters. Five distinct prior distributions can be implemented: uniform, normal, lognormal, beta and a gamma distribution. For the Strait of Georgia herring, a bounded uniform prior was specified for the log of unfished recruitment U(-5.0,15), a non-informative beta prior was assumed for steepness Beta(1.01,1.01), a normal prior was specified for the log of natural mortality rate N(-1.0966,0.05), a bounded uniform prior for the log of average recruitment U(-5.0,15.0), a beta prior for the variance partitioning parameter ρ Beta(15,60), and a gamma prior for the precision parameter ϑ , Gamma(156.25,125.0). An example of these prior distributions based on the parameter specified above is show in Figure A.49.

In addition to the priors specified for the six leading parameter, there are several other informative distributions that are invoked for the non-parametric selectivity parameters. In cases were age-specific selectivity coefficients are estimated, or nodes of a spline function are estimated, two additional penalties are added to the objective function to control how smooth the selectivity changes (A.2) and how much dome-shape is allowed in the nonparametric selectivities (A.3).

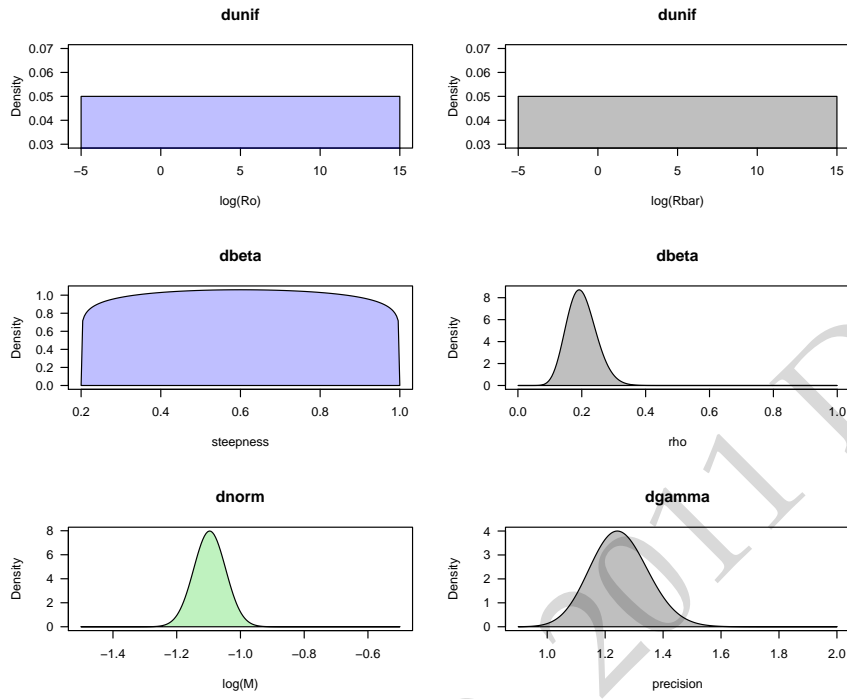


Figure A.49: An example of the prior distributions used for $\ln(R_o)$, h , $\ln(M)$, $\ln(\bar{R})$, ρ , ϑ . The actual values used for the SOG herring assessment can be found in the control file in the appendix.

A.1.16 Survey priors

The scaling parameter q for each of the surveys is not estimated; rather, the maximum likelihood estimate for q conditional on all other parameters is used to scale the predicted spawning biomass to the observed spawn survey index. In the case of Pacific herring, the relationship between fecundity and mature female biomass is relatively invariant at about 227 eggs per gram (Hardwick, 1973). This relationship has been used to convert total egg deposition from the spawn survey to total female spawning biomass, and assuming all spawning was accounted for, then a reasonable estimate for q should be 1.0.

In the Strait of Georgia herring assessment, we specified an informative normal prior on $\ln(q)$ with a mean of 0, and a standard deviation of 0.05 for the contemporary data. For the pre-1988 spawn survey data, we explored three alternative priors including a non-informative prior, and a normal prior with a mean 0 and standard deviations of 0.05, or 0.1. The informative prior for the contemporary data implies a 95% confidence interval of 0.82 to 1.22 for q .

A.1.17 Convergence penalties

For the Strait of Georgia herring assessment, there are well over 200 estimated parameters, the exact number depends on the model configuration. Needless to say, non-linear parameter estimation is often very sensitive to the initial starting conditions, and the end results may differ depending on the initial values of the model parameters or even the phase at which parameters are included into the estimation problem. There is no guarantee that the algorithm will converge to the global minimum every time. AD Model Builder is unique in that the estimation process can be conducted in a series of phases where more and more parameters are ‘freed up’ as the model progress through each phase. Furthermore, the actual objective function can change between phases such that during the initial phases large penalties can be used to, as Dave Fournier would say, “regularize the solution”. For example, in the initial phases of parameter estimation *iSCA_M* uses fairly steep quadratic penalties for the annual recruitment deviations and average fishing mortality rates to initially aid in finding reasonable values of the average recruitment, natural mortality and selectivity

parameters. In the final phase, these quadratic penalties are relaxed.

In the case of the annual recruitment deviations, the quadratic penalty term is:

$$100 \sum_{t=1-A}^T \omega_t^2,$$

which is approximately a normal density with a standard deviation equal to 0.07. In the last phase this constraint is relaxed with a large standard deviation of 5.0.

A similar penalty (a normal distribution for the log mean fishing rate) is also invoked for the mean fishing mortality rate, but in this case the user specifies the mean fishing mortality rate and the standard deviations in the initial phases and the last phase. Normally, a rather small standard deviation is used in the initial phases (e.g., 0.01) and this is then relaxed to a much larger value (e.g., 5.0) in the last phase. These standard deviations are specified by the user in the control file.

B.2 Data and Control files

B.2.1 Haida Gwaii

```

#NB The data herein were taken from qc12010_final.dat for the HCAM model.
## -----
## ____Model Dimensions____
1951 #first year of data
2011 #last year of data
2 #age of youngest age class
10 #age of plus group
5 #number of gears (ngear)
## flags for fishery (1) or survey (0) in ngears
#1 1 0 0
0.0686819 0.4137555 0.5175626 0.0000000 0.0000000
## -----
##Age-schedule and population parameters
#natural mortality rate (m)
0.334
#growth parameters (linf,k,to) (from fishbase)
27.0, 0.48, 0
#length-weight allometry (a,b)
4.5e-6, 3.1270
#maturity at age (am=log(3)/k) & gm=std for logistic
2.055, 0.05
## -----
#Time series data
#Observed catch (1951-2011, 1000s metric t)
#Year P1 P2 P3 S1 S2
1951 2.847 0.000 0.000 0 0
1952 10.147 0.000 0.000 0 0
1953 0.000 0.000 0.000 0 0
1954 1.786 0.000 0.000 0 0
1955 1.234 0.000 0.000 0 0
1956 77.681 0.000 0.000 0 0
1957 23.711 0.000 0.000 0 0
1958 11.168 0.000 0.000 0 0
1959 7.027 0.000 0.000 0 0
1960 0.000 0.000 0.000 0 0
1961 0.653 0.000 0.000 0 0
1962 7.632 0.000 0.000 0 0
1963 14.980 0.000 0.000 0 0
1964 28.777 0.000 0.000 0 0
1965 35.448 0.000 0.000 0 0
1966 2.746 0.000 0.000 0 0
1967 0.213 0.000 0.000 0 0
1968 0.080 0.000 0.000 0 0
1969 0.000 0.000 0.000 0 0
1970 0.000 0.000 0.000 0 0
1971 0.102 0.000 0.000 0 0
1972 0.849 3.124 0.000 0 0
1973 0.000 7.520 0.000 0 0
1974 0.000 6.191 0.127 0 0
1975 0.000 7.619 0.105 0 0
1976 0.374 11.939 1.802 0 0
1977 0.000 11.146 1.489 0 0
1978 0.000 9.172 2.553 0 0
1979 0.000 5.867 2.086 0 0
1980 0.000 2.106 1.210 0 0
1981 0.000 3.926 1.705 0 0
1982 0.000 2.371 1.407 0 0
1983 0.067 4.661 0.929 0 0
1984 0.096 4.016 0.535 0 0
1985 0.000 4.616 1.493 0 0
1986 0.000 2.613 0.890 0 0
1987 0.000 2.061 0.000 0 0
1988 0.000 0.032 0.000 0 0
1989 0.000 1.461 0.000 0 0
1990 0.000 5.542 1.170 0 0
1991 0.000 3.899 0.543 0 0
1992 0.000 2.524 0.000 0 0
1993 0.000 2.699 0.000 0 0
1994 0.000 0.299 0.000 0 0
1995 0.000 0.000 0.000 0 0
1996 0.000 0.000 0.000 0 0
1997 0.000 0.000 0.000 0 0
1998 0.000 1.372 0.000 0 0
1999 0.000 2.500 0.473 0 0
2000 0.000 1.764 0.000 0 0
2001 0.000 0.000 0.000 0 0
2002 0.000 0.706 0.000 0 0
2003 0.000 0.000 0.000 0 0
2004 0.000 0.000 0.000 0 0
2005 0.000 0.000 0.000 0 0
2006 0.000 0.000 0.000 0 0
2007 0.000 0.000 0.000 0 0
2008 0.000 0.000 0.000 0 0
2009 0.000 0.000 0.000 0 0
2010 0.000 0.000 0.000 0 0
2011 0.000 0.000 0.000 0 0
#Relative Abundance index from fisheries independent survey (it) 1970-2008
#nit
#it
2
#nit_nobs
37 24
#Survey type
## 1 = survey is proportional to vulnerable numbers
## 2 = survey is proportional to vulnerable biomass
## 3 = survey is proportional to spawning biomass (e.g., herring spawn survey)
3 3
#it gear wt survey timing

```


C.3 Bayesian prior for the dive survey spawn index proportionality constant q

C.3.1 The process

A Bayesian prior for the herring dive survey spawn index proportionality constant (q) is developed using a process that combines expert knowledge (in some cases best guesses) and data associated with factors influencing the prior. The process, used to develop acoustic and trawl survey priors for New Zealand fisheries stock assessments (e.g., [Cordue, 2006](#)), is comprised of the following steps:

1. List all factors affecting q .
2. For each factor, determine the statistical distribution that best describes the uncertainty associated with that factor. Where available, the distribution is based on data (not data that will be used in the assessment); otherwise it is based on expert knowledge.
3. The prior distribution for q is estimated by integrating across the distributions for each factor. This can be approximated by generating joint random samples from the distributions.
4. Finally, a parametric model is fit to the resulting distribution of replicate random samples to approximate the q prior.

C.3.2 Factors affecting q and their distributions

The factors that contribute to the spawn index q prior include: the proportion of the total spawn that is surveyed; the amount of egg loss that occurs prior to the spawn survey; bias in the estimate of mean egg density; and drift in spawn survey observations over time. The distributions for each of these factors should reflect uncertainty in their average affect over years, not capture inter-annual variation in them.

Proportion of total spawn surveyed

The proportion of the total spawn that is surveyed has a natural upper bound of 1, though its central tendency is not known. Reasons for not surveying herring spawns include non-detection (early or late in season or very deep and not observed) or lack of resources to conduct the survey. For the latter case the spawns will be reported, and this occurrence is rare. The proportion of the total spawn that is not-detected is likely higher in more remote locations and when spawning abundance is low. With limited information, we assume a uniform distribution on 0.9–1.0 for the average proportion of total spawn surveyed.

Egg loss prior to survey

This factor accounts for egg loss due to predation (seabirds, invertebrates, marine mammals) and translocation between the time of egg deposition and the spawn surveys. The amount of egg loss prior to spawn surveys is determined by the daily egg loss rate and the number of days between a spawn and the subsequent survey.

The herring egg loss literature, recently summarized by ([Hay et al., 2011](#), their Appendix 7), is used to estimate a distribution for daily egg loss rates. All studies conducted on the west coast of North America that estimated total egg loss over the incubation period (or daily egg loss rates) were considered for inclusion in the egg loss rate distribution. Those criteria substantially reduce the available literature (Table C-3). Egg loss estimates from the selected studies were standardized to instantaneous (daily) rates (Table C-4). A normal distribution for the daily egg loss rate, based on the mean and standard deviation of the selected estimates, is assumed.

The second component of the egg loss distribution is the average number of days between the spawn event and the surveys. Information to inform the distribution of this factor was available in the B.C. herring spawn survey database. Only dive survey records were selected, and numerous error checks imposed to remove erroneous data (Table C-4). For each spawn record, the number of days between the spawn event

and subsequent survey was estimated as the difference between the mid-spawn date and the mid-survey date. The mean time between a spawn deposition event and the subsequent survey ranges from 6.4 to 9.2 days across the stock assessment regions (Table C-6). A normal distribution for the average time between egg deposition and surveys is assumed, based on the mean and standard deviation of the mean values for the stock assessment regions (mean=7.7; standard deviation =1.13).

Bias in mean egg density

The equation predicting egg density from dive survey observations was calculated from field studies conducted through much of the B.C. coast in the mid 1980s. These studies included diver observations of egg layers and percent cover by vegetation classes and subsequent laboratory egg counts of the observed quadrats. While the egg density prediction equation is unbiased, the unexplained residual error is large and the error in the mean egg densities predicted at the stock assessment region/year level were often greater than expected based on the assumption of unbiased iid observations. To allow for potential bias in predicted mean egg density at the stock assessment region level, we assume a normal distribution for this factor with mean 1 and standard deviation 0.2.

Drift in dive survey observations

The studies to calibrate field observations of herring spawns to egg density estimates were primarily conducted during the mid 1980s by research divers. Since then, Fisheries Officers and subsequently research divers have conducted the coast wide herring spawn surveys. While there is considerable effort to ensure standardization of the surveys, it is possible that there has been drift in how observations are made. There is no direct information on how survey observations may have changed over time, however Hay (in press) suggests that if drift has occurred its direction is to observations that result in lower density estimates (i.e. there has been an increase in trace observations.) For now, we do not include this factor in calculating a prior distribution for the spawn survey q .

Table C-1 summarizes the factors affecting the q prior and their assumed distributions.

Table C-1: Factors affecting the q prior and their assumed distributions.

Factor affecting the q prior	Distribution	Parameters of distribution
Proportion of total spawn surveyed (p_i)	Uniform	0.9-1.0
Egg loss prior to survey:		
Instantaneous daily egg loss rate (Z_i)	Normal	Mean 0.0642 Std. dev 0.0187
Days between spawn deposition and survey (d_i)	Normal	Mean 7.7 Std. dev. 1.13
Bias in mean egg density (b_i)	Normal	Mean 1 Std. dev. 0.2

C.3.3 Simulating the dive survey spawn index q

Monte-Carlo simulations were conducted, randomly sampling from each factors distribution. The factors will operate independently so covariance structure does not need to be considered. For each of 10,000 replicates (i), a random draw was made for each factor to generate a point in the joint distribution for the q prior (\tilde{q}_i):

$$\tilde{q}_i = p_i b_i \exp(-d_i Z_i)$$

For the $i\text{SCA}_M$ herring stock assessments, a lognormal prior for the spawn index q is assumed (i.e., $\ln(q)$ is assumed normally distributed). The distribution of the simulated \tilde{q}_i is reasonably approximated by a lognormal distribution (Figure C.1). Means and standard deviations for the simulated and the natural log of the \tilde{q}_i are presented in Table C-2

Table C-2: Estimated means and standard deviations for the simulated q prior and natural log of the q prior.

	\tilde{q}_i	$\ln(\tilde{q}_i)$
Mean	0.587	-0.569
Std	0.155	0.274

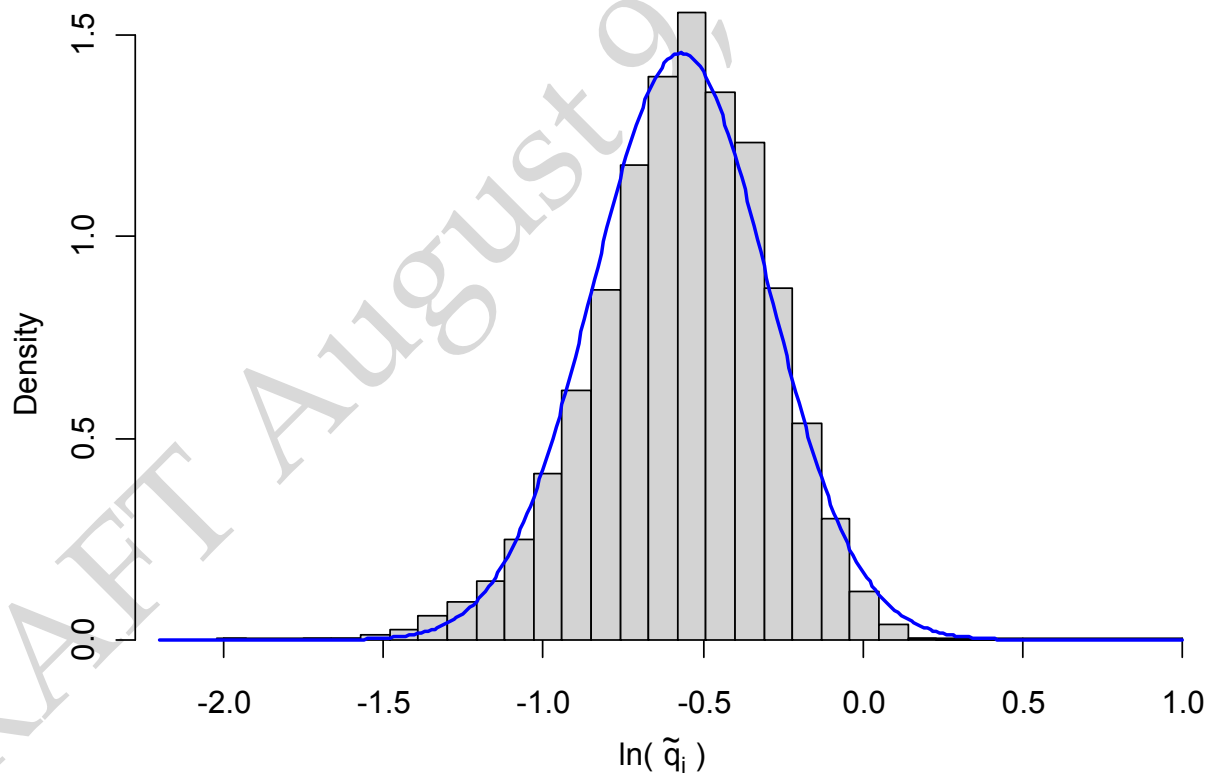


Figure C.1: Distribution of the log of the simulated spawn index q estimates, overlaid with a normal distribution based on the mean and standard deviation of the simulated values.

Table C-3: Summary of west coast North America herring egg loss literature.

Study and summary of pertinent egg loss estimates:	Rationale for inclusion/exclusion from prior estimation:
Bishop and Green (2001) Estimated 31% of herring egg deposition was consumed by 5 species of birds (1994, Prince William Sound), based on a bioenergetics model.	Not included because study estimated only bird predation effect.
Haegele and Schweigert (1991) Estimated 58% herring egg loss over 14 day incubation period (Lambert Channel 1989). Bird and invertebrate predation accounted for 7.1% egg loss; the remainder from physical removal and translocation could not be directly estimated.	Included because comprehensive B.C. study.
Haegele and Schweigert (1989) Estimated 19.5% egg loss from predation based on predator counts and consumption rates (birds and invertebrates). From egg counts, total egg loss estimated at 68.8% over a 14 day incubation period (their Table 3 egg loss equations). Modelled changes in observations of egg layers over the incubation period: egg layers on sea grasses= 2.17 0.07 (day); egg layers on filamentous algae= 3.47 0.13 (day). Equations result in 45% and 52% decrease in egg layers over 14 days incubation period, respectively.	Included because comprehensive B.C. study.
Outram (1958) Seabird predator exclusion study, West coast Vancouver Island (1951-1953). Overall, estimated 39% egg loss due to seabirds over the incubation period. Total egg loss over incubation period ranged from 56% to 99% (based on change in egg biomass for the control plots). Study was restricted to eelgrass beds.	Not included because study restricted to eel grass beds
Paulson (1984) Estimated daily egg loss rates from 16.9% to 51.8% (positively correlated with egg density just after spawning). Large predators account for 20% to 50% of daily egg loss. Initial egg densities were very low, ranging from 400 to 80,000 eggs/m ² across 9 study sites. Paulsons thesis cites additional egg loss literature that is not included here because the studies generally focussed on a limited range of habitat types.	Not included because study egg densities were much lower than densities generally seen in B.C. spawns.
Rooper et al. (1999) Surveys conducted 1991, 1992, 1994 and 1995. Depth is factor that best accounts for egg loss rates (higher egg loss in shallower waters). Mean daily egg loss rates (Z) were (their Table 2): <ul style="list-style-type: none">• 1990 0.076• 1991 0.042• 1994 0.096• 1995 0.096	Comprehensive study in Prince William Sound. Estimates for 1990 and 1991 only are included because population had crashed by 1994 and abundance was low.
Note that population was much lower in 1994 and 1995.	

Table C-4: Estimates of the instantaneous daily egg loss rate (Z) from herring egg loss studies conducted in the Pacific Northwest. The Z estimates for the Haegele and Schweigert (1989, 1991) studies were calculated from their reported egg loss rates over the study period.

Publication	Study Location	Year	Z
Haegele & Schweigert (1991)	SoG	1989	0.056
Haegele & Schweigert (1989)	WCVI	1988	0.083
Rooper et al. (1999)	PWS	1991	0.076
Rooper et al. (1999)	PWS	1992	0.042
		Mean	0.0642
		Std	0.0187

Table C-5: Criteria for selecting herring spawn survey data records for estimating days between spawning and surveys. The "number of records" is the records retained after each successive selection criterion.

Selection criterion	Number of Records
Total dive survey records (1985-2010)	3457
Spawn and survey start/end dates completed	3188
End spawn date \leq start spawn date	
End spawn date - start spawn date < 20	
Survey days ≤ 14 3130	3130
End spawn date-end survey date ≤ 2	
End survey date- end spawn date < 20	3074

Table C-6: Average number of days between spawn deposition and spawn survey by stock assessment region and year.

Year	A2W	HG	PRD	CC	SoG	WCVI	A27
1985					5.2	6.6	8.8
1986			6.0	5.5	5.8	9.2	2.2
1987					10.6		
1988		7.4	11.2	8.3	11.0	8.2	
1989		8.2	10.8	5.8	14.5	8.6	10.7
1990	8.9	12.2	8.3	7.9	12.8	7.6	7.8
1991	10.5	5.9	7.5	11.0	12.4	9.2	2.3
1992	3.6	0.1	6.6	10.0	8.1	9.4	5.7
1993	12.2	9.3	4.9	9.1	13.1	7.6	16.8
1994	4.8	12.2	10.8	8.7	12.8	6.2	
1995		10.3	6.1	7.9	9.3	6.4	11.1
1996		7.9	5.7		10.2	4.5	7.9
1997		8.6	10.3	6.1	9.4	7.5	2.8
1998	10.5	13.3	5.5	12.4	10.4	6.4	4.2
1999		10.0	8.1	6.4	8.0	4.9	
2000	6.5	10.8	10.8	7.4	8.8	6.1	6.9
2001	9.0	7.4	8.3	6.8	8.0	6.9	3.8
2002	6.5	9.0	5.7	5.6	9.9	5.5	2.3
2003		7.5	6.2	5.0	9.5	7.0	7.3
2004	8.6	14.0	8.2	4.1	9.5	7.1	8.2
2005	6.3	9.4	8.8	9.2	5.8	5.1	3.3
2006			7.6	6.5	11.7	3.1	5.8
2007		6.0	10.8	0.7	9.3	3.4	
2008		7.4	7.2	4.3	9.5	3.8	2.0
2009	5.3	6.0	9.6	5.3	4.2	5.5	5.6
2010					7.1	5.2	
Mean	7.8	8.7	8.3	6.8	9.2	6.6	6.4

D.4 Landings and Survey data

The following tables present the herring catch by gear and year for each Stock Assessment Region and the spawn survey data. Note that the units are in 1000's of tonnes.

